Unstructured Finite Volume Techniques for Boussinesq type modelling

Maria Kazolea[2]
Argiris I. Delis[1]
Costas. E. Synolakis[2]

[1]Department of Sciences-Division of Mathematics, Technical University of Crete, Greece
[2] Environmental Engineering Department, TUC, Greece

December 2012

Motivation

Discretize **depth-integrated** equations that model free surface flows, using mass and momentum conservation, by well-established FV approximations.

Motivation

Discretize **depth-integrated** equations that model free surface flows, using mass and momentum conservation, by well-established FV approximations.

* Most popular (applied): Nonlinear Shallow Water Equations (NSWE)

Motivation

Discretize **depth-integrated** equations that model free surface flows, using mass and momentum conservation, by well-established FV approximations.

* Most popular (applied): Nonlinear Shallow Water Equations (NSWE)
  - Limitation: Not applicable for wave propagation in intermediate/deeper waters (dispersion has an effect on free surface flow)

Motivation

Discretize **depth-integrated** equations that model free surface flows, using mass and momentum conservation, by well-established FV approximations.

* Most popular (applied): Nonlinear Shallow Water Equations (NSWE)
  - Limitation: Not applicable for wave propagation in intermediate/deeper waters (dispersion has an effect on free surface flow)
* Popular Boussinesq-type (BT) models for **intermediate water** depths:
  - Peregrine's standard equations (1967) but for $\frac{h}{L} \approx \frac{1}{5}$

Motivation

Discretize **depth-integrated** equations that model free surface flows, using mass and momentum conservation, by well-established FV approximations.

* Most popular (applied): Nonlinear Shallow Water Equations (NSWE)
  – Limitation: Not applicable for wave propagation in intermediate/deeper waters (dispersion has an effect on free surface flow)
* Popular Boussinesq-type (BT) models for **intermediate water** depths:
  – Peregrine's standard equations (1967) but for $\frac{h}{L} \approx \frac{1}{5}$
  – Madsen and Sörensen's (MS) (1992), **Nowgu's (1993)** and Beji and Nadaoka (BN) equations (1996) for $\frac{h}{L} \approx \frac{1}{2}$

Motivation

Discretize **depth-integrated** equations that model free surface flows, using mass and momentum conservation, by well-established FV approximations.

* Most popular (applied): Nonlinear Shallow Water Equations (NSWE)
  – Limitation: Not applicable for wave propagation in intermediate/deeper waters (dispersion has an effect on free surface flow)
* Popular Boussinesq-type (BT) models for **intermediate water** depths:
  – Peregrine's standard equations (1967) but for $\frac{h}{L} \approx \frac{1}{5}$
  – Madsen and Sörensen's (MS) (1992), **Nowgu's (1993)** and Beji and Nadaoka (BN) equations (1996) for $\frac{h}{L} \approx \frac{1}{2}$
  – Gobbi, Kirby and Wei BT model (2000)
  – Variety of BT models that include higher-order nonlinear and dispersive terms: P.A. Madsen et al. (2002-2009), Lynett et al. (2004-2010) and Tissier, Bonneton et al. (2010-2012).

(Some) Numerical Works

* Until recently, **Finite-Differences** (FD) was the predominant method based on the work of Wei & Kirby (1995), for 1D & 2D computations

(Some) Numerical Works

* Until recently, **Finite-Differences** (FD) was the predominant method based on the work of Wei & Kirby (1995), for 1D & 2D computations

* More recently **hybrid FV/FD** schemes in 1D & 2D:
  – Nwogu's, MS, BN, Serre Green-Green Naghdi S-GN equations using: Riemann solvers (Roe's and HLL-type), MUSCL-type reconstructions.

    Erduran et al. (2005 & 2007), Cienfuegos et al (2006 & 2007), Tonelli & Petti (2009), Shiach & Mingham (2009), Roeber et al. (2010), Bonneton et al. (2010), Kazolea & Delis (2011), Dutykh et al. (2011).

(Some) Numerical Works

* Until recently, **Finite-Differences** (FD) was the predominant method based on the work of Wei & Kirby (1995), for 1D & 2D computations

* More recently **hybrid FV/FD** schemes in 1D & 2D:
  – Nwogu's, MS, BN, Serre Green-Green Naghdi S-GN equations using: Riemann solvers (Roe's and HLL-type), MUSCL-type reconstructions. Erduran et al. (2005 & 2007), Cienfuegos et al (2006 & 2007), Tonelli & Petti (2009), Shiach & Mingham (2009), Roeber et al. (2010), Bonneton et al. (2010), Kazolea & Delis (2011), Dutykh et al. (2011).
  – MS equations in 2D Tonelli & Petti (2009 & 2010), two-layer BT equations Lynnet et al., (2006-2010), TVD Boussinesq solver Shi, Kirby et. al. (2012).

(Some) Numerical Works

* Until recently, **Finite-Differences** (FD) was the predominant method based on the work of Wei & Kirby (1995), for 1D & 2D computations

* More recently **hybrid FV/FD** schemes in 1D & 2D:
  - Nwogu's, MS, BN, Serre Green-Green Naghdi S-GN equations using: Riemann solvers (Roe's and HLL-type), MUSCL-type reconstructions. Erduran et al. (2005 & 2007), Cienfuegos et al (2006 & 2007), Tonelli & Petti (2009), Shiach & Mingham (2009), Roeber et al. (2010), Bonneton et al. (2010), Kazolea & Delis (2011), Dutykh et al. (2011).
  - MS equations in 2D Tonelli & Petti (2009 & 2010), two-layer BT equations Lynnet et al., (2006-2010), TVD Boussinesq solver Shi, Kirby et. al. (2012).

* 2D **Finite Element** (FE) on unstructured meshes: Walkey & Berzins (2002), Sorensen et al. (2004), Escilsson & Sherwin (2006) and Engsig-Karup et al. (2008).

(Some) Numerical Works

* Until recently, **Finite-Differences** (FD) was the predominant method based on the work of Wei & Kirby (1995), for 1D & 2D computations

* More recently **hybrid FV/FD** schemes in 1D & 2D:
  - Nwogu's, MS, BN, Serre Green-Green Naghdi S-GN equations using: Riemann solvers (Roe's and HLL-type), MUSCL-type reconstructions. Erduran et al. (2005 & 2007), Cienfuegos et al (2006 & 2007), Tonelli & Petti (2009), Shiach & Mingham (2009), Roeber et al. (2010), Bonneton et al. (2010), Kazolea & Delis (2011), Dutykh et al. (2011).
  - MS equations in 2D Tonelli & Petti (2009 & 2010), two-layer BT equations Lynnet et al., (2006-2010), TVD Boussinesq solver Shi, Kirby et. al. (2012).

* 2D **Finite Element** (FE) on unstructured meshes: Walkey & Berzins (2002), Sorensen et al. (2004), Escilsson & Sherwin (2006) and Engsig-Karup et al. (2008).

* **FV for unstructured meshes**: Only one work by Asmar and Nwogu (2006) using a low-order staggered scheme

Physical problem setup

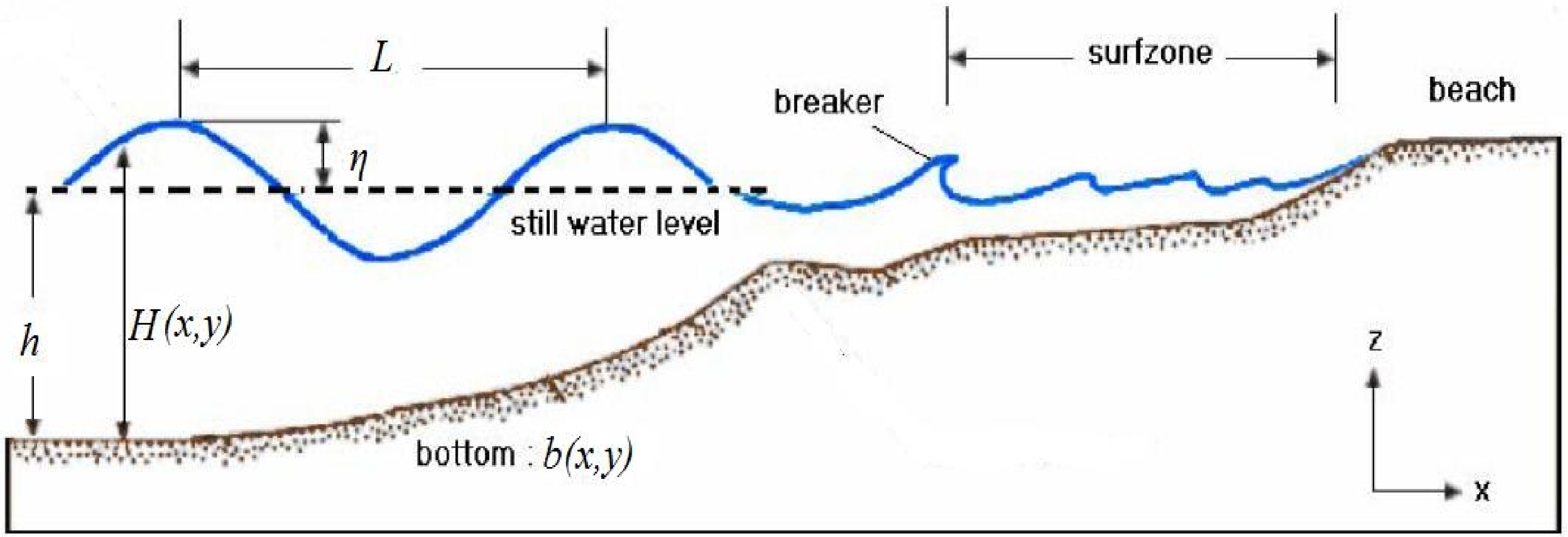

η: **free surface elevation**;

h: **steel water level**;

$H = \eta + h$: **total water depth**;

b: **bottom topography**;

L: **wave length**;

A: **wave amplitude**

Physical problem setup

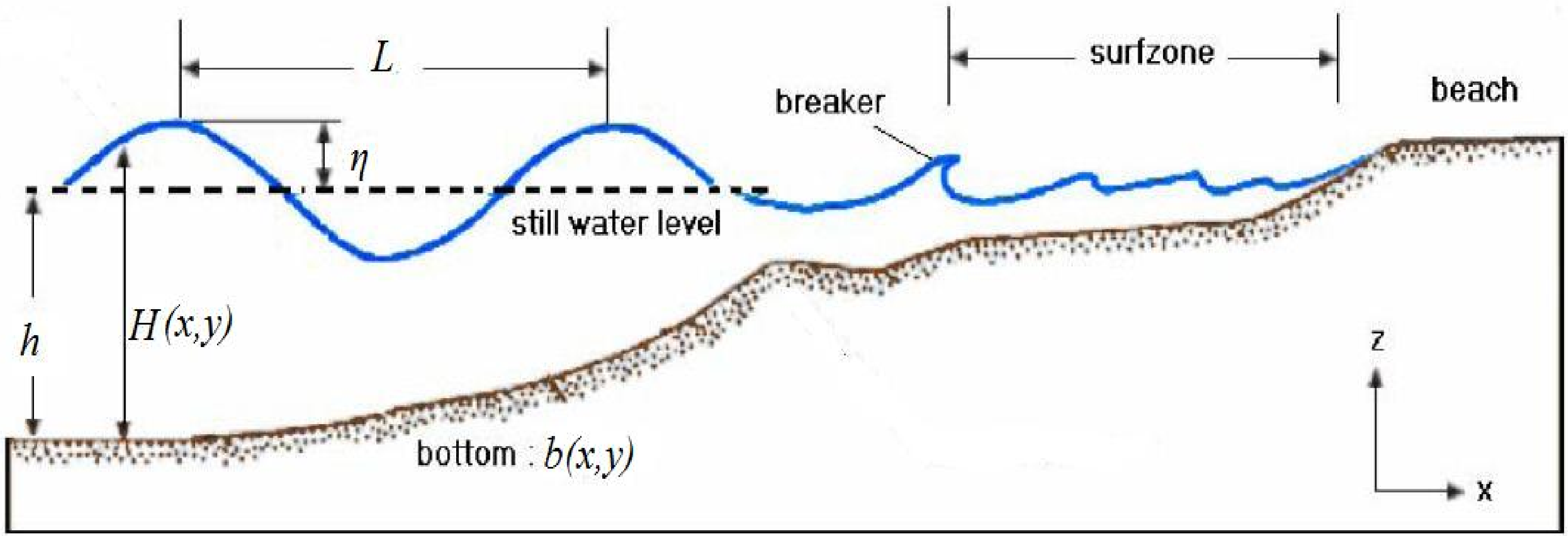

η: **free surface elevation**;

h: **steel water level**;

$H = \eta + h$: **total water depth**;

b: **bottom topography**;

L: **wave length**;

A: **wave amplitude**

Deep water: $\frac{h}{L} > \frac{1}{2}$

Intermediate water: $\frac{1}{20} < \frac{h}{L} \leq \frac{1}{2}$

Shallow water: $\frac{h}{L} \leq \frac{1}{20}$

Mathematical Model: Nowgu's extended Boussinesq equations

Using $\mathbf{z_a = -0.531h}$ as optimal reference depth and $\mathbf{u} \equiv \mathbf{u}_a$ at $z = z_a$

$$
\begin{aligned}
\eta_t \quad &+ \quad (Hu)_x + (Hv)_y + \left[\left(\frac{z_a^2}{2} - \frac{h^2}{6} \right) h(u_x + v_y)_x + \left(z_a + \frac{h}{2} \right) h \left((hu)_x + (hv)_y \right)_x \right]_x \\
&+ \quad \left[\left(\frac{z_a^2}{2} - \frac{h^2}{6} \right) h(u_x + v_y)_y + \left(z_a + \frac{h}{2} \right) h \left((hu)_x + (hv)_y \right)_y \right]_y = 0, \qquad (1)
\end{aligned}
$$

$$
u_t \quad + \quad g\eta_x + uu_x + vu_y + \left[\frac{z_a^2}{2}(u_{xx} + v_{yx}) + z_a \left((hu)_{xx} + (hv)_{yx} \right) \right]_t = R_{f_x} + R_{b_x}, \qquad (2)
$$

$$
v_t \quad + \quad g\eta_y + uv_x + vv_y + \left[\frac{z_a^2}{2}(u_{xy} + v_{yy}) + z_a \left((hu)_{xy} + (hv)_{yy} \right) \right]_t = R_{f_y} + R_{b_y}, \qquad (3)
$$

Mathematical Model: Nowgu's extended Boussinesq equations

Using $\mathbf{z_a = -0.531h}$ as optimal reference depth and $\mathbf{u} \equiv \mathbf{u}_a$ at $z = z_a$

$$
\begin{aligned}
\eta_t \quad &+ \quad (Hu)_x + (Hv)_y + \left[\left(\frac{z_a^2}{2} - \frac{h^2}{6} \right) h(u_x + v_y)_x + \left(z_a + \frac{h}{2} \right) h\left((hu)_x + (hv)_y \right)_x \right]_x \\
&+ \quad \left[\left(\frac{z_a^2}{2} - \frac{h^2}{6} \right) h(u_x + v_y)_y + \left(z_a + \frac{h}{2} \right) h\left((hu)_x + (hv)_y \right)_y \right]_y = 0, \qquad (1) \\
u_t \quad &+ \quad g\eta_x + uu_x + vu_y + \left[\frac{z_a^2}{2}(u_{xx} + v_{yx}) + z_a\left((hu)_{xx} + (hv)_{yx} \right) \right]_t = R_{f_x} + R_{b_x}, \qquad (2) \\
v_t \quad &+ \quad g\eta_y + uv_x + vv_y + \left[\frac{z_a^2}{2}(u_{xy} + v_{yy}) + z_a\left((hu)_{xy} + (hv)_{yy} \right) \right]_t = R_{f_y} + R_{b_y}, \qquad (3)
\end{aligned}
$$

Equations derived under the assumption that

$$
\epsilon := A/h \ll 1, \qquad \mu^2 := h^2/L^2 \ll 1, \qquad S := \epsilon/\mu^2 = O(1),
$$

and provide good linear accuracy to $kh = \frac{2\pi h}{L} \approx 3$ (intermediate water).

Vector conservative form

$$\mathbf{U}_t + \nabla \cdot \mathcal{H}(\mathbf{U}^\star) = \mathbf{S}(\mathbf{U}) \quad \text{on} \quad \Omega \times [0,t] \subset \mathbb{R}^2 \times \mathbb{R}^+,$$

$\mathbf{U}$ vector of the **new variables**, $\mathbf{U}^\star = [H, Hu, Hv]^{\mathrm{T}}$ and $\mathcal{H} = [\mathbf{F}, \mathbf{G}]$

$$\mathbf{U} = \begin{bmatrix} H \\ P_1 \\ P_2 \end{bmatrix}, \ \mathbf{F}(\mathbf{U}^\star) = \begin{bmatrix} Hu \\ Hu^2 + \frac{1}{2}gH^2 \\ Huv \end{bmatrix}, \ \mathbf{G}(\mathbf{U}^\star) = \begin{bmatrix} Hv \\ Huv \\ Hv^2 + \frac{1}{2}gH^2 \end{bmatrix},$$

with $\mathbf{P} = \begin{bmatrix} P_1 \\ P_2 \end{bmatrix} = H\left[\frac{z_a^2}{2}\nabla(\nabla \cdot \mathbf{u}) + z_a \nabla(\nabla \cdot h\mathbf{u}) + \mathbf{u}\right]$

and $\mathbf{S} = \mathbf{S_b} + \mathbf{S_d} + \mathbf{S_f}$

Vector conservative form

$$\mathbf{U}_t + \nabla \cdot \mathcal{H}(\mathbf{U}^\star) = \mathbf{S}(\mathbf{U}) \quad \text{on} \quad \Omega \times [0,t] \subset \mathbb{R}^2 \times \mathbb{R}^+,$$

$\mathbf{U}$ vector of the **new variables**, $\mathbf{U}^\star = [H, Hu, Hv]^{\mathrm{T}}$ and $\mathcal{H} = [\mathbf{F}, \mathbf{G}]$

$$\mathbf{U} = \begin{bmatrix} H \\ P_1 \\ P_2 \end{bmatrix}, \; \mathbf{F}(\mathbf{U}^\star) = \begin{bmatrix} Hu \\ Hu^2 + \frac{1}{2}gH^2 \\ Huv \end{bmatrix}, \; \mathbf{G}(\mathbf{U}^\star) = \begin{bmatrix} Hv \\ Huv \\ Hv^2 + \frac{1}{2}gH^2 \end{bmatrix},$$

with $\mathbf{P} = \begin{bmatrix} P_1 \\ P_2 \end{bmatrix} = H\left[\frac{z_a^2}{2}\nabla(\nabla \cdot \mathbf{u}) + z_a \nabla(\nabla \cdot h\mathbf{u}) + \mathbf{u}\right]$

and $\mathbf{S} = \mathbf{S_b} + \mathbf{S_d} + \mathbf{S_f}$

$$\mathbf{S_b} = \begin{bmatrix} 0 \\ -gHb_x \\ -gHb_y \end{bmatrix}, \quad \mathbf{S_d} = \begin{bmatrix} -\psi_c \\ -u\psi_c + \psi_{M_x} \\ -v\psi_c + \psi_{M_y} \end{bmatrix}, \quad \mathbf{S_f} = \begin{bmatrix} 0 \\ R_{f_x} + R_{b_x} \\ R_{f_y} + R_{b_y} \end{bmatrix}$$

where

$$\psi_c \quad = \quad \nabla \cdot \left[\left(\frac{z_a^2}{2} - \frac{h^2}{6}\right) h\nabla(\nabla \cdot \mathbf{u}) + \left(z_a + \frac{h}{2}\right) h\nabla(\nabla \cdot h\mathbf{u})\right]$$

Vector conservative form (cont.)

$$\psi_{\mathbf{M}} = \begin{bmatrix} \psi_{M_x} \\ \psi_{M_y} \end{bmatrix} = H_t \frac{z_a^2}{2} \nabla(\nabla \cdot \mathbf{u}) + H_t z_a \nabla(\nabla \cdot h\mathbf{u})$$

Vector conservative form (cont.)

$$\psi_{\mathbf{M}} = \begin{bmatrix} \psi_{M_x} \\ \psi_{M_y} \end{bmatrix} = H_t \frac{z_a^2}{2} \nabla(\nabla \cdot \mathbf{u}) + H_t z_a \nabla(\nabla \cdot h\mathbf{u})$$

$$\mathbf{R}_f = [R_{f_x} \; R_{f_y}] = [-gHS_f^x \; - gHS_f^y]^{\mathrm{T}}$$

where

$$S_f^x = n_m^2 \frac{u||\mathbf{u}||}{H^{-4/3}} \text{ and } S_f^y = n_m^2 \frac{v||\mathbf{u}||}{H^{-4/3}} \text{ Friction force, } n_m = \text{Manning coef.}$$

Vector conservative form (cont.)

$$\psi_{\mathbf{M}} = \begin{bmatrix} \psi_{M_x} \\ \psi_{M_y} \end{bmatrix} = H_t \frac{z_a^2}{2} \nabla(\nabla \cdot \mathbf{u}) + H_t z_a \nabla(\nabla \cdot h\mathbf{u})$$

$$\mathbf{R}_f = [R_{f_x} \; R_{f_y}] = [-gHS_f^x \; -gHS_f^y]^{\mathrm{T}}$$

where

$$S_f^x = n_m^2 \frac{u||\mathbf{u}||}{H^{-4/3}} \text{ and } S_f^y = n_m^2 \frac{v||\mathbf{u}||}{H^{-4/3}} \text{ Friction force, } n_m = \text{Manning coef.}$$

$R_b = [R_{b_x}, \; R_{b_y}]^{\mathrm{T}}$ = parametrization of wave breaking characteristics where

$$\begin{aligned} R_{b_x} &= \nabla \cdot \tilde{\mathbf{R}}_{b_x}, \text{ where } \tilde{\mathbf{R}}_{b_x} = \left[\nu(Hu)_x \quad \frac{\nu}{2}((Hu)_y + (Hv)_x) \right]^{\mathrm{T}} \text{ and} \\ R_{b_y} &= \nabla \cdot \tilde{\mathbf{R}}_{b_y}, \text{ where } \tilde{\mathbf{R}}_{b_y} = \left[\frac{\nu}{2}((Hu)_y + (Hv)_x) \quad \nu(Hv)_y \right]^{\mathrm{T}}. \end{aligned}$$

Numerical Model: Spatial discretization (overview)

- Advective (nonlinear) part and topography source term: Well-balanced FV formulation.

- Roe's approximate Riemann solver is used (Roe, 1981).

Numerical Model: Spatial discretization (overview)

- Advective (nonlinear) part and topography source term: Well-balanced FV formulation.

- Roe's approximate Riemann solver is used (Roe, 1981).

- Upwinding of the topography source term (Bermudez et al., 1994 & Nikolos and Delis, 2009).

Numerical Model: Spatial discretization (overview)

- Advective (nonlinear) part and topography source term: Well-balanced FV formulation.
- Roe's approximate Riemann solver is used (Roe, 1981).
- Upwinding of the topography source term (Bermudez et al., 1994 & Nikolos and Delis, 2009).
- High-order spatial accuracy: third-order **MUSCL**-type scheme (Barth, 1993).

Numerical Model: Spatial discretization (overview)

- Advective (nonlinear) part and topography source term: Well-balanced FV formulation.
- Roe's approximate Riemann solver is used (Roe, 1981).
- Upwinding of the topography source term (Bermudez et al., 1994 & Nikolos and Delis, 2009).
- High-order spatial accuracy: third-order **MUSCL**-type scheme (Barth, 1993).
- Dispersion terms: consistent FV approximations based on gradient and divergence computations (Kazolea et al., 2012)

Numerical Model: Spatial discretization (overview)

- Advective (nonlinear) part and topography source term: Well-balanced FV formulation.
- Roe's approximate Riemann solver is used (Roe, 1981).
- Upwinding of the topography source term (Bermudez et al., 1994 & Nikolos and Delis, 2009).
- High-order spatial accuracy: third-order **MUSCL**-type scheme (Barth, 1993).
- Dispersion terms: consistent FV approximations based on gradient and divergence computations (Kazolea et al., 2012)
- Satisfy the C-property (flow at rest) to higher spatial order: Addition of an extra term to bed upwinding (Hubbard and Garcia-Navarro, 2000 & Nikolos and Delis, 2009)

Numerical Model: Spatial discretization (overview)

- Advective (nonlinear) part and topography source term: Well-balanced FV formulation.
- Roe's approximate Riemann solver is used (Roe, 1981).
- Upwinding of the topography source term (Bermudez et al., 1994 & Nikolos and Delis, 2009).
- High-order spatial accuracy: third-order **MUSCL**-type scheme (Barth, 1993).
- Dispersion terms: consistent FV approximations based on gradient and divergence computations (Kazolea et al., 2012)
- Satisfy the C-property (flow at rest) to higher spatial order: Addition of an extra term to bed upwinding (Hubbard and Garcia-Navarro, 2000 & Nikolos and Delis, 2009)
- Special treatment of **wet/dry fronts**:
  * Identify dry cells: through an adaptive (grid dependant) tolerance parameter
  * Consistent depth reconstruction: satisfy $\nabla H = -\nabla b$ to high-order on wet/dry fronts (Delis et al., 2011)
  * Satisfy an extended C-property: Redefinition of the bed slope, numerical fluxes are computed assuming temporarily zero velocity at wet/dry faces (Brufau et al., 2004)

Numerical Model: Spatial discretization

Use of **node-centered median dual** approach to create control volume C_P:

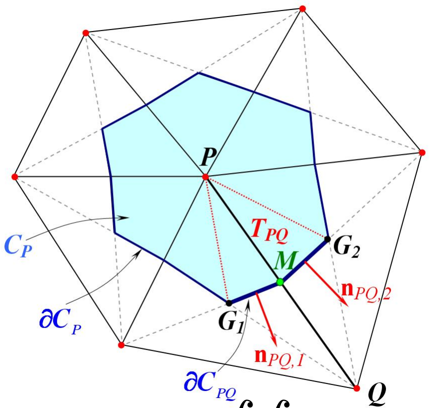

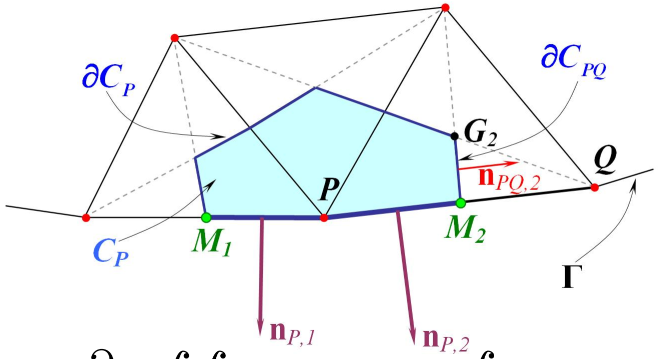

$$\iint_{C_P} \frac{\partial \mathbf{U}}{\partial t} d\Omega + \iint_{C_P} \nabla \cdot \mathcal{H} d\Omega = \iint_{C_P} \mathbf{S} d\Omega \ \Rightarrow \ \frac{\partial}{\partial t} \iint_{C_P} \mathbf{U} d\Omega + \oint_{\partial C_P} \mathcal{H} \cdot \tilde{\mathbf{n}} dl = \iint_{C_P} \mathbf{S} d\Omega$$

Numerical Model: Spatial discretization

Use of **node-centered median dual** approach to create control volume C_P:

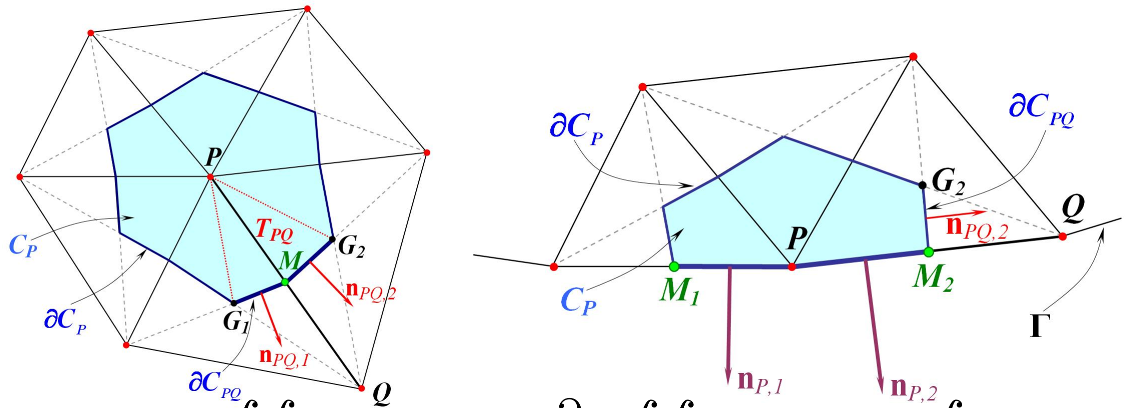

$$\iint_{C_P} \frac{\partial \mathbf{U}}{\partial t} d\Omega + \iint_{C_P} \nabla \cdot \mathcal{H} d\Omega = \iint_{C_P} \mathbf{S} d\Omega \Rightarrow \frac{\partial}{\partial t} \iint_{C_P} \mathbf{U} d\Omega + \oint_{\partial C_P} \mathcal{H} \cdot \tilde{\mathbf{n}} dl = \iint_{C_P} \mathbf{S} d\Omega$$

Introducing the flux vectors

$$\mathbf{\Phi}_{PQ} = \int_{\partial C_{PQ}} \Big(\mathbf{F} \tilde{n}_x + \mathbf{G} \tilde{n}_y \Big) dl \quad \text{and} \quad \mathbf{\Phi}_{P,\Gamma} = \int_{\partial C_P \cap \Gamma} \Big(\mathbf{F} \tilde{n}_x + \mathbf{G} \tilde{n}_y \Big) dl$$

Hence, FV scheme reads

$$\frac{\partial \mathbf{U}_P}{\partial t} = -\frac{1}{|C_P|} \sum_{Q \in K_P} \mathbf{\Phi}_{PQ} - \frac{1}{|C_P|} \mathbf{\Phi}_{P,\Gamma} + \frac{1}{|C_P|} \iint_{C_P.} \left(\mathbf{S_b} + \mathbf{S_d} + \mathbf{S_f} \right) d\Omega$$

Gradient and divergence edge formulas: Green-Gauss linear reconstruction on Ω_P

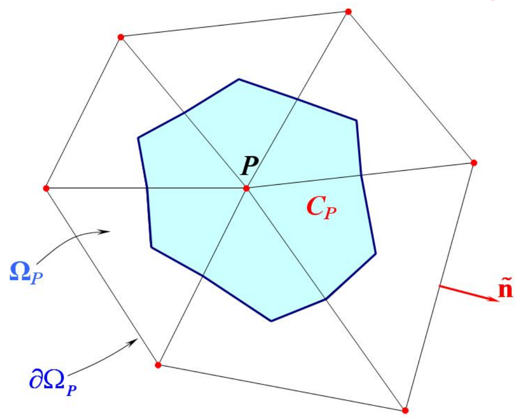

$$|C_P| = \tfrac{1}{3}|\Omega_P|$$

$$\iint_{\Omega_P} \nabla w dA = \oint_{\partial\Omega_P} w\tilde{\mathbf{n}} dl \;\Rightarrow\; (\nabla w)_P = \frac{1}{|C_P|}\sum_{Q\in K_P}\frac{1}{2}\Big(w_P + w_Q\Big)\mathbf{n}_{PQ}$$

Gradient and divergence edge formulas: Green-Gauss linear reconstruction on Ω_P

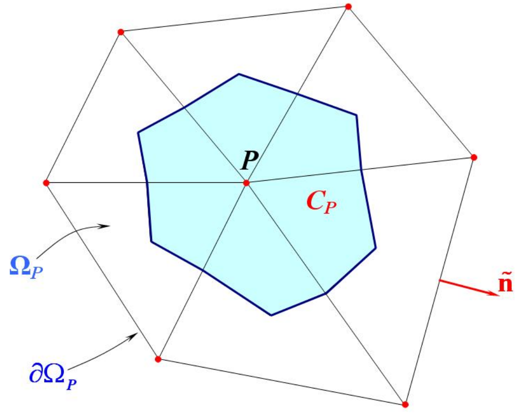

$$|C_P| = \frac{1}{3}|\Omega_P|$$

$$\iint_{\Omega_P} \nabla w dA = \oint_{\partial\Omega_P} w\tilde{\mathbf{n}} dl \;\Rightarrow\; (\nabla w)_P = \frac{1}{|C_P|}\sum_{Q\in K_P}\frac{1}{2}\Big(w_P + w_Q\Big)\mathbf{n}_{PQ}$$

$$\iint_{\Omega_P} \nabla\cdot\mathbf{u} d\Omega = \oint_{\partial\Omega_P} \mathbf{u}\cdot\tilde{\mathbf{n}} dl = \sum_{Q\in K_P}\frac{3}{2}(\mathbf{u}_P+\mathbf{u}_Q)\cdot\mathbf{n}_{PQ} \Rightarrow (\nabla\cdot\mathbf{u})_P = \frac{1}{2|C_P|}\sum_{Q\in K_P}(\mathbf{u}_P+\mathbf{u}_Q)\cdot\mathbf{n}_{PQ}$$

Gradient and divergence edge formulas: Green-Gauss linear reconstruction on Ω_P

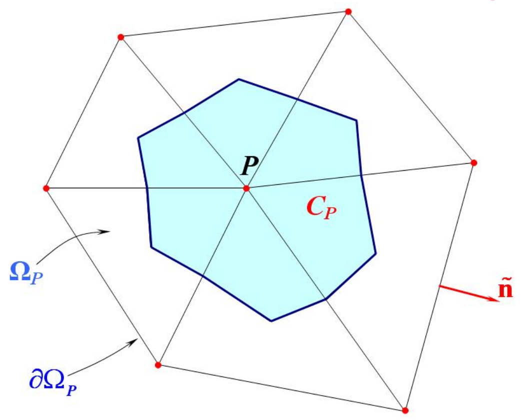

$$|C_P| = \tfrac{1}{3}|\Omega_P|$$

$$\iint_{\Omega_P} \nabla w dA = \oint_{\partial\Omega_P} w\tilde{\mathbf{n}} dl \;\Rightarrow\; (\nabla w)_P = \frac{1}{|C_P|}\sum_{Q\in K_P} \frac{1}{2}\Big(w_P + w_Q\Big)\mathbf{n}_{PQ}$$

$$\iint_{\Omega_P} \nabla\cdot\mathbf{u} d\Omega = \oint_{\partial\Omega_P} \mathbf{u}\cdot\tilde{\mathbf{n}} dl = \sum_{Q\in K_P} \frac{3}{2}(\mathbf{u}_P+\mathbf{u}_Q)\cdot\mathbf{n}_{PQ} \Rightarrow (\nabla\cdot\mathbf{u})_P = \frac{1}{2|C_P|}\sum_{Q\in K_P}(\mathbf{u}_P+\mathbf{u}_Q)\cdot\mathbf{n}_{PQ}$$

For boundary cells:

$$(\nabla w)_P = \frac{1}{|C_P|}\Big[\sum_{Q\in K_P}\frac{1}{2}\Big(w_P + w_Q\Big)\mathbf{n}_{PQ} + w_P\Big(\mathbf{n}_{P,1} + \mathbf{n}_{P,2}\Big)\Big]$$

$$(\nabla\cdot\mathbf{u})_P = \frac{1}{|C_P|}\Big[\sum_{Q\in K_P}\frac{1}{2}(\mathbf{u}_P + \mathbf{u}_Q)\cdot\mathbf{n}_{PQ} + \mathbf{u}_P\cdot(\mathbf{n}_{P,1} + \mathbf{n}_{P,2})\Big]$$

Discretization of the dispersion terms (mass equation): Integral averaging

$$
\begin{aligned}
(\psi_c)_P &= \frac{1}{|C_P|}\iint_{C_P} \nabla\cdot\left[\left(\frac{z_a^2}{2}-\frac{h^2}{6}\right) h\nabla(\nabla\cdot\mathbf{u}) + \left(z_a+\frac{h}{2}\right) h\nabla(\nabla\cdot h\mathbf{u})\right] d\Omega \\
&= \frac{1}{|C_P|}\sum_{Q\in K_P}\left\{\int_{\partial C_{PQ}}\left[\left(\frac{z_a^2}{2}-\frac{h^2}{6}\right) h\nabla(\nabla\cdot\mathbf{u})\right]\cdot\tilde{\mathbf{n}}dl + \int_{\partial C_{PQ}}\left[\left(z_a+\frac{h}{2}\right) h\nabla(\nabla\cdot h\mathbf{u})\right]\cdot\tilde{\mathbf{n}}dl\right\}
\end{aligned}
$$

Discretization of the dispersion terms (mass equation): Integral averaging

$$
\begin{aligned}
(\psi_c)_P &= \frac{1}{|C_P|}\iint_{C_P} \nabla\cdot\left[\left(\frac{z_a^2}{2}-\frac{h^2}{6}\right)h\nabla(\nabla\cdot\mathbf{u}) + \left(z_a+\frac{h}{2}\right)h\nabla(\nabla\cdot h\mathbf{u})\right]d\Omega \\
&= \frac{1}{|C_P|}\sum_{Q\in K_P}\left\{\int_{\partial C_{PQ}}\left[\left(\frac{z_a^2}{2}-\frac{h^2}{6}\right)h\nabla(\nabla\cdot\mathbf{u})\right]\cdot\tilde{\mathbf{n}}dl + \int_{\partial C_{PQ}}\left[\left(z_a+\frac{h}{2}\right)h\nabla(\nabla\cdot h\mathbf{u})\right]\cdot\tilde{\mathbf{n}}dl\right\}
\end{aligned}
$$

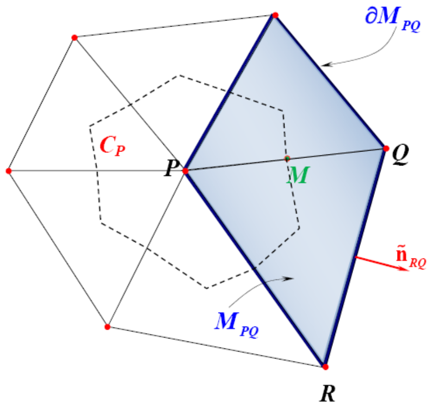

$$
\int_{\partial C_{PQ}}\left(\frac{z_a^2}{2}-\frac{h^2}{6}\right)h\nabla(\nabla\cdot\mathbf{u})\cdot\tilde{\mathbf{n}}dl \approx \left[\left(\frac{z_a^2}{2}-\frac{h^2}{6}\right)h\right]_M \left[\nabla(\nabla\cdot\mathbf{u})\cdot\mathbf{n}_{PQ}\right]_M,
$$

$$
\int_{\partial C_{PQ}}\left(z_a+\tfrac{h}{2}\right)h\nabla(\nabla\cdot h\mathbf{u})\cdot\tilde{\mathbf{n}}dl \approx \left[\left(z_a+\tfrac{h}{2}\right)h\right]_M \left[\nabla(\nabla\cdot h\mathbf{u})\cdot\mathbf{n}_{PQ}\right]_M
$$

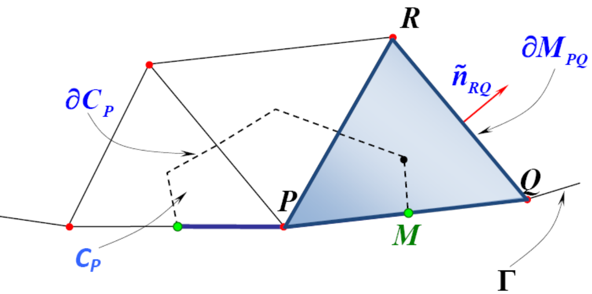

$$
K_{PQ} := \{R\in\mathbb{N}\mid R \text{ is a vertex of } M_{PQ} \text{ and } RQ\in\partial M_{PQ}\}
$$

$$
(\nabla w)_M = \frac{1}{|M_{PQ}|}\sum_{\substack{R,Q\in K_{PQ}\\ R\neq Q}}\frac{1}{2}(w_R+w_Q)\,\mathbf{n}_{RQ}
$$

Discretization of the dispersion terms (momentum equations):

$$\frac{1}{|C_P|}\iint_{C_P}\left(-\mathbf{u}\psi_c+\psi_{\mathbf{M}}\right)d\Omega=-\frac{\mathbf{u}_P}{|C_P|}\iint_{C_P}\psi_c d\Omega+\frac{1}{|C_P|}\iint_{C_P}\psi_{\mathbf{M}}d\Omega.$$

The ψ_c is discretized as before and the second term takes the discrete form:

$$\begin{aligned}
(\psi_{\mathbf{M}})_P=\frac{1}{|C_P|}\iint_{C_P}\psi_{\mathbf{M}}d\Omega &= \frac{1}{|C_P|}\iint_{C_P}H_t\frac{z_a^2}{2}\nabla(\nabla\cdot\mathbf{u})+H_t z_a\nabla(\nabla\cdot h\mathbf{u})d\Omega\\
&= \frac{1}{|C_P|}\iint_{C_P}H_t\frac{z_a^2}{2}\nabla(\nabla\cdot\mathbf{u})d\Omega+\frac{1}{|C_P|}\iint_{C_P}H_t z_a\nabla(\nabla\cdot h\mathbf{u})d\Omega\\
&\approx \left[H_t\frac{z_a^2}{2}\right]_P\left[\nabla(\nabla\cdot\mathbf{u})\right]_P+\left[H_t z_a\right]_P\left[\nabla(\nabla\cdot h\mathbf{u})\right]_P,
\end{aligned}$$

Numerical Model (continued)

Consider the semi-discrete scheme:

$$\frac{\partial \mathbf{U}_P}{\partial t} = \mathcal{L}\left(\mathbf{U}\right)$$

Time Integration (match the order of truncation errors from dispersion terms):

Use 3rd order explicit Strong Stability-Preserving Runge-Kutta (SSP-RK):

$$\begin{aligned}
\mathbf{U}_P^{(1)} &= \mathbf{U}_P^{(n)} + \Delta t^n \mathcal{L}\left(\mathbf{U}^{(n)}\right); \\
\mathbf{U}_P^{(2)} &= \frac{3}{4}\mathbf{U}_P^{(n)} + \frac{1}{4}\mathbf{U}_P^{(1)} + \Delta t^n \frac{1}{4}\mathcal{L}\left(\mathbf{U}^{(1)}\right); \\
\mathbf{U}_P^{(n+1)} &= \frac{1}{3}\mathbf{U}_P^{(n)} + \frac{2}{3}\mathbf{U}_P^{(2)} + \Delta t^n \frac{2}{3}\mathcal{L}\left(\mathbf{U}^{(2)}\right)
\end{aligned}$$

Time step Δt^n estimated by a CFL stability condition as

$$\Delta t^n = CFL \cdot \min_P \left(\frac{R_P}{\left(\sqrt{u^2+v^2}+c\right)_P^n} \right)$$

Velocity field recovery: from new solution variables $\mathbf{P} = [P_1, P_2]^{\mathrm{T}}$

At each step in the RK scheme a linear system $\mathbf{MV} = \mathbf{C}$ with $\mathbf{M} \in \mathbb{R}^{2N\times 2N}$ and $\mathbf{C} = [\mathbf{P}_1\ \mathbf{P}_2 \cdots\ \mathbf{P}_N]^{\mathrm{T}}$, has to be solved to obtain the velocities $\mathbf{V} = [\mathbf{u}_1\ \mathbf{u}_2\ \cdots\ \mathbf{u}_N]^{\mathrm{T}}$. Each two rows of the system read as

$$H_P^{(i)} \left[\frac{z_a^2}{2} \nabla(\nabla \cdot \mathbf{u}) + z_a \nabla(\nabla \cdot h\mathbf{u}) + \mathbf{u} \right]_P^{(i)} = \mathbf{P}_P^{(i)}, \quad i = 1, 2, n+1.$$

Velocity field recovery: from new solution variables $\mathbf{P} = [P_1, P_2]^{\mathrm{T}}$

At each step in the RK scheme a linear system $\mathbf{MV} = \mathbf{C}$ with $\mathbf{M} \in \mathbb{R}^{2N\times 2N}$ and $\mathbf{C} = [\mathbf{P}_1\ \mathbf{P}_2 \cdots\ \mathbf{P}_N]^{\mathrm{T}}$, has to be solved to obtain the velocities $\mathbf{V} = [\mathbf{u}_1\ \mathbf{u}_2\ \cdots\ \mathbf{u}_N]^{\mathrm{T}}$. Each two rows of the system read as

$$H_P^{(i)} \left[\frac{z_a^2}{2} \nabla(\nabla\cdot\mathbf{u}) + z_a \nabla(\nabla\cdot h\mathbf{u}) + \mathbf{u} \right]_P^{(i)} = \mathbf{P}_P^{(i)}, \quad i = 1, 2, n+1.$$

Important to (a) keep the unknown information needed at the minimum possible level and (b) exploit already computed geometrical information.

$$H_P \left[\frac{(z_a^2)_P}{2} \frac{1}{|C_P|} \sum_{Q\in K_P} (\nabla\cdot\mathbf{u})_M \mathbf{n}_{PQ} + \frac{(z_a)_P}{|C_P|} \sum_{Q\in K_P} (\nabla\cdot h\mathbf{u})_M \mathbf{n}_{PQ} + \mathbf{u}_P \right] = \mathbf{P}_P$$

Velocity field recovery: from new solution variables $\mathbf{P} = [P_1, P_2]^{\mathrm{T}}$

At each step in the RK scheme a linear system $\mathbf{MV} = \mathbf{C}$ with $\mathbf{M} \in \mathbb{R}^{2N \times 2N}$ and $\mathbf{C} = [\mathbf{P}_1 \; \mathbf{P}_2 \cdots \; \mathbf{P}_N]^{\mathrm{T}}$, has to be solved to obtain the velocities $\mathbf{V} = [\mathbf{u}_1 \; \mathbf{u}_2 \; \cdots \; \mathbf{u}_N]^{\mathrm{T}}$. Each two rows of the system read as

$$H_P^{(i)} \left[\frac{z_a^2}{2} \nabla (\nabla \cdot \mathbf{u}) + z_a \nabla (\nabla \cdot h\mathbf{u}) + \mathbf{u} \right]_P^{(i)} = \mathbf{P}_P^{(i)}, \quad i = 1, 2, n+1.$$

Important to (a) keep the unknown information needed at the minimum possible level and (b) exploit already computed geometrical information.

$$H_P \left[\frac{(z_a^2)_P}{2} \frac{1}{|C_P|} \sum_{Q \in K_P} (\nabla \cdot \mathbf{u})_M \mathbf{n}_{PQ} + \frac{(z_a)_P}{|C_P|} \sum_{Q \in K_P} (\nabla \cdot h\mathbf{u})_M \mathbf{n}_{PQ} + \mathbf{u}_P \right] = \mathbf{P}_P$$

$$\frac{(z_a^2)_P}{2|C_P|} \sum_{Q \in K_P} \mathbf{A}_Q \mathbf{u}_Q + \mathbf{A}_P \mathbf{u}_P + \frac{(z_a)_P}{|C_P|} \sum_{Q \in K_P} \mathbf{B}_Q \mathbf{u}_Q + \mathbf{B}_P \mathbf{u}_P + \mathbf{I} \mathbf{u}_P = \frac{1}{H_P} \mathbf{P}_P, \; P = 1 \ldots N$$

Solution of the linear system:

* The matrix $\mathbf{M}$ is **sparse and structurally symmetric** but is also mesh dependent.

Solution of the linear system:

* The matrix $\mathbf{M}$ is **sparse and structurally symmetric** but is also mesh dependent.
* Matrix $\mathbf{M}$ is stored in the **compressed sparse row (CSR)** format

Solution of the linear system:

* The matrix $\mathbf{M}$ is **sparse and structurally symmetric** but is also mesh dependent.

* Matrix $\mathbf{M}$ is stored in the **compressed sparse row (CSR)** format

* The **ILUT preconditioner** from SPARSKIT package is used

Solution of the linear system:

* The matrix M is **sparse and structurally symmetric** but is also mesh dependent.
* Matrix M is stored in the **compressed sparse row (CSR)** format
* The **ILUT preconditioner** from SPARSKIT package is used
* The **reverse Cuthill–McKee (RCM)** algorithm is also employed to reorder the matrix elements as to minimize the matrix bandwidth.

Solution of the linear system:

* The matrix M is **sparse and structurally symmetric** but is also mesh dependent.
* Matrix M is stored in the **compressed sparse row (CSR)** format
* The **ILUT preconditioner** from SPARSKIT package is used
* The **reverse Cuthill–McKee (RCM)** algorithm is also employed to reorder the matrix elements as to minimize the matrix bandwidth.
* System is solved using **Bi-Conjugate Gradient Stabilized** method (BiCGStab), with tolerance $5 \cdot 10^{-6}$

Solution of the linear system:

* The matrix M is **sparse and structurally symmetric** but is also mesh dependent.
* Matrix M is stored in the **compressed sparse row (CSR)** format
* The **ILUT preconditioner** from SPARSKIT package is used
* The **reverse Cuthill–McKee (RCM)** algorithm is also employed to reorder the matrix elements as to minimize the matrix bandwidth.
* System is solved using **Bi-Conjugate Gradient Stabilized** method (BiCGStab), with tolerance $5 \cdot 10^{-6}$
* Convergence to the solution was obtained in one or two steps with the numerical solution for the velocities at the previous time step given as initial guess.

Wave breaking models

- Two wave breaking models are implemented and tested

1. **Eddy viscosity** approach (Keneddy et al., 2000)

$$
\begin{aligned}
(\mathbf{R_b})_P &= \frac{1}{|C_P|}\iint_{C_P} \mathbf{R_b} d\Omega = \frac{1}{|C_P|}\iint_{C_P} \left[\begin{array}{c} \nabla \cdot \tilde{\mathbf{R}}_{b_y} \\ \nabla \cdot \tilde{\mathbf{R}}_{b_x} \end{array} \right] d\Omega \\
&= \frac{1}{|C_P|}\int_{\partial C_{PQ}} \left[\begin{array}{c} \tilde{\mathbf{R}}_{b_x} \cdot \widetilde{\mathbf{n}} \\ \tilde{\mathbf{R}}_{b_y} \cdot \widetilde{\mathbf{n}} \end{array} \right] dl \approx \frac{1}{|C_P|} \left[\begin{array}{c} \tilde{\mathbf{R}}_{b_x} \cdot \mathbf{n}_{PQ} \\ \tilde{\mathbf{R}}_{b_y} \cdot \mathbf{n}_{PQ} \end{array} \right]_M
\end{aligned}
$$

$$
\begin{aligned}
R_{b_x} &= \nabla \cdot \tilde{\mathbf{R}}_{b_x}, \quad \text{where } \tilde{\mathbf{R}}_{b_x} = \left[\nu (Hu)_x \quad \frac{\nu}{2}((Hu)_y + (Hv)_x) \right]^{\mathrm{T}} \\
R_{b_y} &= \nabla \cdot \tilde{\mathbf{R}}_{b_y}, \quad \text{where } \tilde{\mathbf{R}}_{b_y} = \left[\frac{\nu}{2}((Hu)_y + (Hv)_x) \quad \nu (Hv)_y \right]^{\mathrm{T}}
\end{aligned}
$$

where $\nu = B\delta_b^2 H \eta_t$ is the eddy viscosity coefficient with $0 < B < 1$ and δ_b is a mixing length coefficient.

Wave breaking models (cont.)

Wave breaking models (cont.)

2. **Hybrid model**

   Idea: switching off the dispersive terms.

   Boussinesq degenerate into NSWE as dispersive terms become negligible (Tonelli and Petti, 2009 & 2010 for the MS equations).

   * Criterion: If $\epsilon = \frac{A}{h} \leq 0.8$, Boussinesq equations are solved otherwise NSWE are solved.

   Value of ϵ is computed and checked in each computational cell at every time step.

Wave breaking models (cont.)

2. **Hybrid model**
   Idea: switching off the dispersive terms.
   Boussinesq degenerate into NSWE as dispersive terms become negligible (Tonelli and Petti, 2009 & 2010 for the MS equations).

   * Criterion: If $\epsilon = \frac{A}{h} \leq 0.8$, Boussinesq equations are solved otherwise NSWE are solved.
   Value of ϵ is computed and checked in each computational cell at every time step.

   * Make the scheme more stable: In post breaking region $\epsilon < 0.4$ in order to switch from NSWE to Boussinesq (Tonelli and Petti, 2012).

Wave breaking models (cont.)

2. **Hybrid model**

   Idea: switching off the dispersive terms.
   Boussinesq degenerate into NSWE as dispersive terms become negligible (Tonelli and Petti, 2009 & 2010 for the MS equations).

   * Criterion: If $\epsilon = \frac{A}{h} \leq 0.8$, Boussinesq equations are solved otherwise NSWE are solved.
   Value of ϵ is computed and checked in each computational cell at every time step.

   * Make the scheme more stable: In post breaking region $\epsilon < 0.4$ in order to switch from NSWE to Boussinesq (Tonelli and Petti, 2012).

   * Need of a ”clever” implementation.

Boundary conditions and internal source function:

- **Wall (reflective) boundary condition**: $\mathbf{u} \cdot \widetilde{\mathbf{n}} = 0 \;\; \text{for} \;\; \mathbf{x} \in \partial\Omega$
  By conservation of mass (no loss or gain through the wall)

$$\frac{\partial}{\partial t} \iint_{\Omega} H \, d\Omega + \int_{\partial\Omega} \left[H\mathbf{u} + \left(\frac{z_a^2}{2} - \frac{h^2}{6} \right) h\nabla(\nabla \cdot \mathbf{u}) + \left(z_a + \frac{h}{2} \right) h\nabla(\nabla \cdot h\mathbf{u}) \right] \cdot \widetilde{\mathbf{n}} dl = 0$$

Define the normal boundary advective flux in weak form, $\mathbf{\Phi}_{P,\Gamma} = \begin{bmatrix} 0 \\ \frac{1}{2} g (H^\star)^2 n_{P,1x} \\ \frac{1}{2} g (H^\star)^2 n_{P,1y} \end{bmatrix}$
by the **method of characteristics**

Boundary conditions and internal source function:

- **Wall (reflective) boundary condition**: $\mathbf{u}\cdot\widetilde{\mathbf{n}} = 0$ for $\mathbf{x}\in\partial\Omega$
  By conservation of mass (no loss or gain through the wall)

$$\frac{\partial}{\partial t}\iint_{\Omega} H\,d\Omega + \int_{\partial\Omega}\left[H\mathbf{u} + \left(\frac{z_a^2}{2} - \frac{h^2}{6}\right)h\nabla(\nabla\cdot\mathbf{u}) + \left(z_a + \frac{h}{2}\right)h\nabla(\nabla\cdot h\mathbf{u})\right]\cdot\widetilde{\mathbf{n}}\,dl = 0$$

Define the normal boundary advective flux in weak form, $\mathbf{\Phi}_{P,\Gamma} = \begin{bmatrix} 0 \\ \frac{1}{2}g(H^\star)^2 n_{P,1x} \\ \frac{1}{2}g(H^\star)^2 n_{P,1y} \end{bmatrix}$
by the **method of characteristics**

- **Absorbing boundaries:** should dissipate the energy of incoming waves

Sponge layer is defined: $m(\mathbf{x}) = \sqrt{1 - \left(\frac{\mathbf{x} - d(\mathbf{x})}{L_s}\right)^2}$, $L \le L_s \le 1.5L$,

Boundary conditions and internal source function:

- **Wall (reflective) boundary condition**: $\mathbf{u} \cdot \widetilde{\mathbf{n}} = 0$ for $\mathbf{x} \in \partial\Omega$

  By conservation of mass (no loss or gain through the wall)

$$\frac{\partial}{\partial t}\iint_{\Omega} H\, d\Omega + \int_{\partial\Omega}\left[H\mathbf{u} + \left(\frac{z_a^2}{2} - \frac{h^2}{6}\right) h\nabla(\nabla\cdot\mathbf{u}) + \left(z_a + \frac{h}{2}\right) h\nabla(\nabla\cdot h\mathbf{u})\right]\cdot\widetilde{\mathbf{n}}\, dl = 0$$

  Define the normal boundary advective flux in weak form, $\mathbf{\Phi}_{P,\Gamma} = \begin{bmatrix} 0 \\ \frac{1}{2}g(H^\star)^2 n_{P,1x} \\ \frac{1}{2}g(H^\star)^2 n_{P,1y} \end{bmatrix}$
  by the **method of characteristics**

- **Absorbing boundaries:** should dissipate the energy of incoming waves

  Sponge layer is defined: $m(\mathbf{x}) = \sqrt{1 - \left(\frac{\mathbf{x} - d(\mathbf{x})}{L_s}\right)^2}$, $L \le L_s \le 1.5L$,

- **Internal source function** for regular waves (Wei et al., 1993) added to the mass equation

$$S(\mathbf{x}, t) = D^* \exp\left(\gamma(x - x_s)^2\right)\sin(\lambda y - \omega t)$$

I. 2D run-up of a solitary wave on a conical island (Briggs et al. 1995)

Area: $(x, y) = [-5, 28m] \times [0, 30m]$, $A/h = 0.18$, $N = 52,191$, $CFL = 0.8$

Using mesh $h-$ enrichment

I. 2D run-up of a solitary wave on a conical island (Briggs et al. 1995)

Area: $(x, y) = [-5, 28m] \times [0, 30m]$, $A/h = 0.18$, $N = 52,191$, $CFL = 0.8$

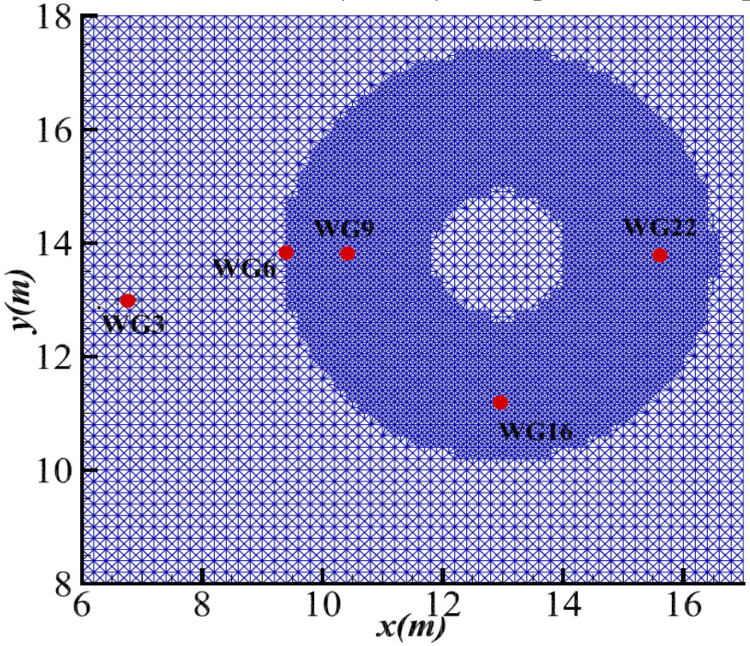

Using mesh $h-$ enrichment

I. 2D run-up of a solitary wave on a conical island (Briggs et al. 1995)

Area: $(x, y) = [-5, 28m] \times [0, 30m], \ A/h = 0.18, \ N = 52,191 \ , CFL = 0.8$

Using mesh $h-$ enrichment

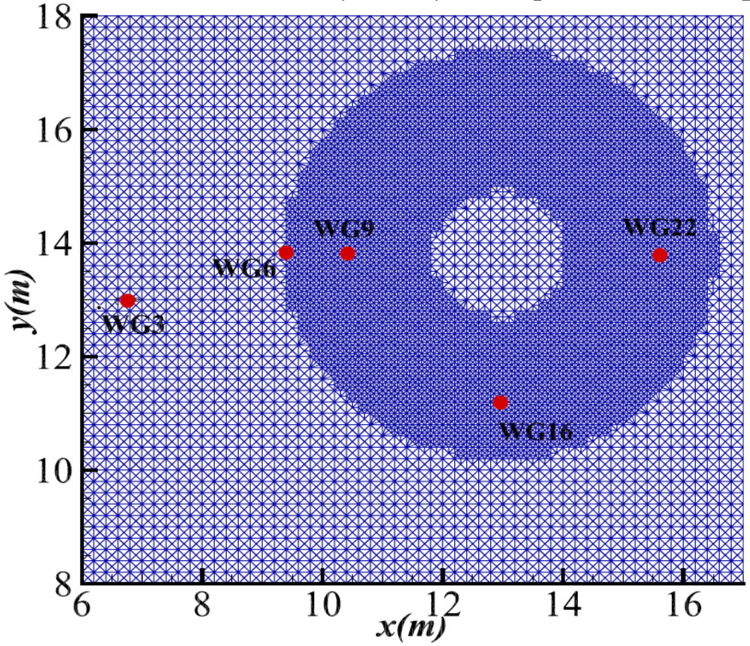

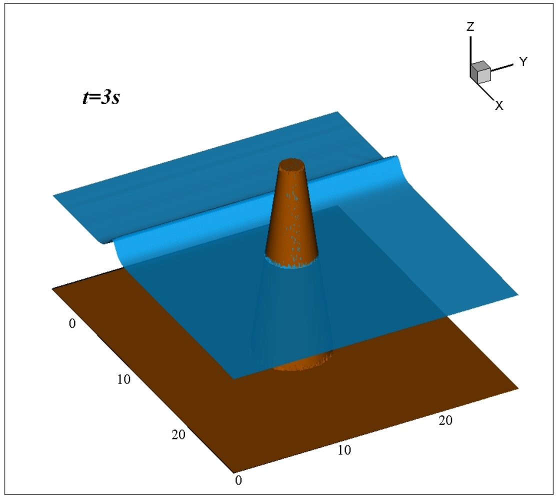

I. 2D run-up of a solitary wave on a conical island (Briggs et al. 1995)

Area: $(x,y) = [-5, 28m] \times [0, 30m]$, $A/h = 0.18$, $N = 52,191$, $CFL = 0.8$

Using mesh $h-$ enrichment

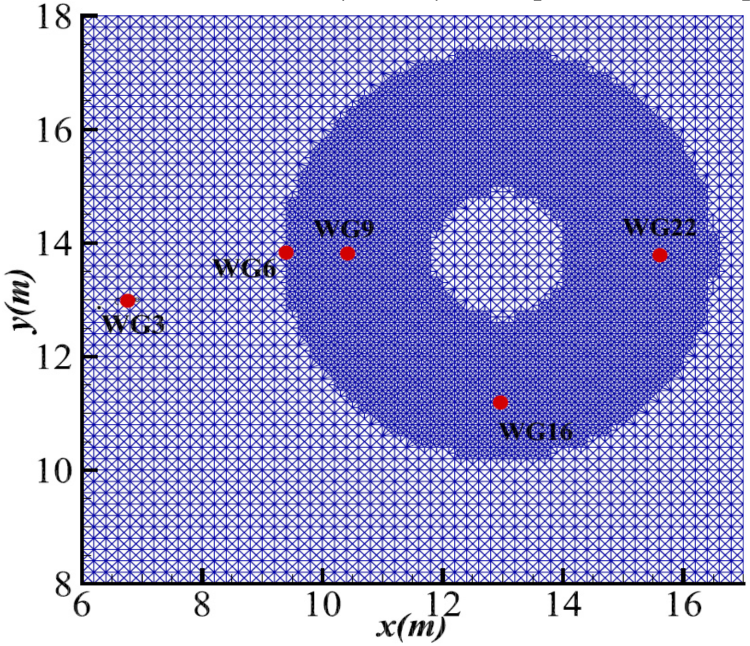

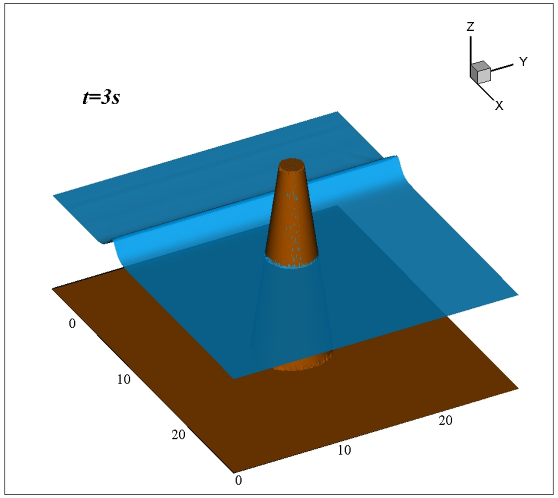

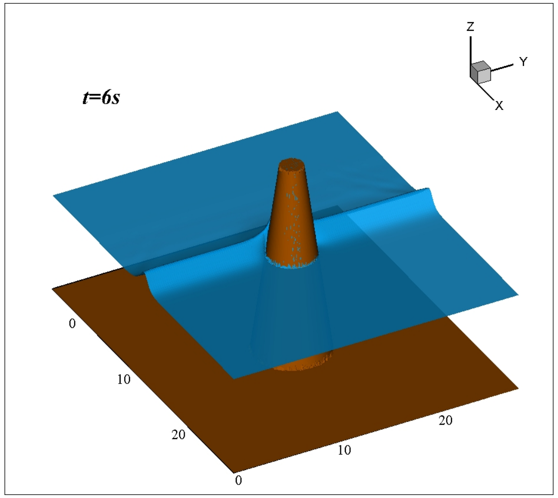

I. 2D run-up of a solitary wave on a conical island (Briggs et al. 1995)

Area: $(x, y) = [-5, 28m] \times [0, 30m]$, $A/h = 0.18$, $N = 52,191$, $CFL = 0.8$

Using mesh $h-$ enrichment

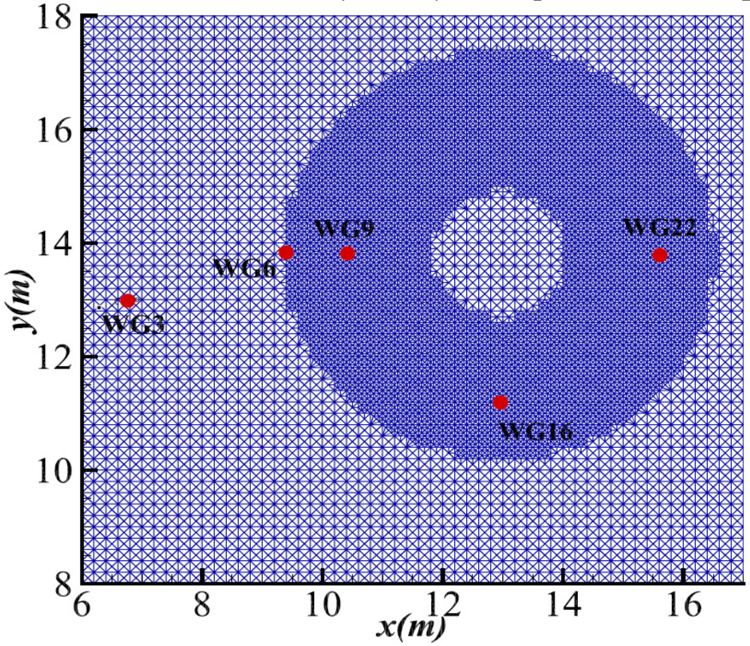

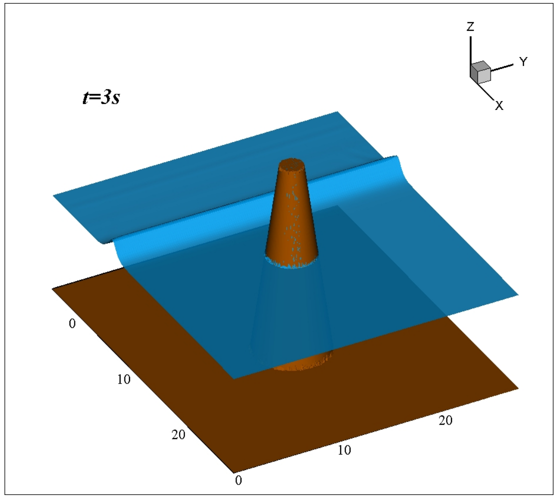

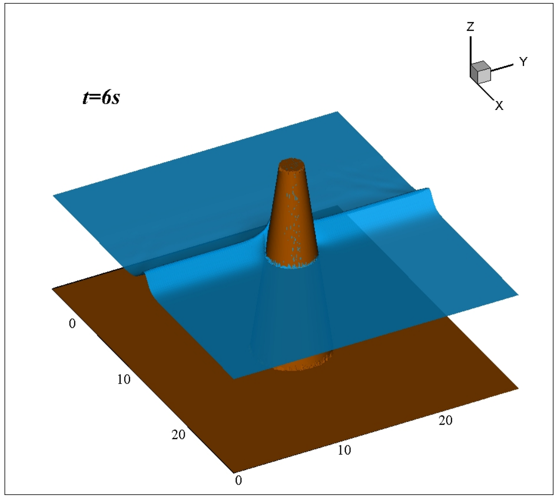

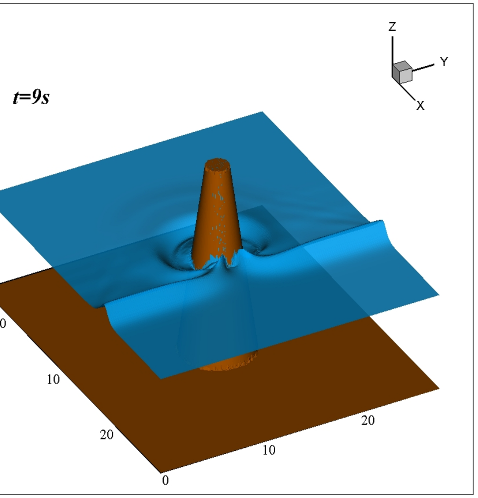

I. 2D run-up of a solitary wave on a conical island (Briggs et al. 1995)

Area: $(x, y) = [-5, 28m] \times [0, 30m]$, $A/h = 0.18$, $N = 52,191$, $CFL = 0.8$

Using mesh $h-$ enrichment

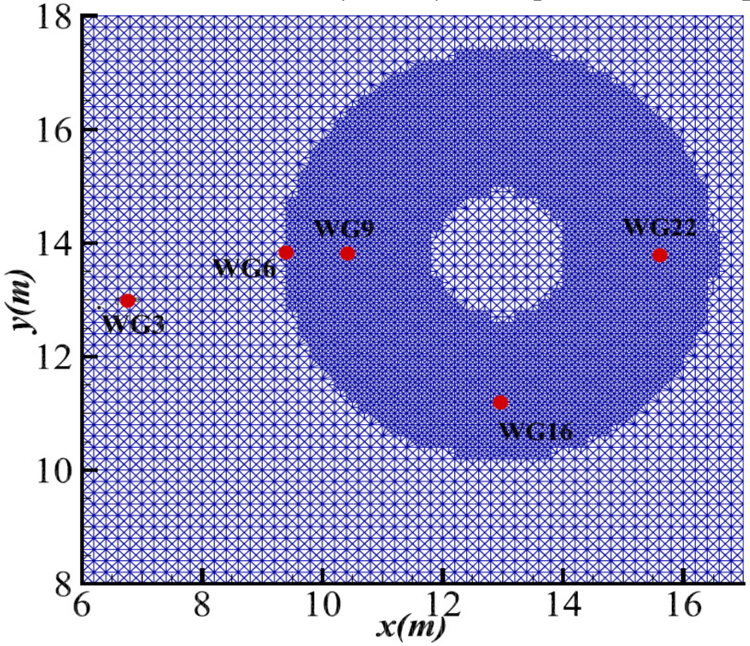

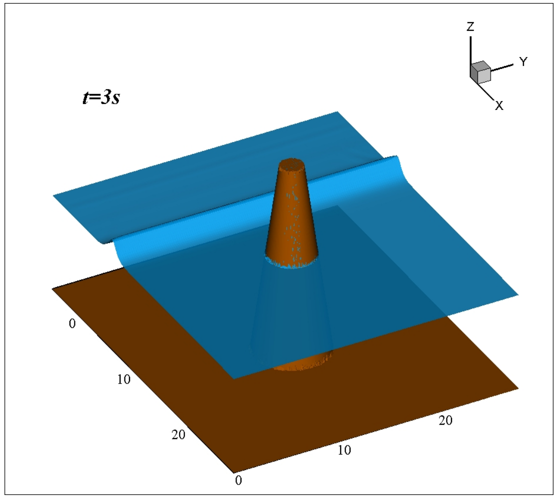

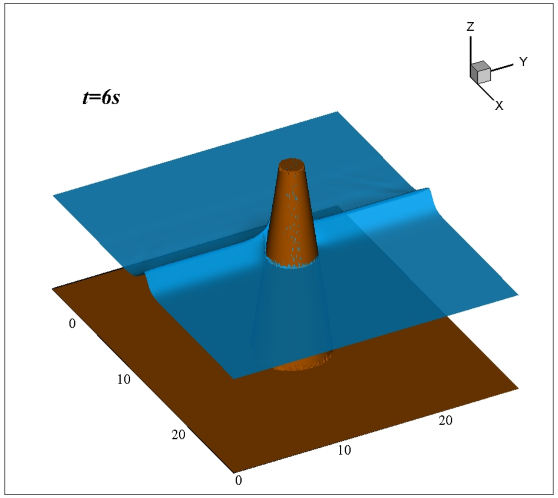

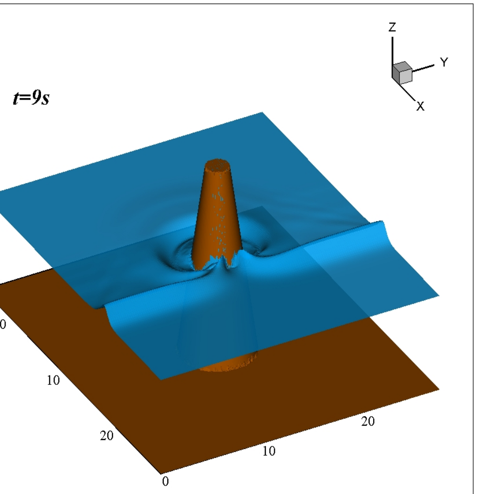

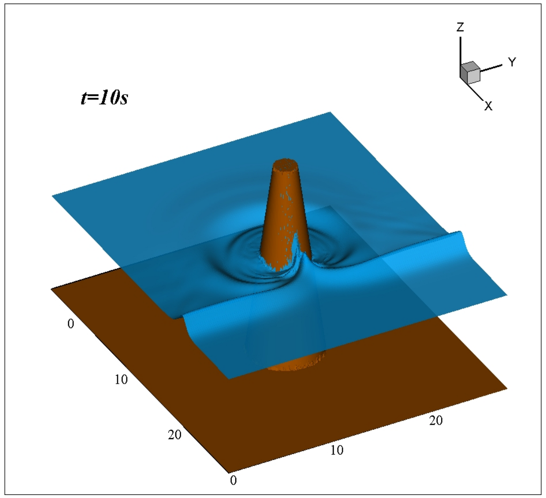

I. 2D run-up of a solitary wave on a conical island (Briggs et al. 1995)

Area: $(x, y) = [-5, 28m] \times [0, 30m]$, $A/h = 0.18$, $N = 52,191$, $CFL = 0.8$

Using mesh $h-$ enrichment

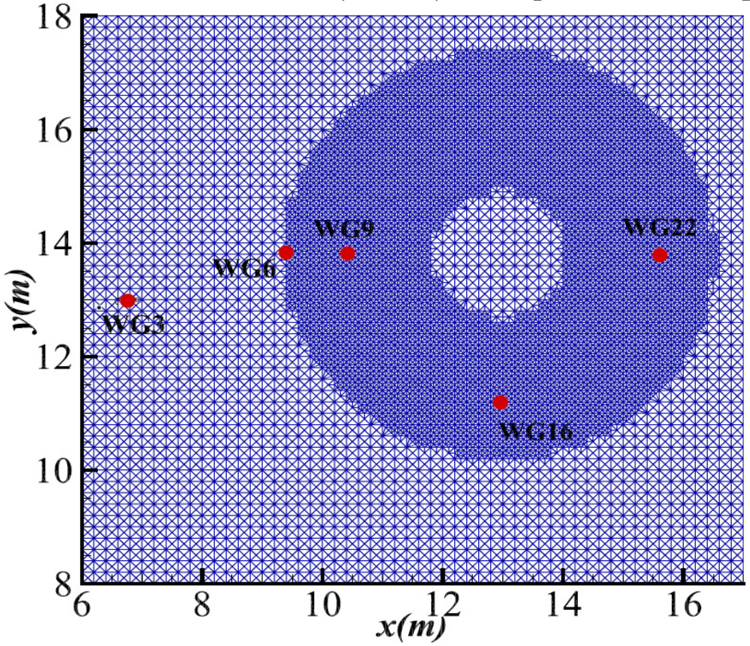

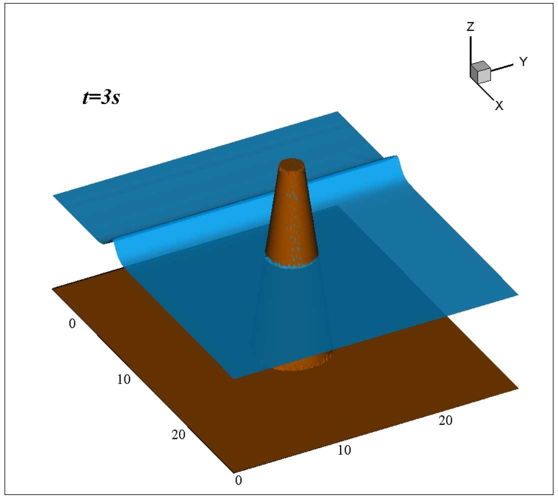

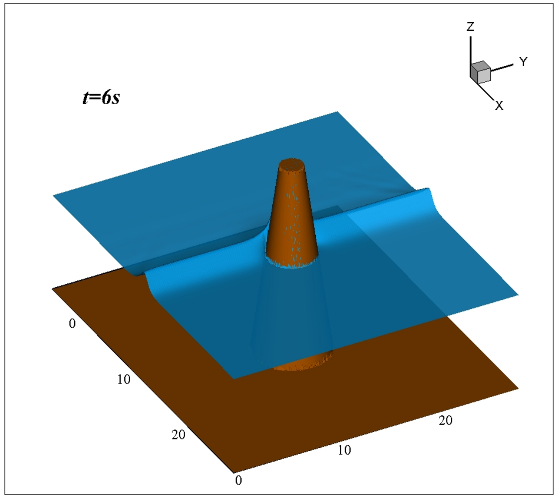

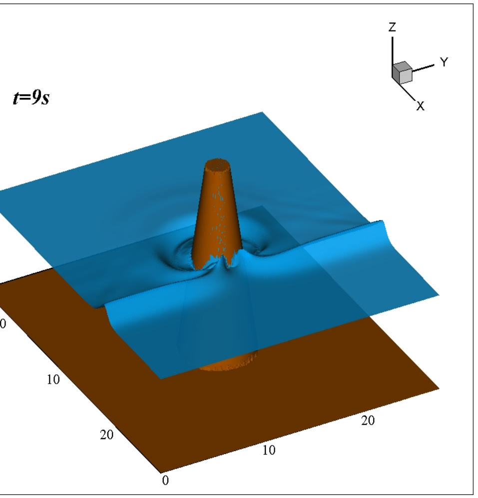

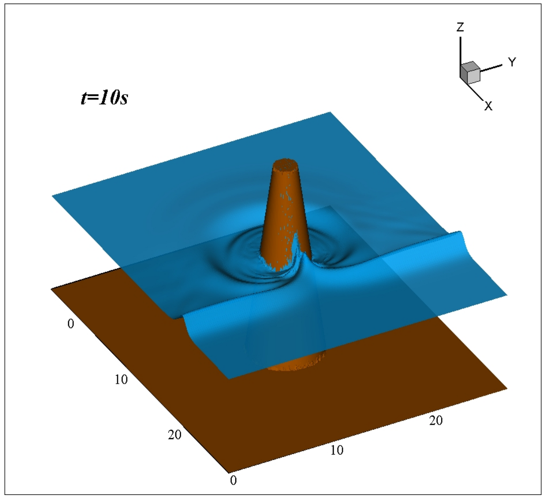

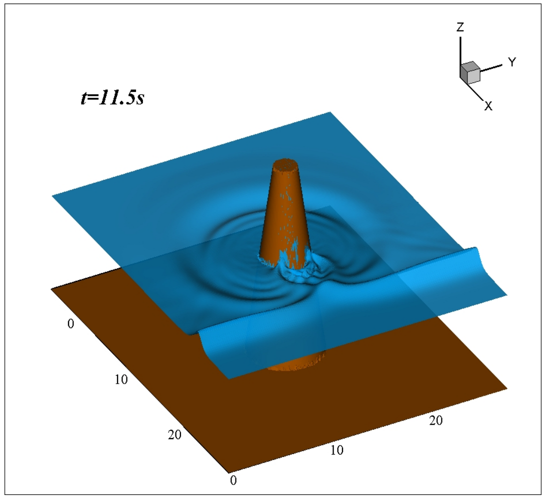

I. 2D run-up of a solitary wave on a conical island (Briggs et al. 1995)

Area: $(x, y) = [-5, 28m] \times [0, 30m]$, $A/h = 0.18$, $N = 52,191$, $CFL = 0.8$

Using mesh $h-$ enrichment

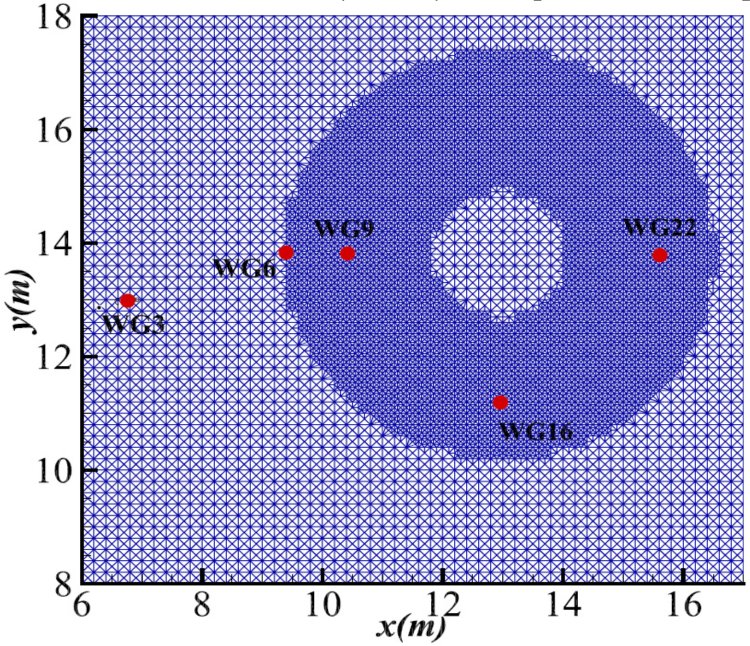

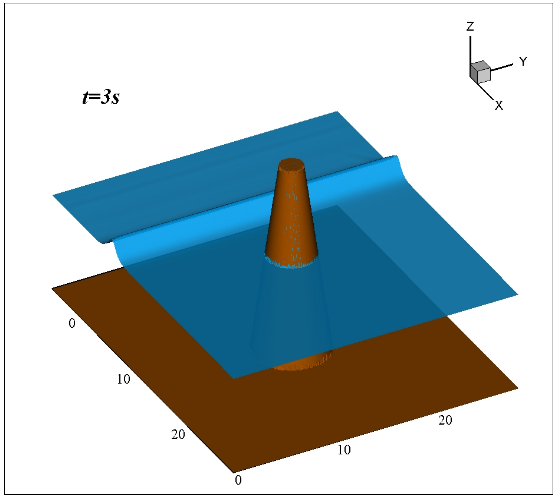

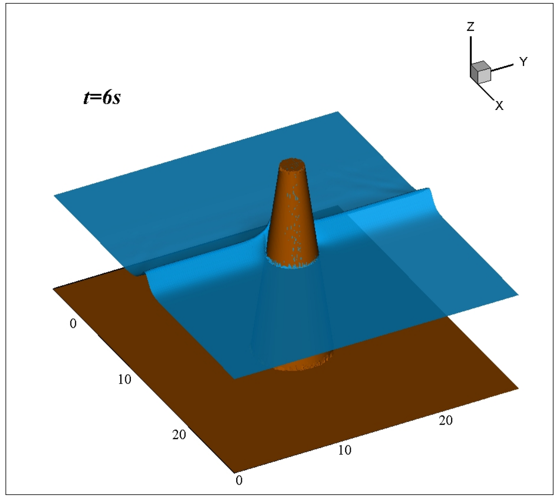

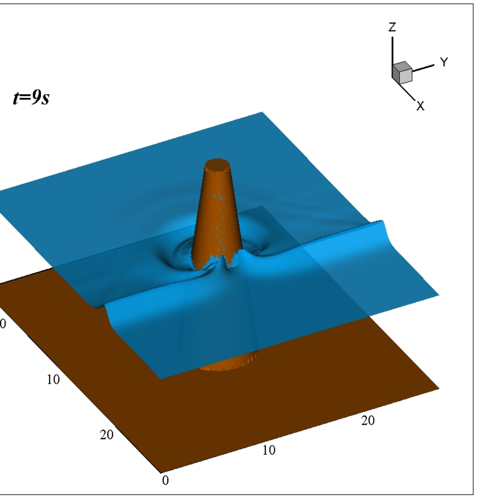

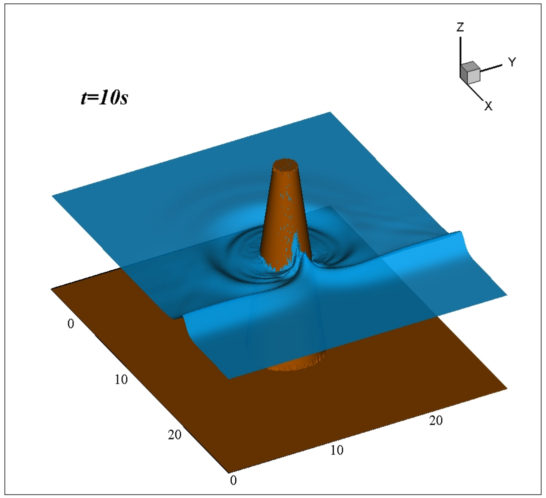

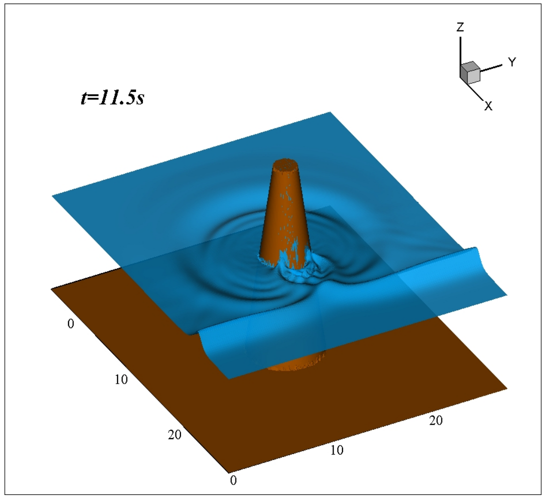

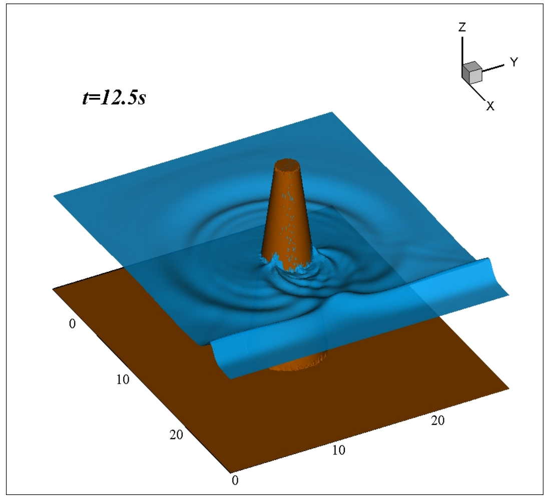

2D run-up of a solitary wave on a conical island (cont)

Time series of surface elevation at wave gauges around the island:

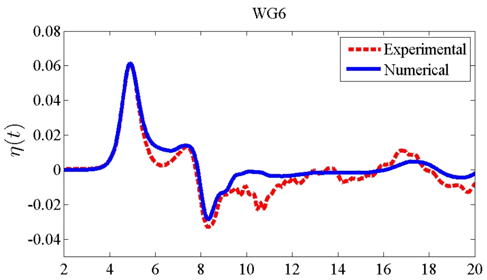

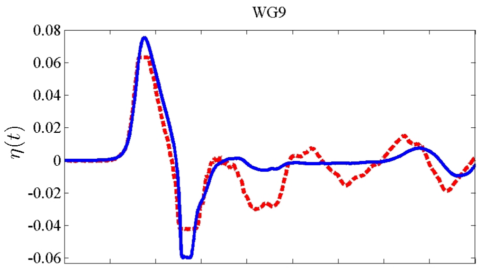

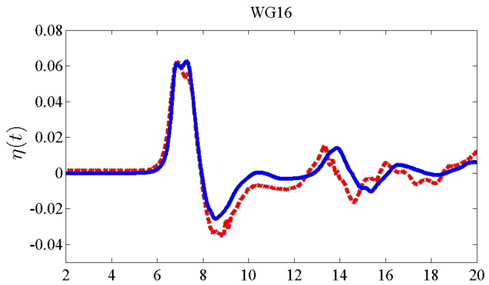

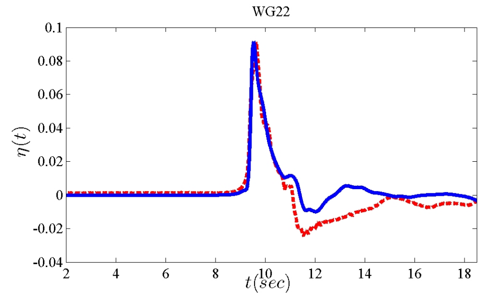

2D run-up of a solitary wave on a conical island (cont)

Time series of surface elevation at wave gauges around the island:

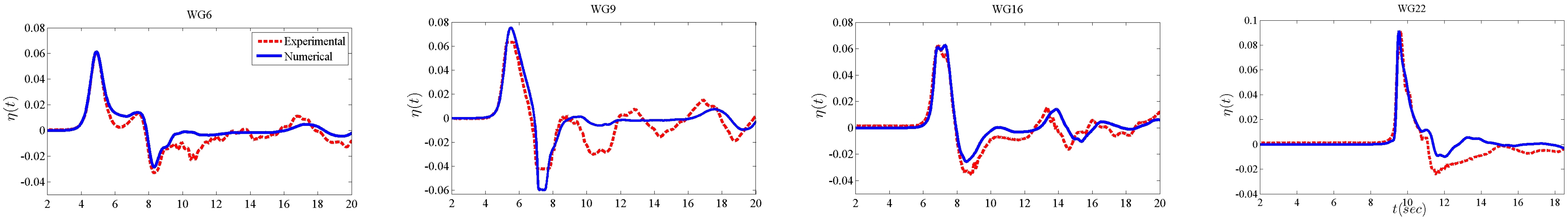

Experimental measurements and numerical runup around the conical island:

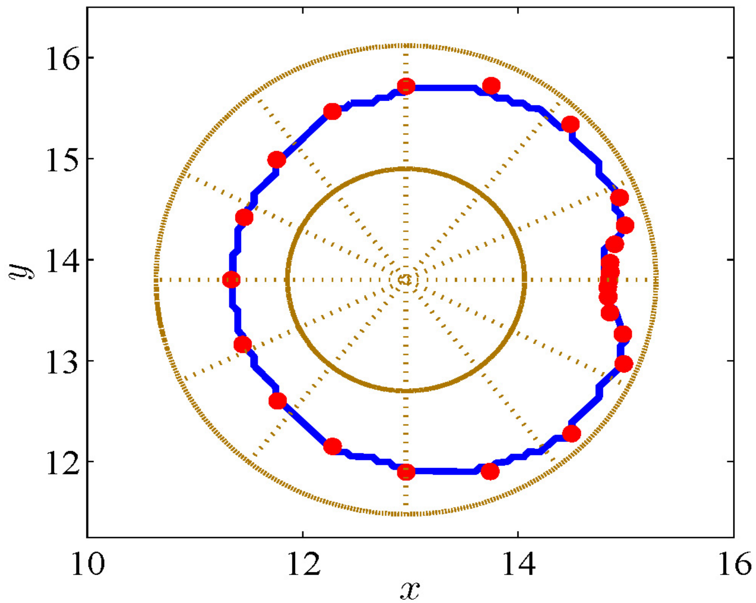

Simulation $\sim$ 28min on a single 2.4GHz Intel Core 2 Quad Q6600 processor

II. Wave propagation over a semicircular shoal (Whalin, 1971)

Case B: $T = 2.0s,\quad h/L = 0.117,\quad A/h = 0.0165,\quad kh = 0.735$ and $S = 1.198$

II. Wave propagation over a semicircular shoal (Whalin, 1971)

Case B: $T = 2.0s, \quad h/L = 0.117, \quad A/h = 0.0165, \quad kh = 0.735$ and $S = 1.198$

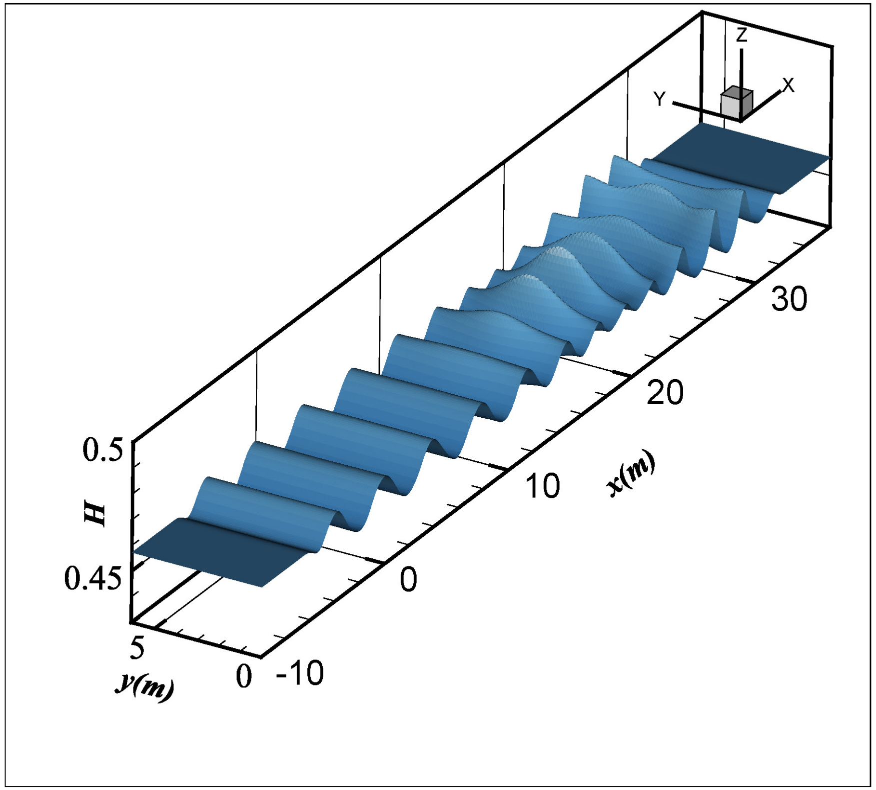

II. Wave propagation over a semicircular shoal (Whalin, 1971)

Case B: $T = 2.0s, \quad h/L = 0.117, \quad A/h = 0.0165, \quad kh = 0.735$ and $S = 1.198$

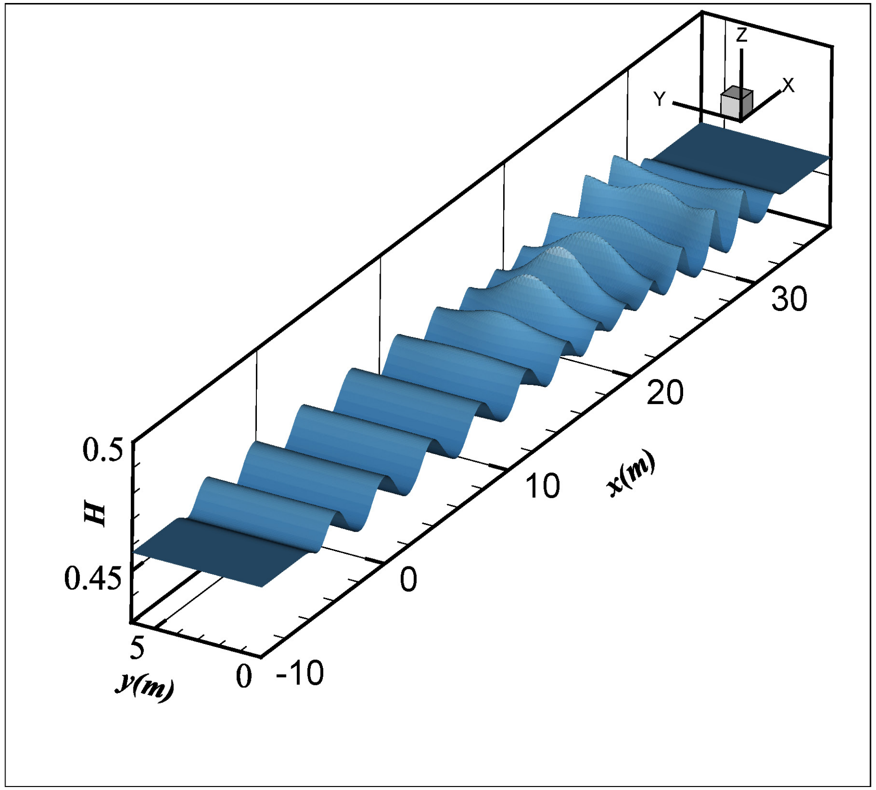

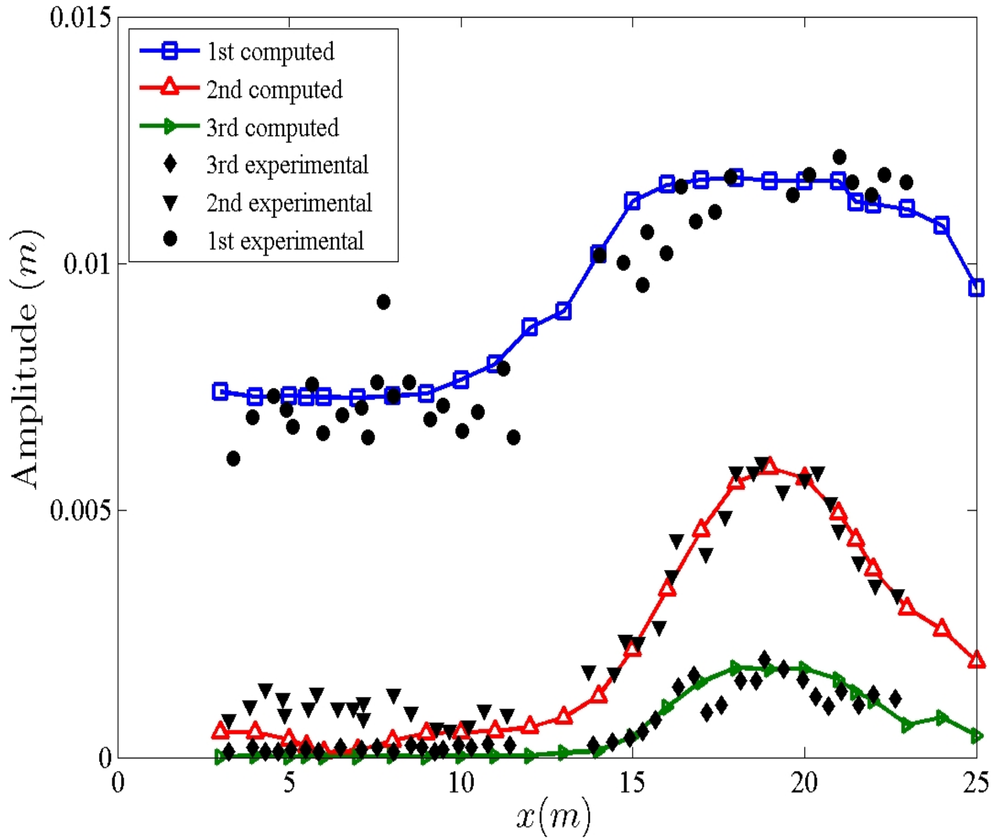

Free surface and spatial evolution of the 1st, 2nd and 3rd harmonic

III. Breaking on a sloping beach (Hansen and Svendsen, 1979)

Area: $(x, y) = [-26, 26m] \times [0, 1m]$, $N = 24,996$, $CFL = 0.4$

Case B (Spilling-plunging):

$T = 2.5s$, $H = 0.39m$, $S = 8.6032$

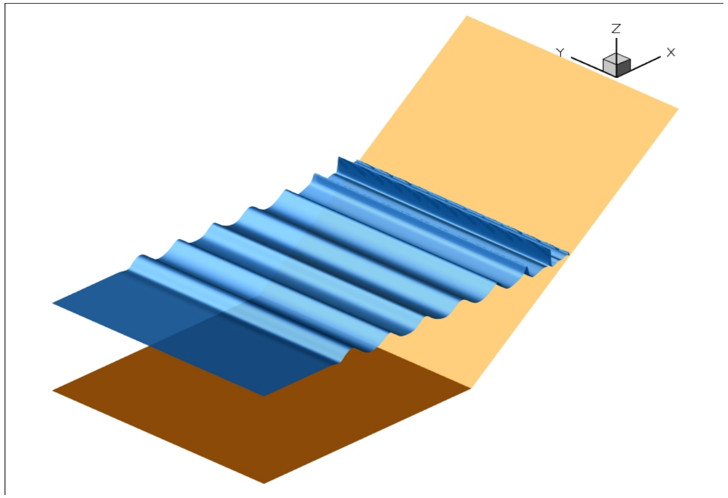

III. Breaking on a sloping beach (Hansen and Svendsen, 1979)

Area: $(x, y) = [-26, 26m] \times [0, 1m]$, $N = 24,996$, $CFL = 0.4$

Case B (Spilling-plunging):

$T = 2.5s$, $H = 0.39m$, $S = 8.6032$

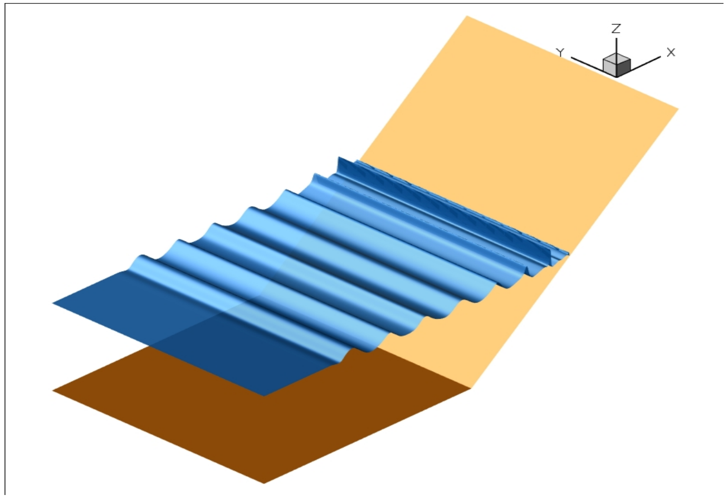

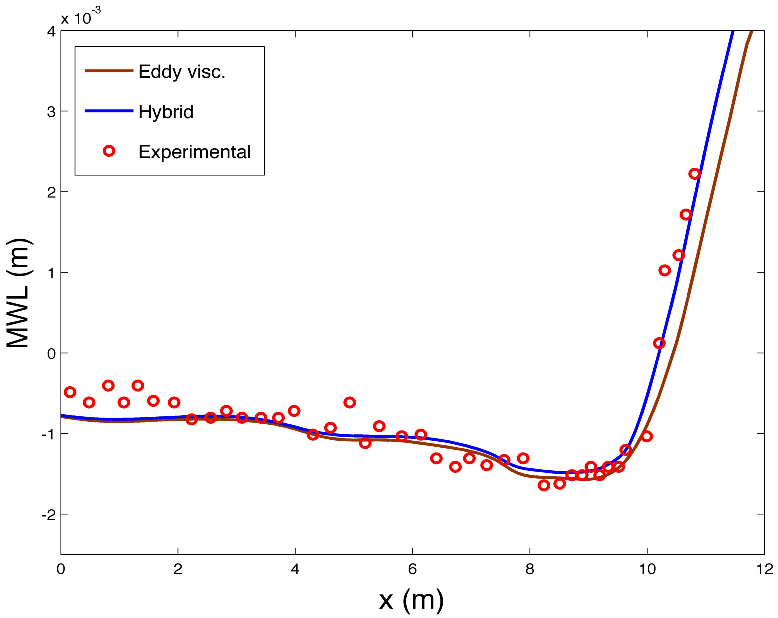

III. Breaking on a sloping beach (Hansen and Svendsen, 1979)

Area: $(x, y) = [-26, 26m] \times [0, 1m]$, $N = 24,996$, $CFL = 0.4$

Case B (Spilling-plunging):

$T = 2.5s$, $H = 0.39m$, $S = 8.6032$

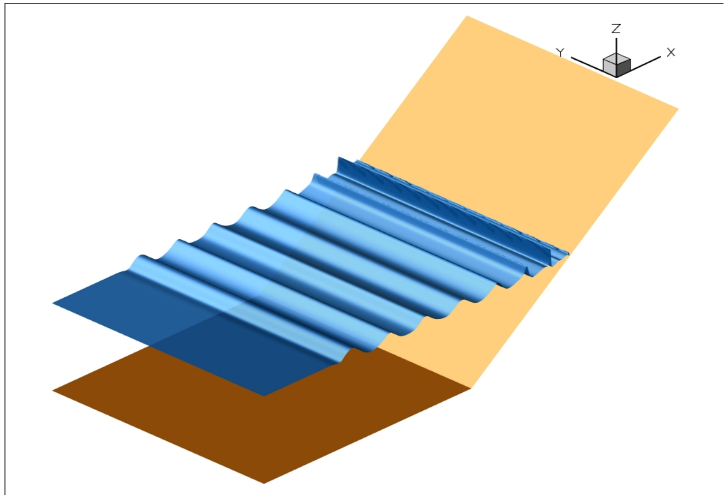

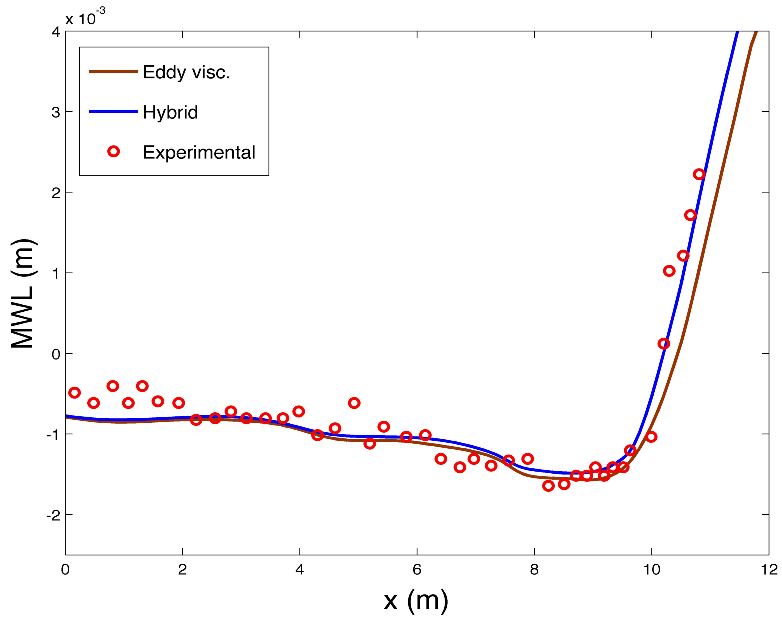

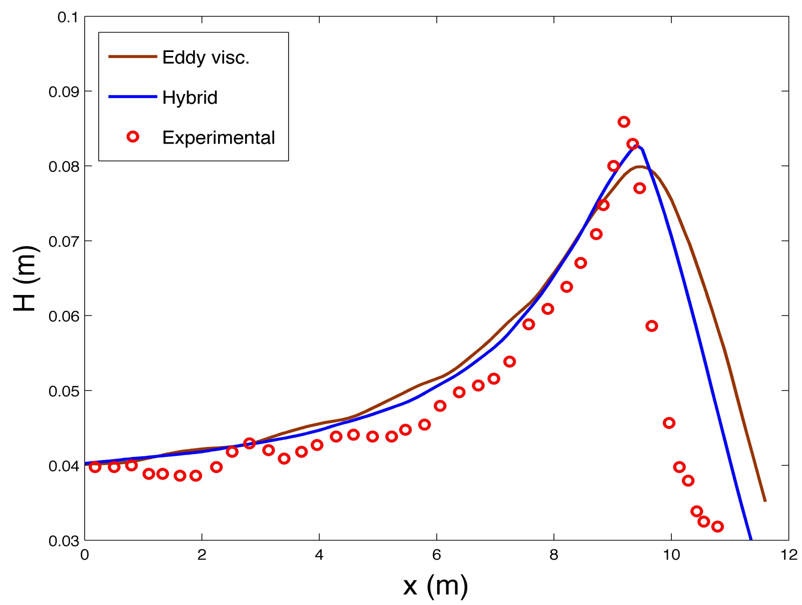

Breaking on a sloping beach

Case C (Spilling): $T = 2.0s$, $H = 0.36m$, $S = 4.8077$

Breaking on a sloping beach

Case C (Spilling): $T = 2.0s$, $H = 0.36m$, $S = 4.8077$

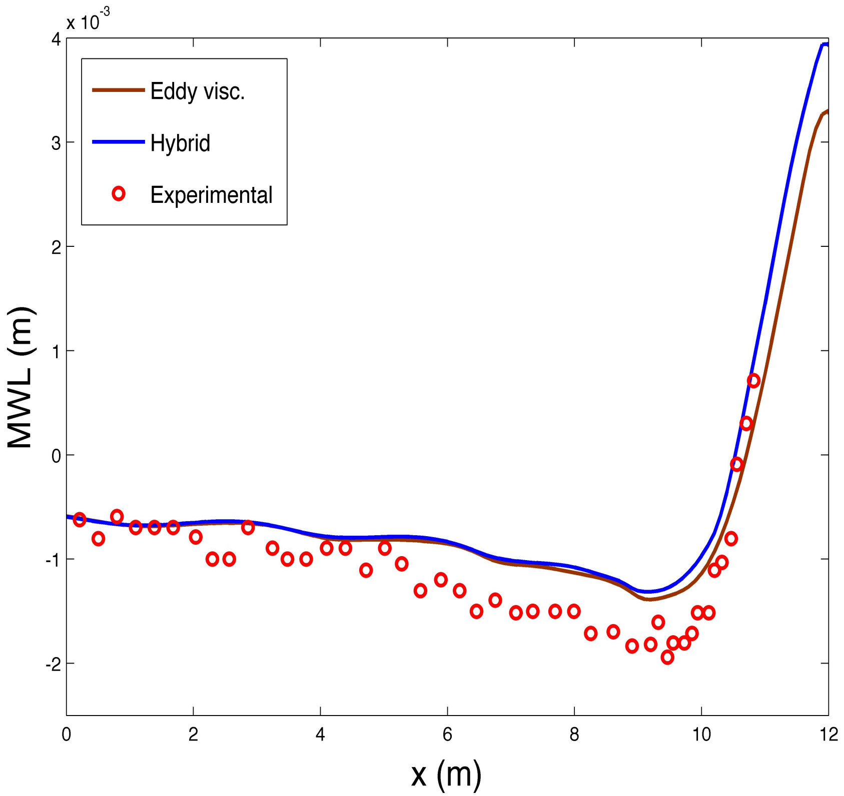

Breaking on a sloping beach

Case C (Spilling): $T = 2.0s$, $H = 0.36m$, $S = 4.8077$

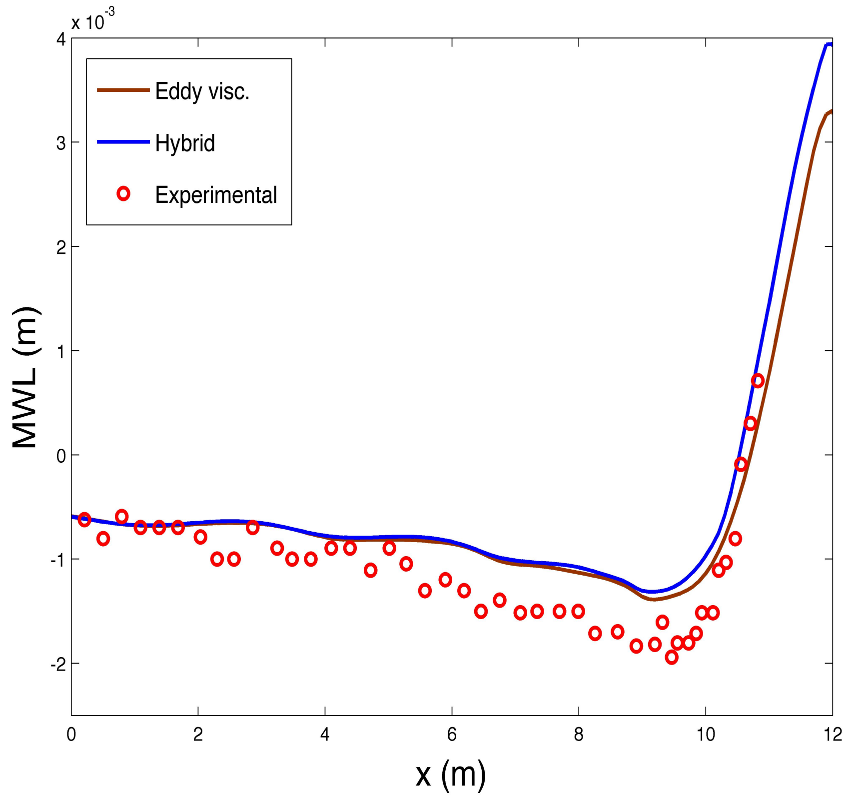

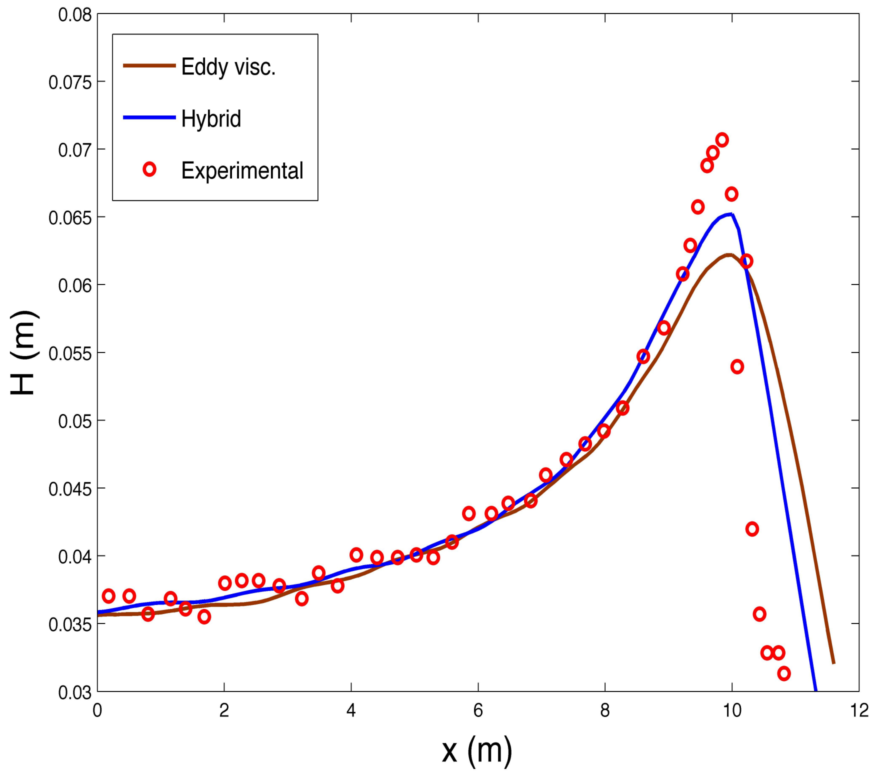

IV. Wave over a bar (Beji and Battjes, 1993)

$(x, y) = [-10, 30m] \times [0, 0.8m],\ H = 0.02m,\ T = 2.02s,\ N = 40,364\ ,\ CFL = 0.4$

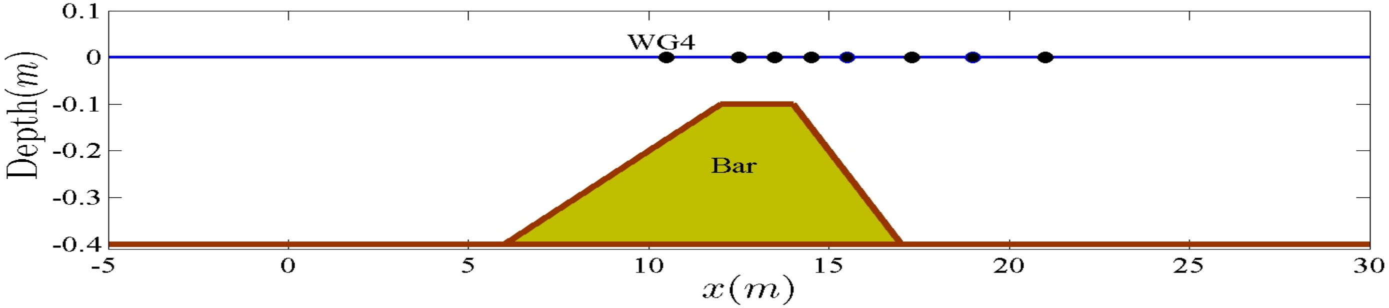

IV. Wave over a bar (Beji and Battjes, 1993)

$$(x, y) = [-10, 30m] \times [0, 0.8m],\ \ H = 0.02m,\ \ T = 2.02s,\ N = 40,364\ ,\ CFL = 0.4$$

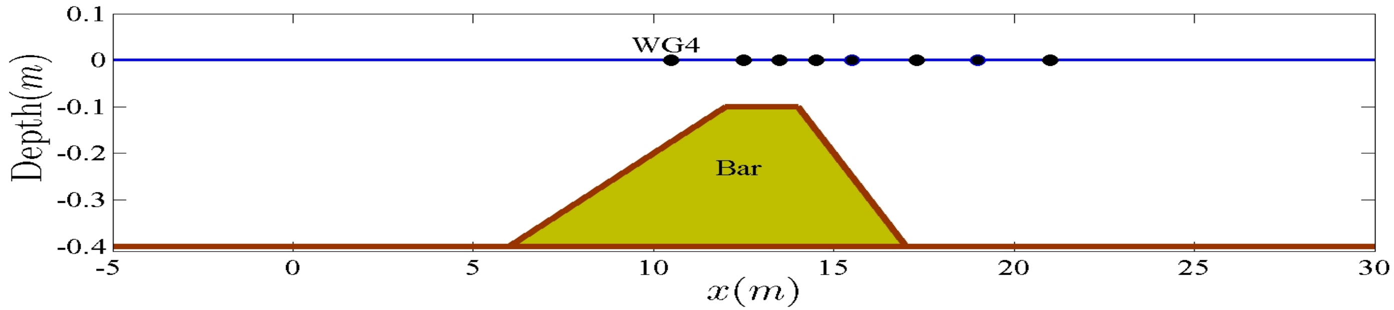

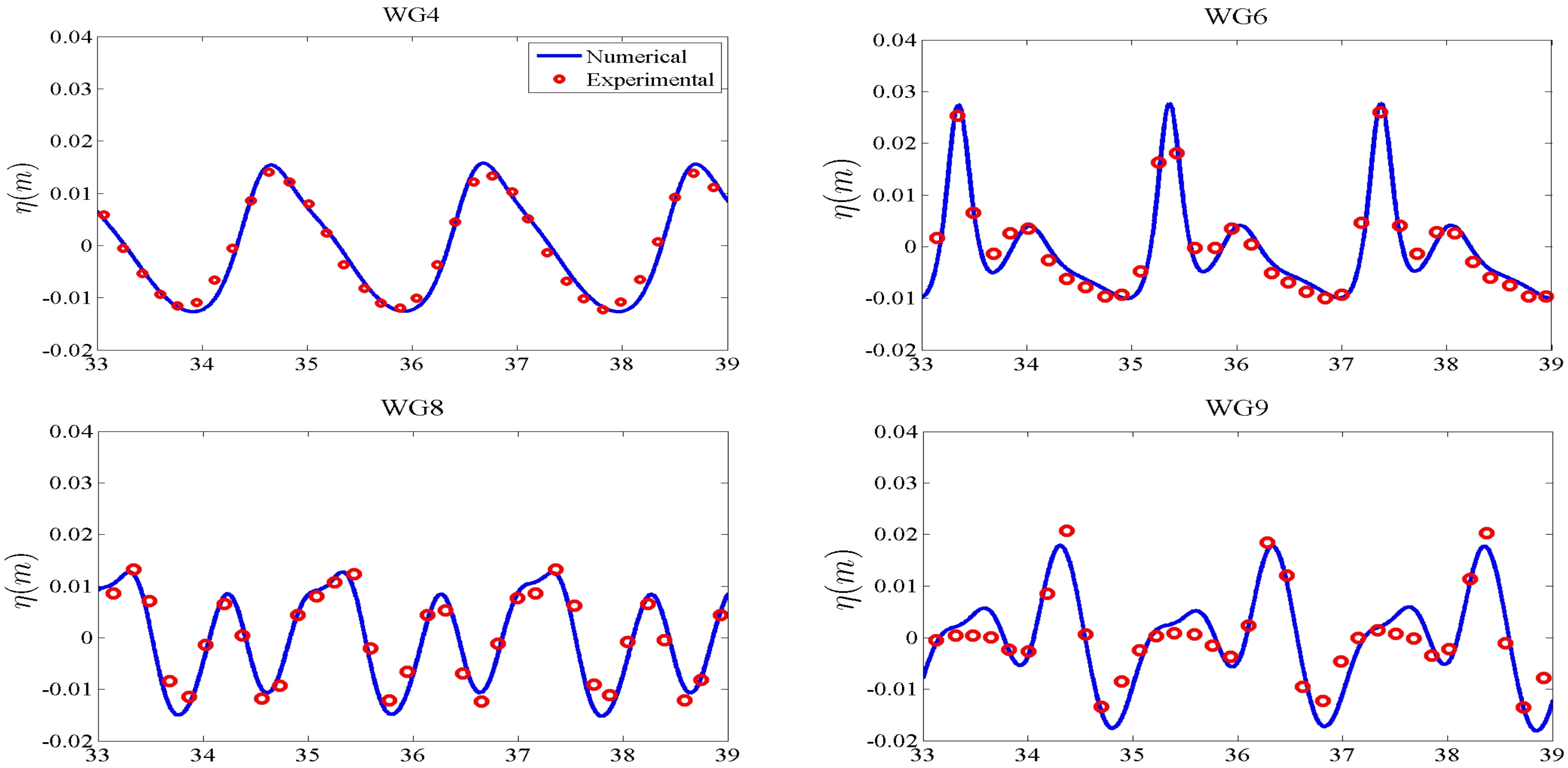

IV. Wave over a bar (breaking case)

$(x, y) = [-10, 30m] \times [0, 0.8m],\ H = 0.029m,\ T = 2.525s,\ N = 40,364\ , CFL = 0.4$

IV. Wave over a bar (breaking case)

$$(x, y) = [-10, 30m] \times [0, 0.8m],\ \ H = 0.029m,\ \ T = 2.525s,\ N = 40,364\ ,\ CFL = 0.4$$

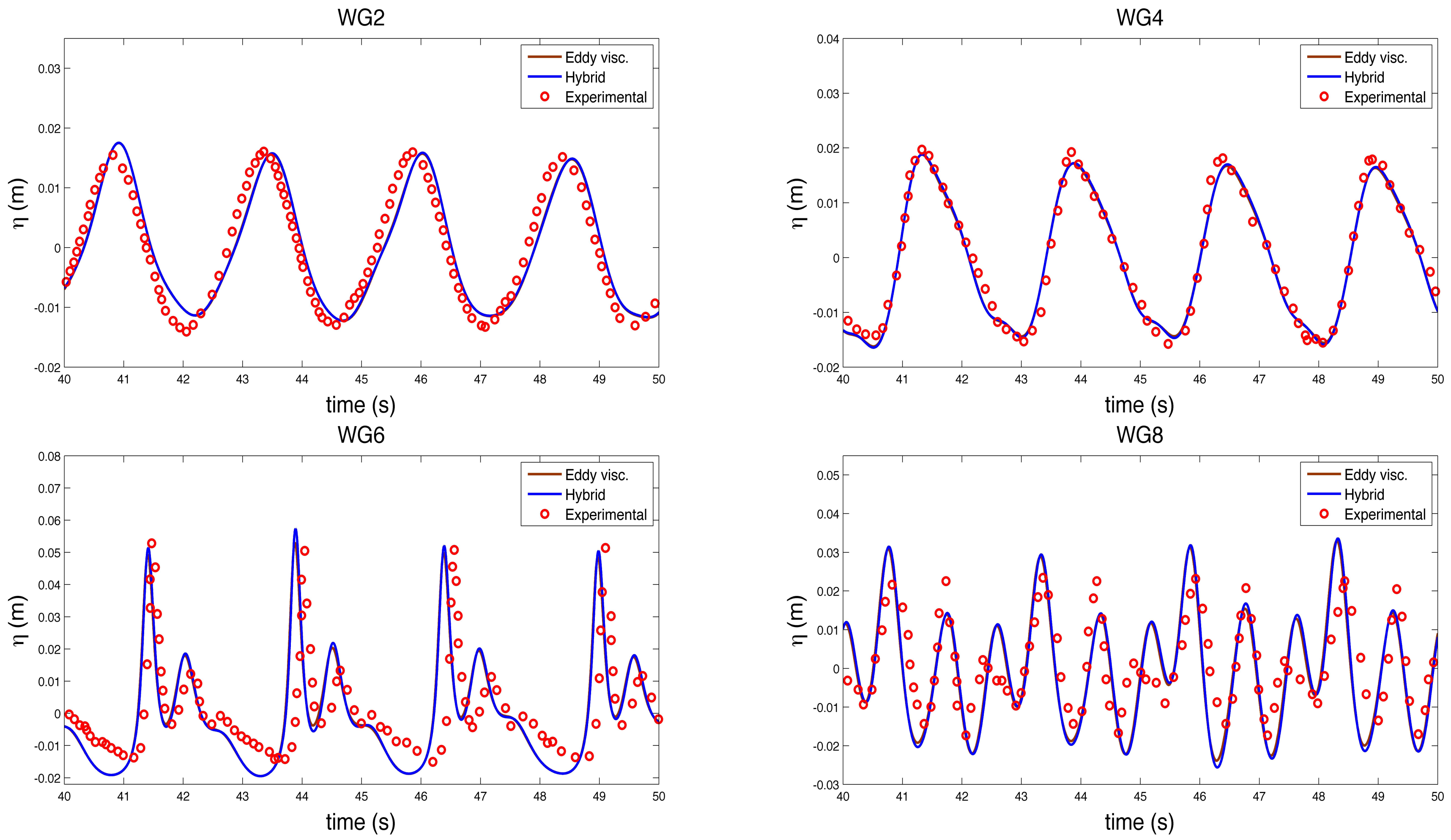

V. Two-dimensional reef (Roeber et al, 2010)

Area: $(x, y) = [0, 83m] \times [0, 1m]$, $A/h = 0.3$, $N = 10,900$, $CFL = 0.4$, $n_m = 0.014$

—Hybrid and — Eddy viscosity

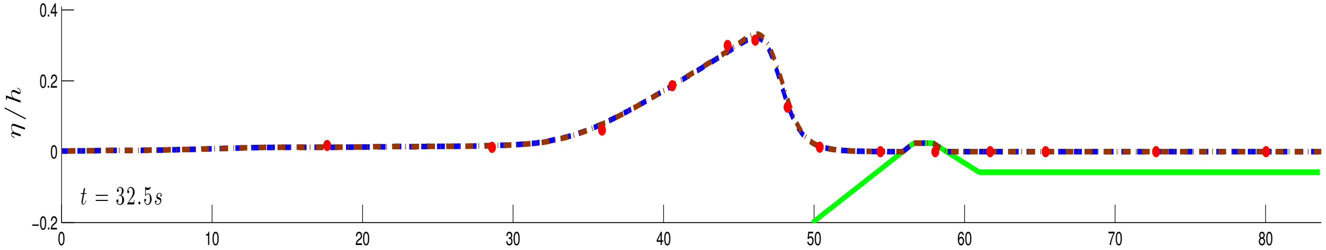

Shoaling, before breaking

V. Two-dimensional reef (Roeber et al, 2010)

Area: $(x, y) = [0, 83m] \times [0, 1m]$, $A/h = 0.3$, $N = 10,900$, $CFL = 0.4$, $n_m = 0.014$

—Hybrid and — Eddy viscosity

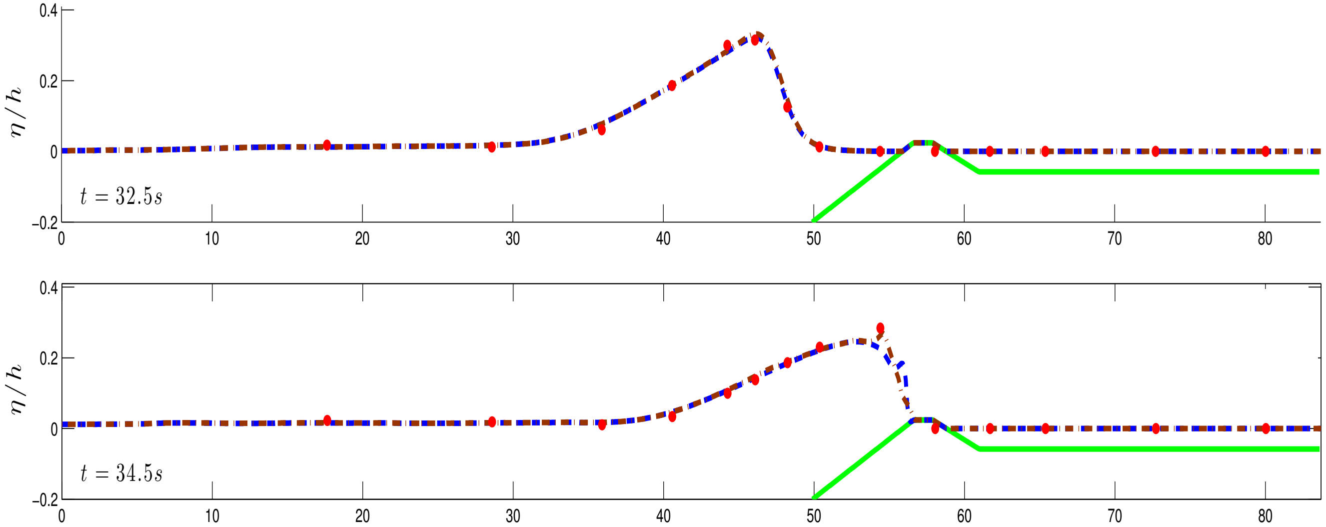

Shoaling, before breaking

During breaking

V. Two-dimensional reef (Roeber et al, 2010)

Area: $(x, y) = [0, 83m] \times [0, 1m]$, $A/h = 0.3$, $N = 10,900$, $CFL = 0.4$, $n_m = 0.014$

—Hybrid and — Eddy viscosity

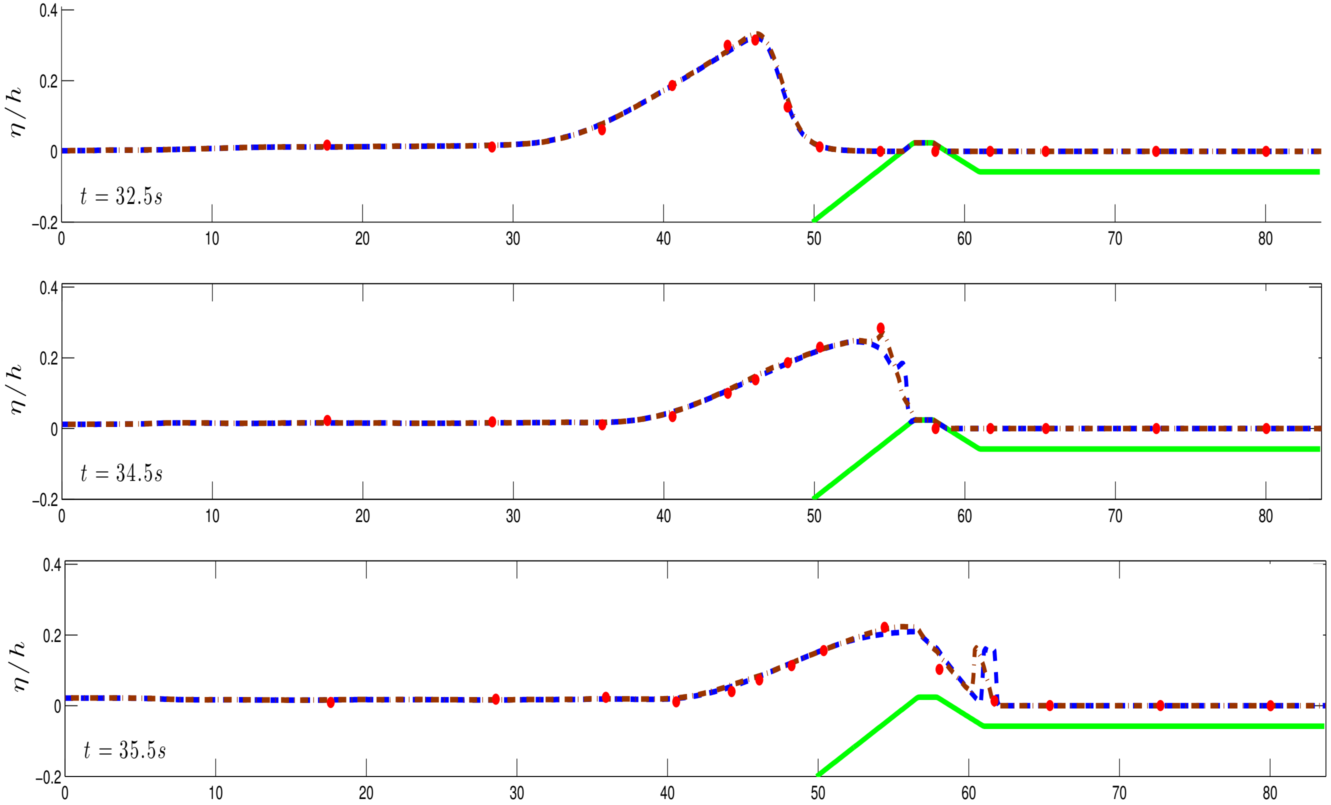

Shoaling, before breaking

During breaking

Wave jet hits still water

V. Two-dimensional reef (Roeber et al, 2010)

Area: $(x, y) = [0, 83m] \times [0, 1m]$, $A/h = 0.3$, $N = 10,900$, $CFL = 0.4$, $n_m = 0.014$

—Hybrid and — Eddy viscosity

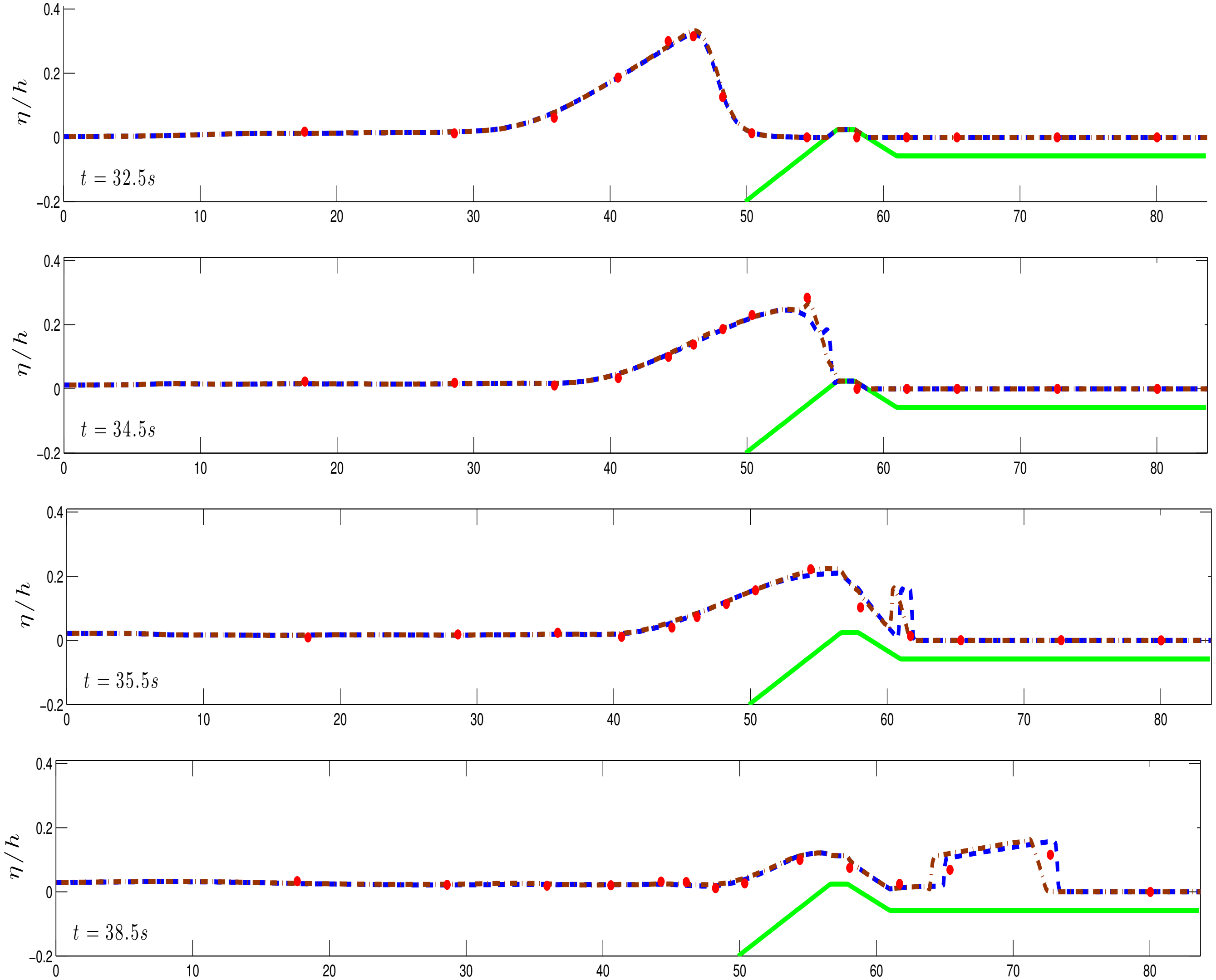

Shoaling, before breaking

During breaking

Wave jet hits still water

Bore propagation

Two-dimensional reef (cont.)

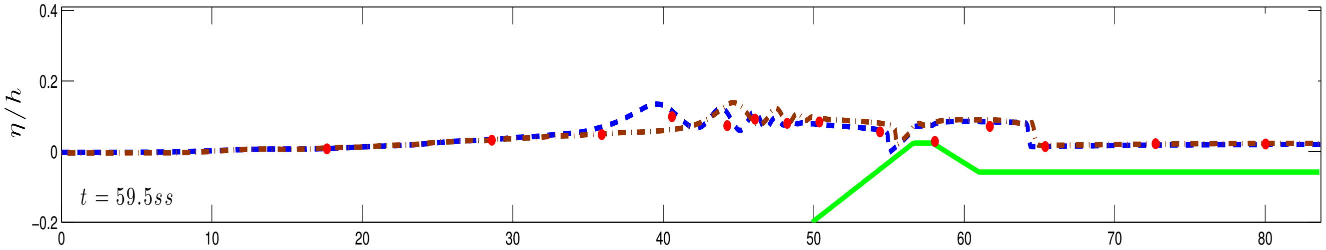

Hydraulic jump on the fore reef

Two-dimensional reef (cont.)

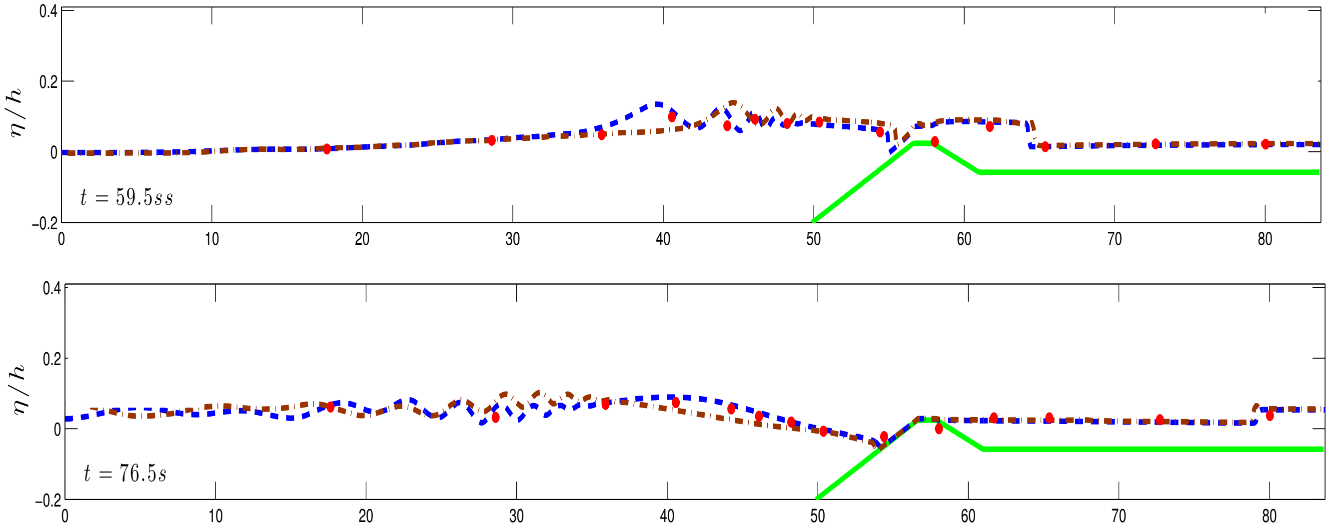

Hydraulic jump on the fore reef

Two-dimensional reef (cont.)

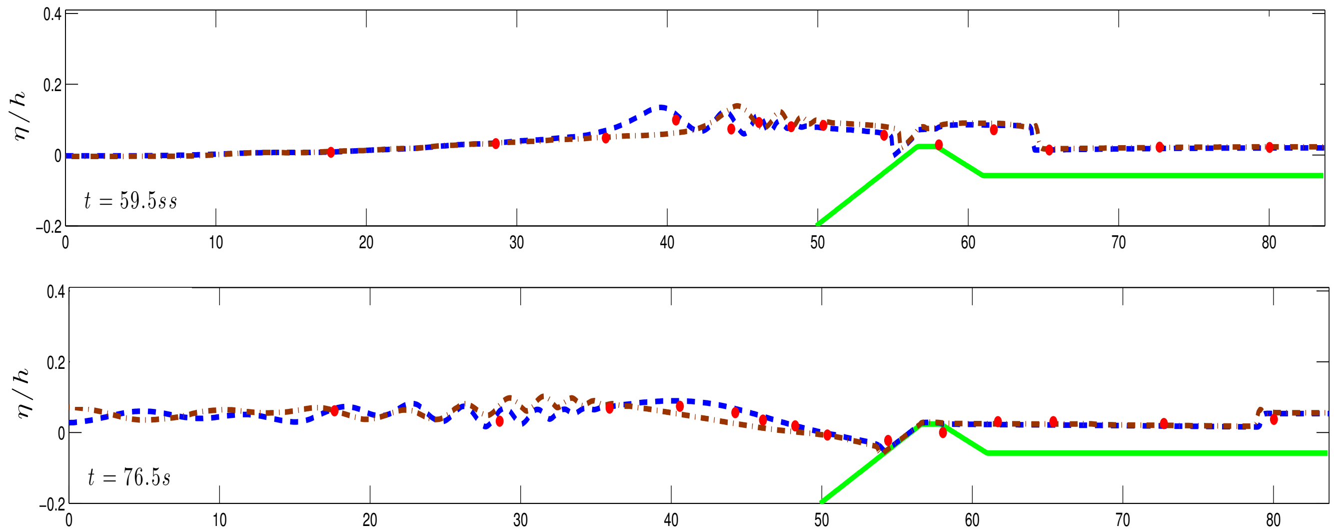

Hydraulic jump on the fore reef

Time series of surface elevation at wave gauges:

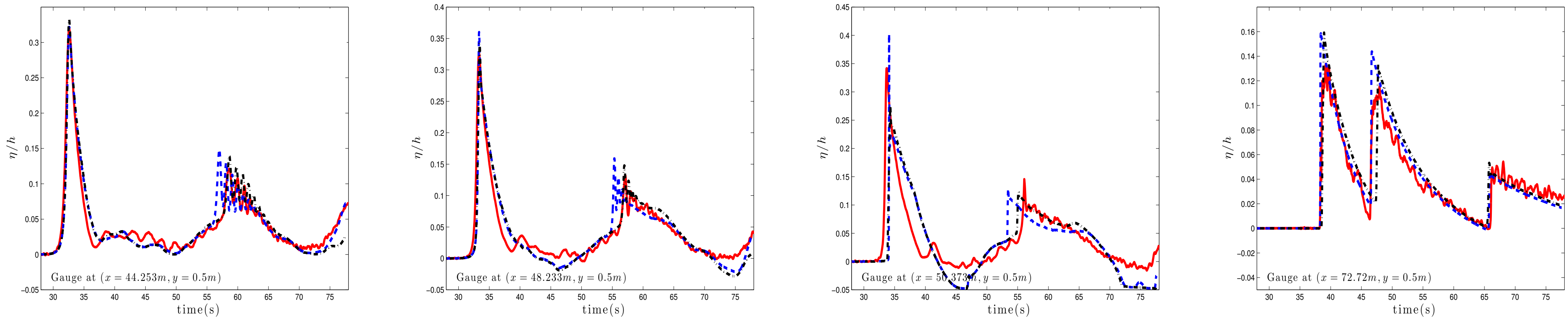

VI. Three-dimensional reef (Lynett et al., 2011)

Area: $(x, y) = [0, 45m] \times [-13m, 13m]$, $A/h = 0.5$, $N = 87,961$, $CFL = 0.4$

VI. Three-dimensional reef (Lynett et al., 2011)

Area: $(x, y) = [0, 45m] \times [-13m, 13m]$, $A/h = 0.5$, $N = 87,961$, $CFL = 0.4$

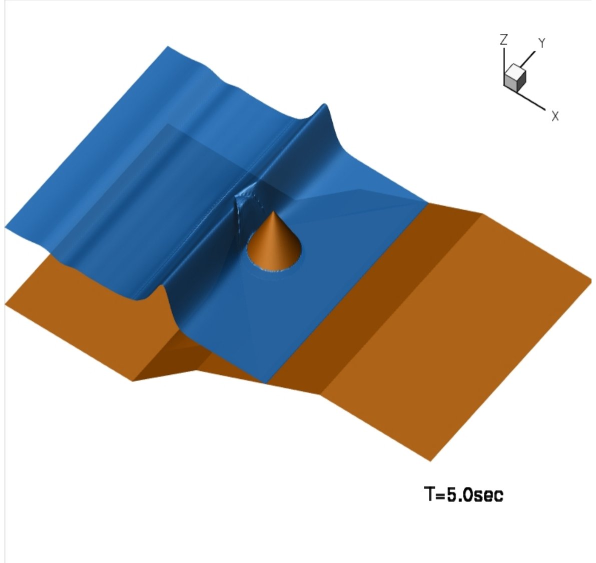

VI. Three-dimensional reef (Lynett et al., 2011)

Area: $(x, y) = [0, 45m] \times [-13m, 13m]$, $A/h = 0.5$, $N = 87,961$, $CFL = 0.4$

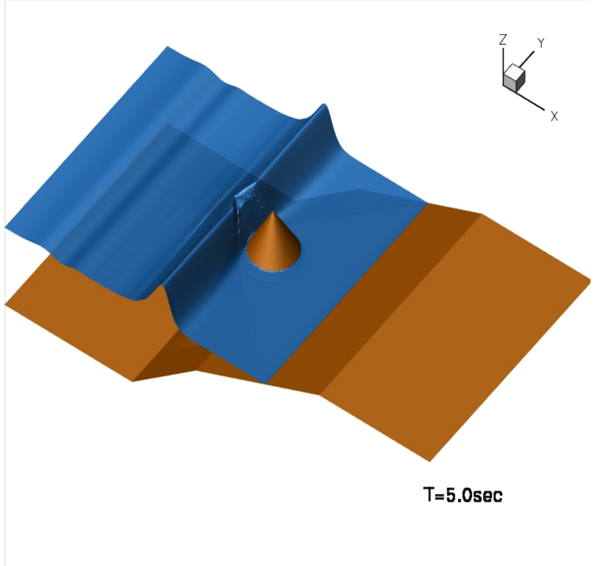

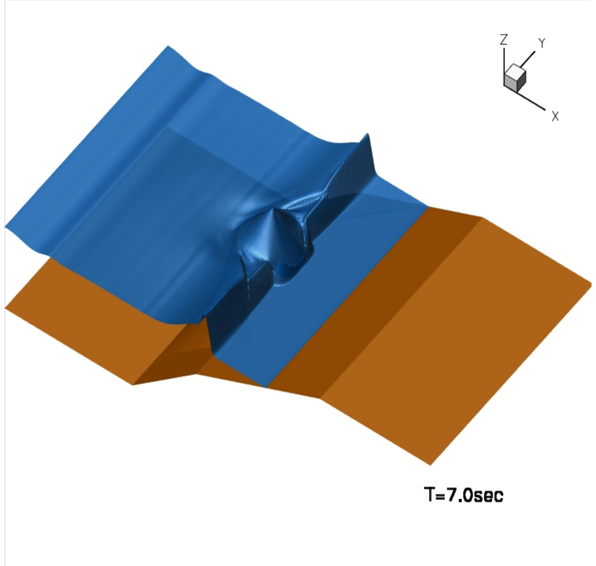

VI. Three-dimensional reef (Lynett et al., 2011)

Area: $(x, y) = [0, 45m] \times [-13m, 13m]$, $A/h = 0.5$, $N = 87,961$, $CFL = 0.4$

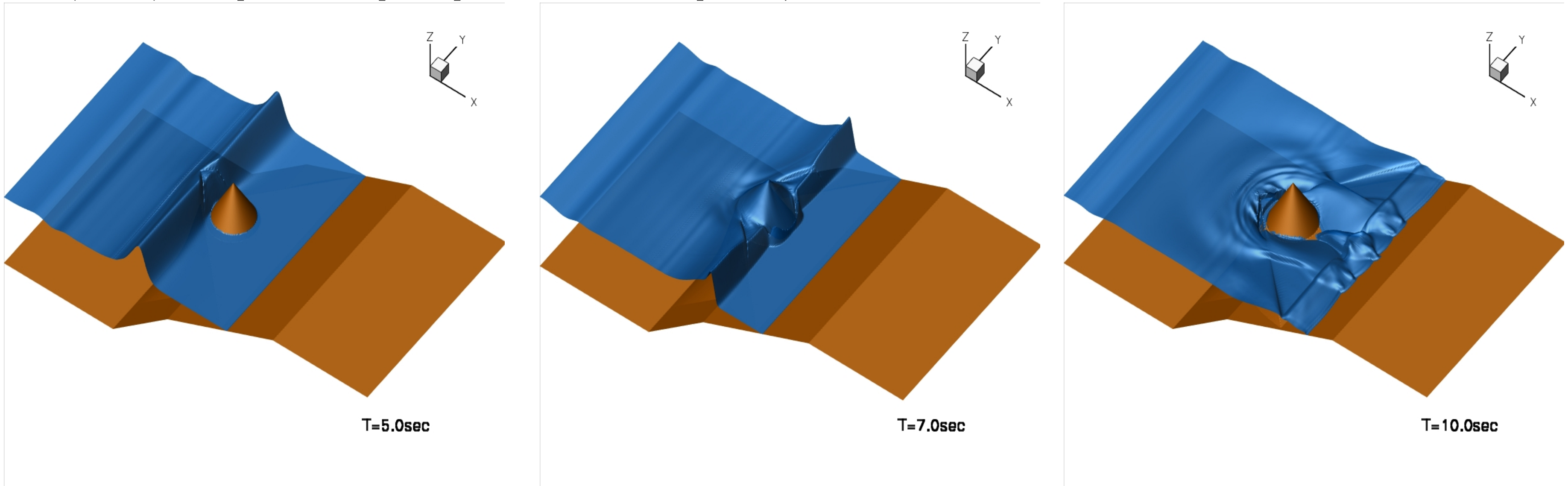

VI. Three-dimensional reef (Lynett et al., 2011)

Area: $(x, y) = [0, 45m] \times [-13m, 13m]$, $A/h = 0.5$, $N = 87,961$, $CFL = 0.4$

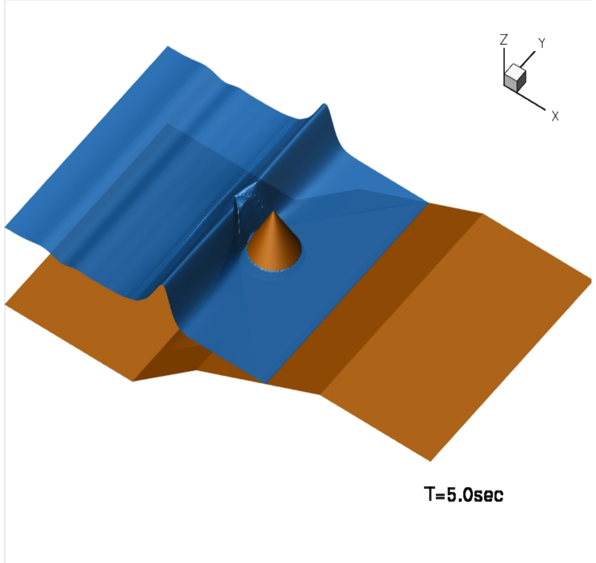

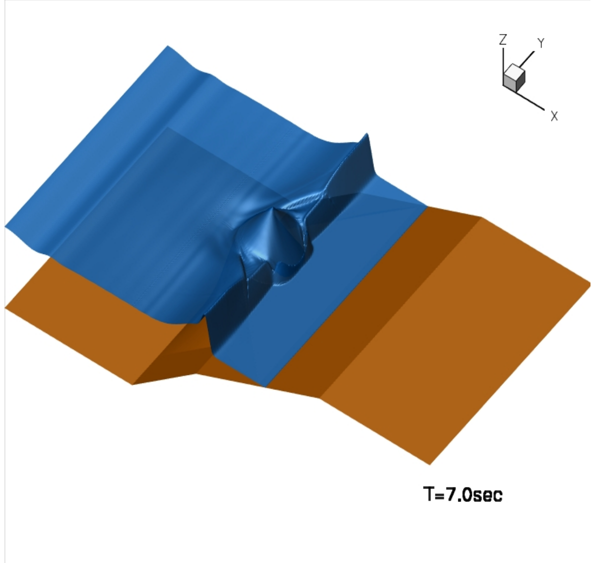

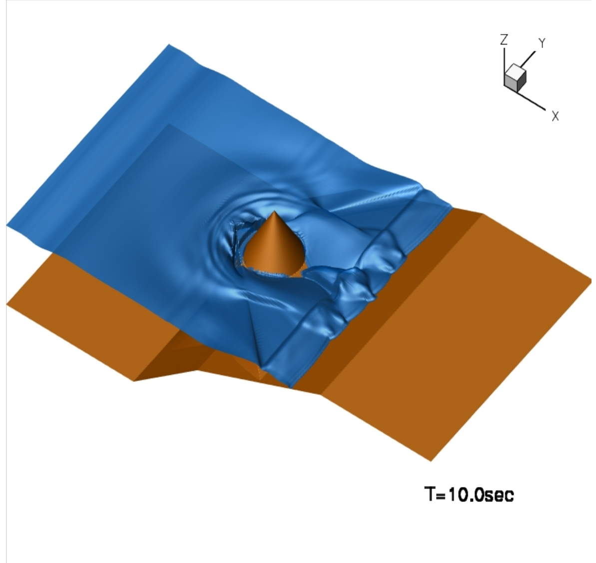

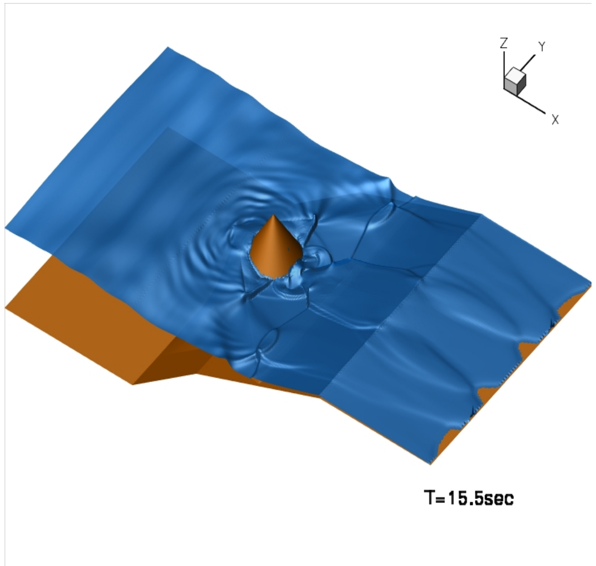

VI. Three-dimensional reef (Lynett et al., 2011)

Area: $(x, y) = [0, 45m] \times [-13m, 13m]$, $A/h = 0.5$, $N = 87,961$, $CFL = 0.4$

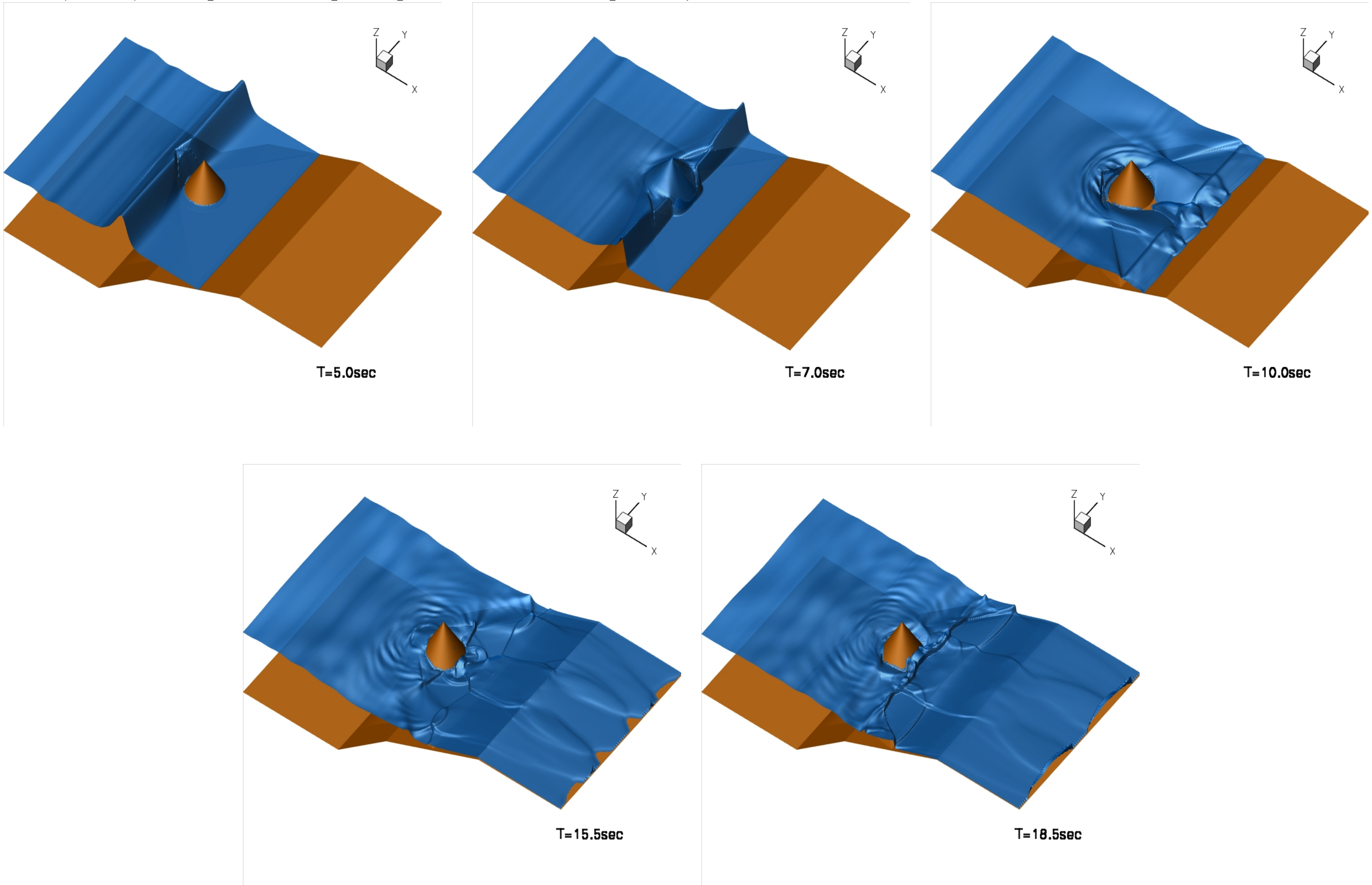

VI. Three-dimensional reef (Lynett et al., 2011)

Area: $(x, y) = [0, 45m] \times [-13m, 13m],\ \ A/h = 0.5,\ \ N = 87,961\ ,\ CFL = 0.4$

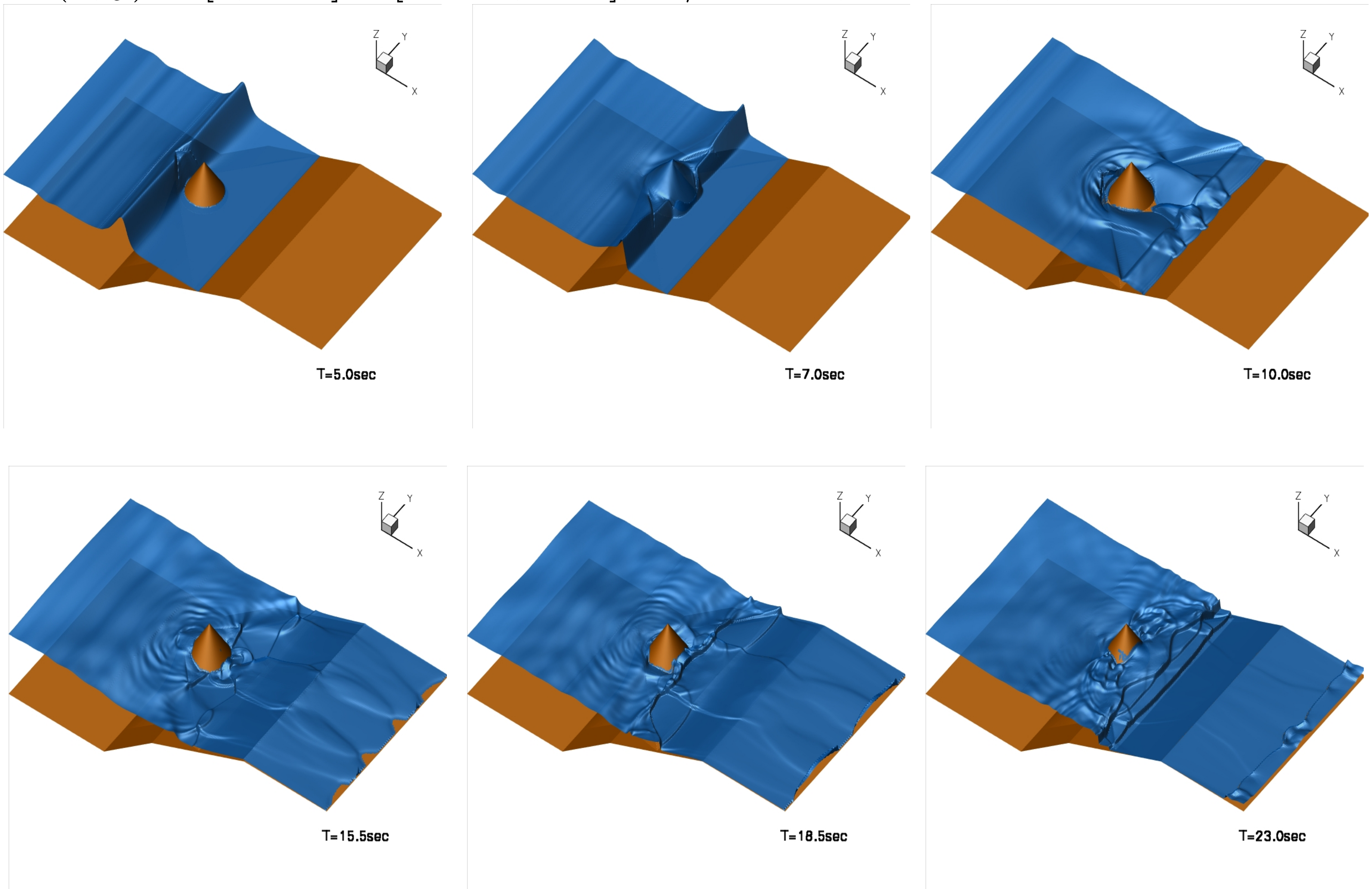

Three-dimensional reef (cont)

Time series of surface elevation at wave gauges:

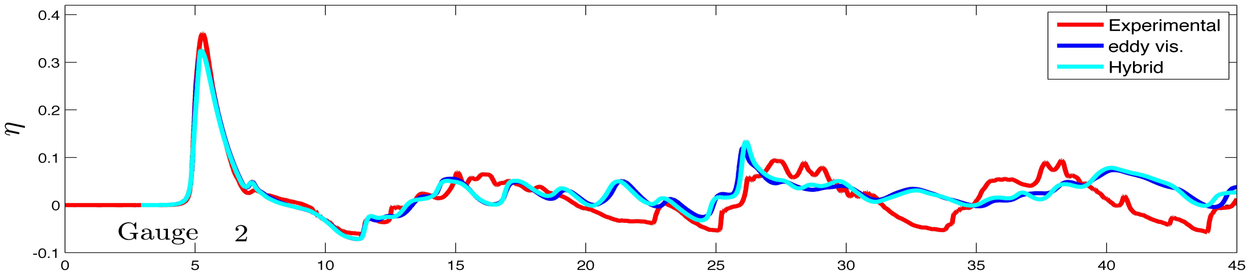

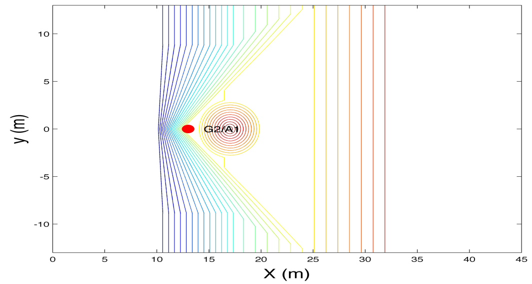

Three-dimensional reef (cont)

Time series of surface elevation at wave gauges:

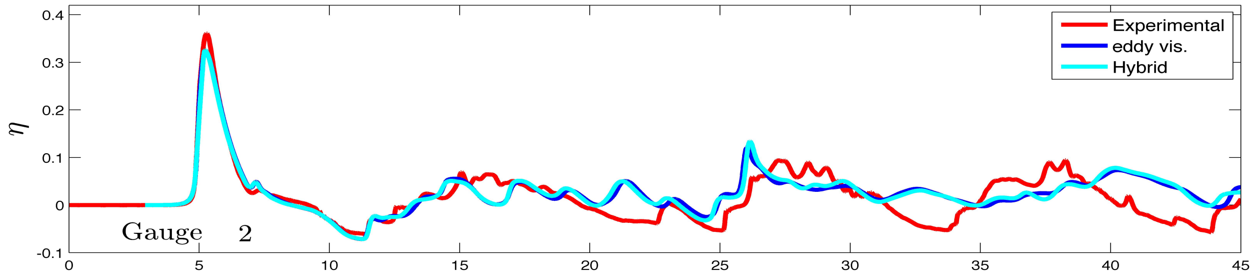

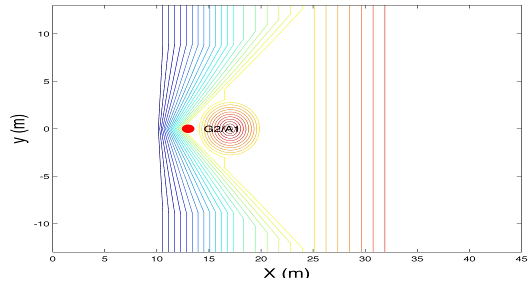

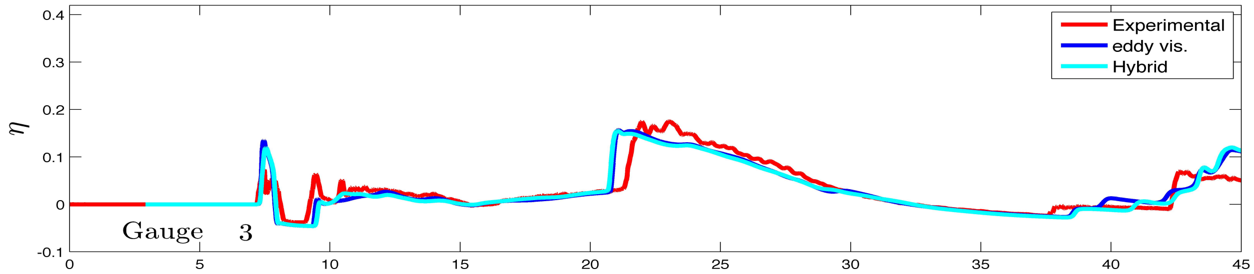

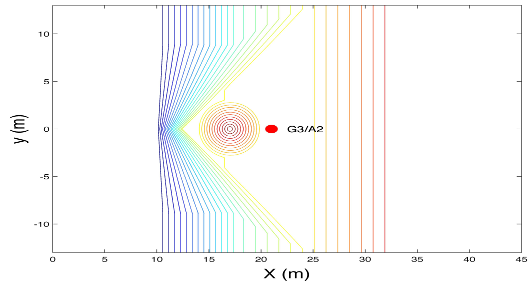

Three-dimensional reef (cont)

Time series of surface elevation at wave gauges:

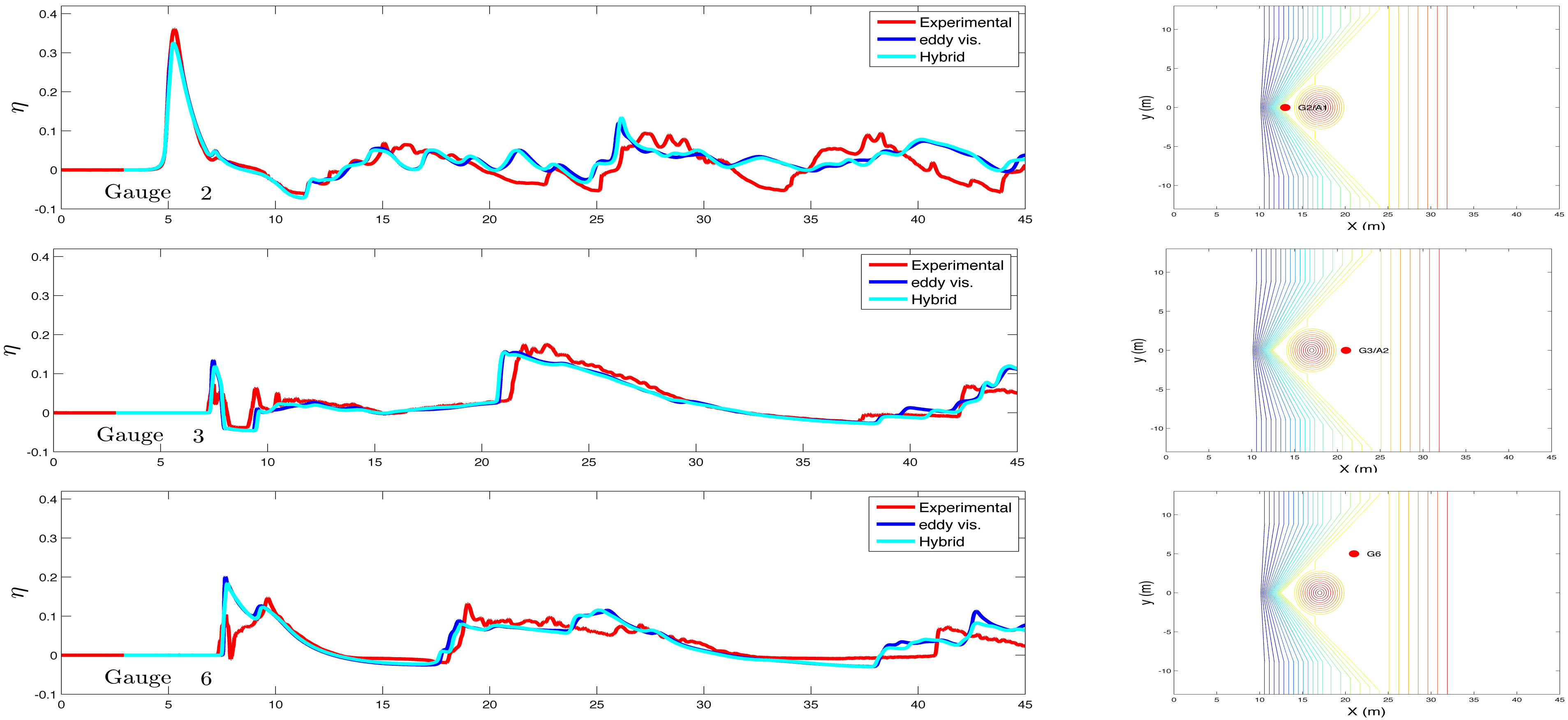

Time series of surface elevation at wave gauges:

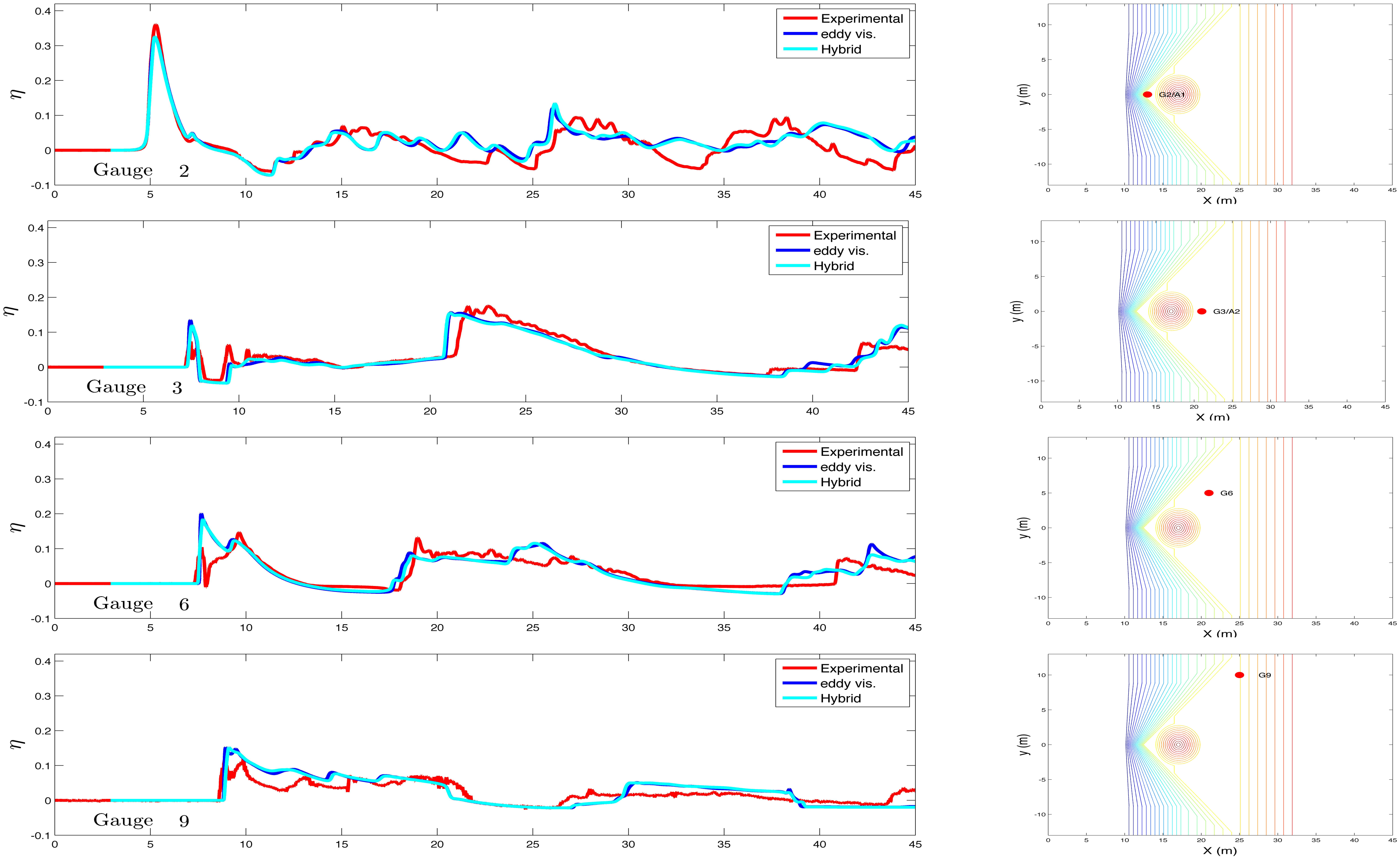

Three-dimensional reef (cont)

Time series of velocities at wave gauges:

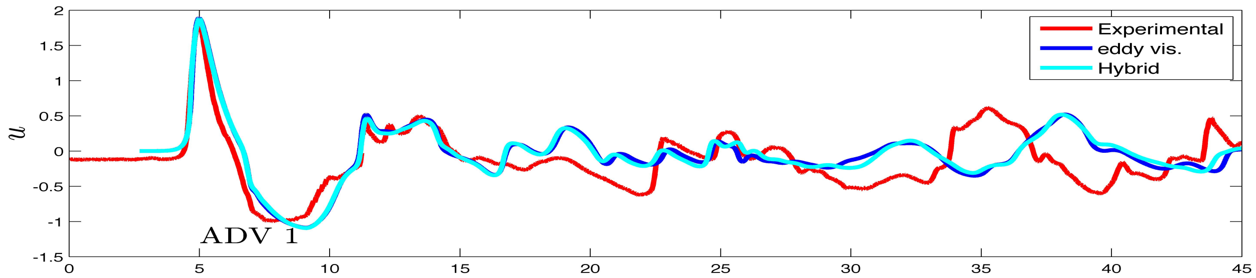

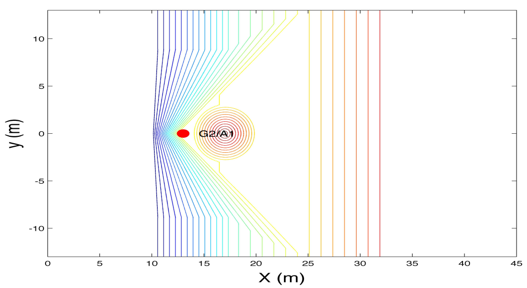

Three-dimensional reef (cont)

Time series of velocities at wave gauges:

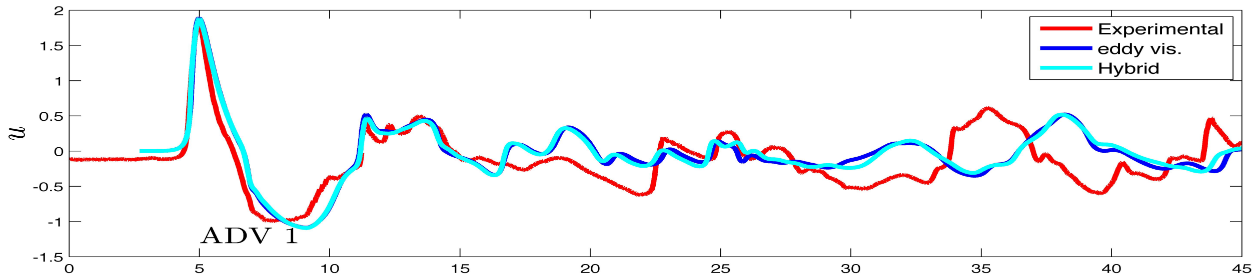

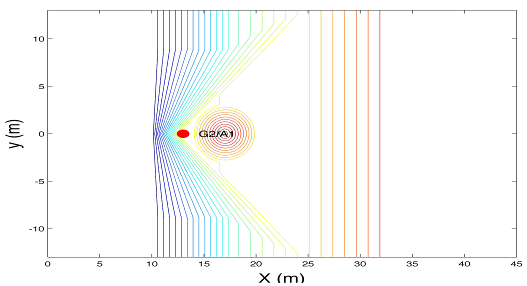

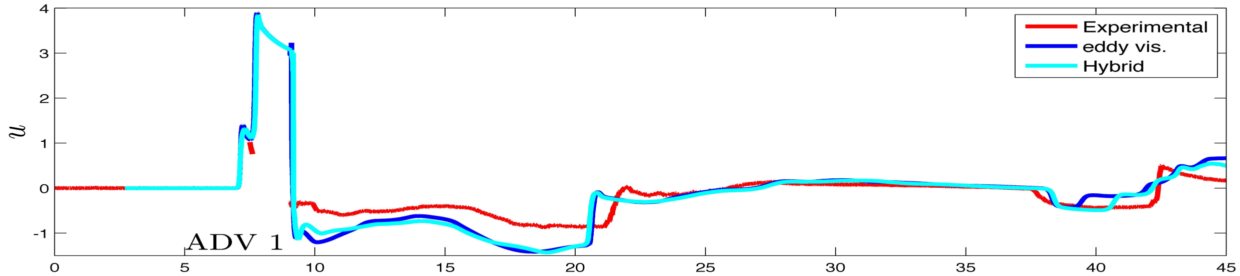

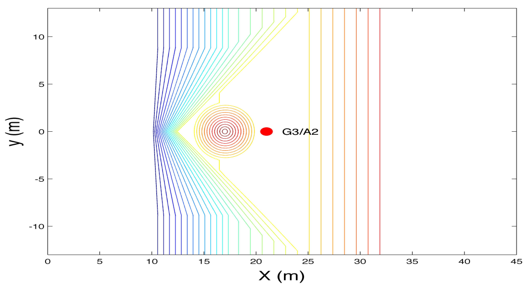

Three-dimensional reef (cont)

Time series of velocities at wave gauges:

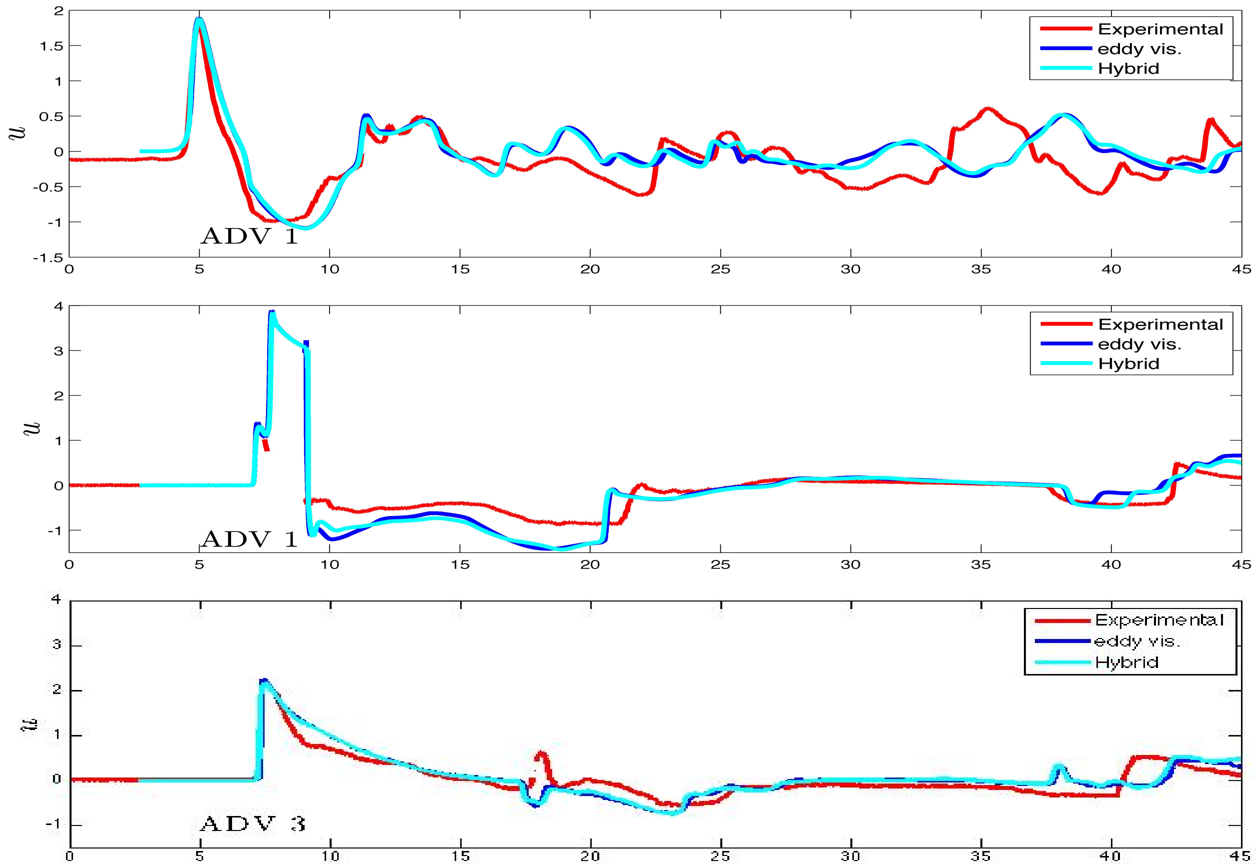

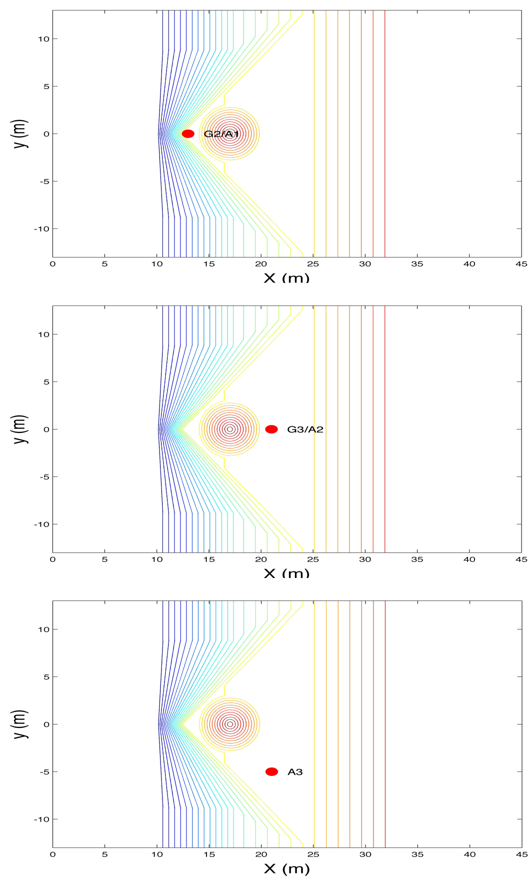

Three-dimensional reef (cont)

Time series of velocities at wave gauges:

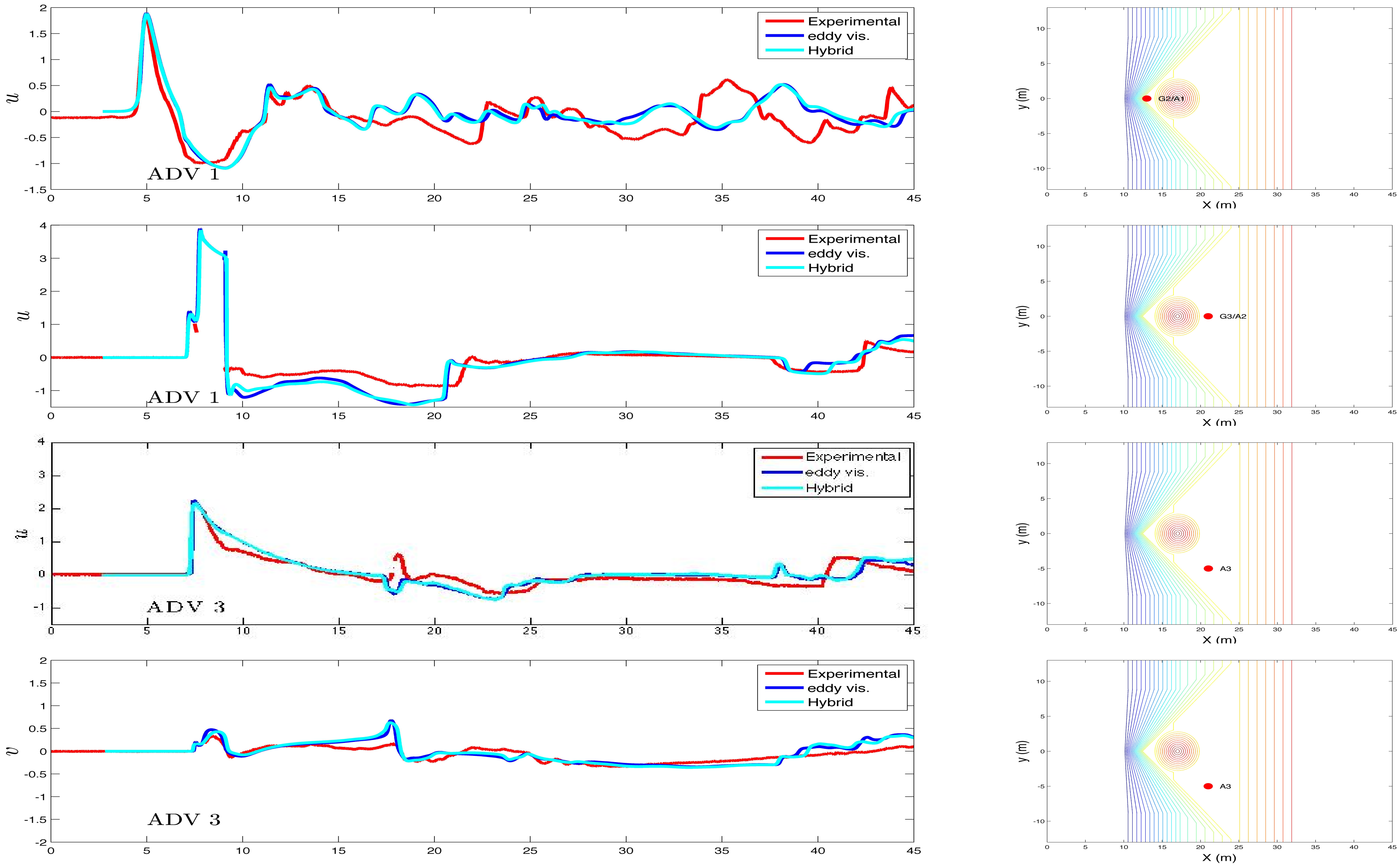

Conclusions

- A 2D unstructured FV numerical model has been developed for solving Nwogu's extended BT equations, formulated as to have identical **flux terms as to the NSWE**.

Conclusions

- A 2D unstructured FV numerical model has been developed for solving Nwogu's extended BT equations, formulated as to have identical **flux terms as to the NSWE**.
- The **conservative formulation** and the **higher-order** FV scheme enhance the applicability of the model without altering its dispersion characteristics.

Conclusions

- A 2D unstructured FV numerical model has been developed for solving Nwogu's extended BT equations, formulated as to have identical **flux terms as to the NSWE**.
- The **conservative formulation** and the **higher-order** FV scheme enhance the applicability of the model without altering its dispersion characteristics.
- The **well-balanced** topography and wet/dry front discretizations provided accurate, conservative and stable wave propagation, shoaling and run-up.

Conclusions

- A 2D unstructured FV numerical model has been developed for solving Nwogu's extended BT equations, formulated as to have identical **flux terms as to the NSWE**.
- The **conservative formulation** and the **higher-order** FV scheme enhance the applicability of the model without altering its dispersion characteristics.
- The **well-balanced** topography and wet/dry front discretizations provided accurate, conservative and stable wave propagation, shoaling and run-up.
- Impose boundary conditions through **weak formulation** and no ghost cells have to be used.

Conclusions

- A 2D unstructured FV numerical model has been developed for solving Nwogu's extended BT equations, formulated as to have identical **flux terms as to the NSWE**.
- The **conservative formulation** and the **higher-order** FV scheme enhance the applicability of the model without altering its dispersion characteristics.
- The **well-balanced** topography and wet/dry front discretizations provided accurate, conservative and stable wave propagation, shoaling and run-up.
- Impose boundary conditions through **weak formulation** and no ghost cells have to be used.
- The flexibility of the FV approach and the use of $h-$ **refinement** are advantageous

Conclusions

- A 2D unstructured FV numerical model has been developed for solving Nwogu's extended BT equations, formulated as to have identical **flux terms as to the NSWE**.
- The **conservative formulation** and the **higher-order** FV scheme enhance the applicability of the model without altering its dispersion characteristics.
- The **well-balanced** topography and wet/dry front discretizations provided accurate, conservative and stable wave propagation, shoaling and run-up.
- Impose boundary conditions through **weak formulation** and no ghost cells have to be used.
- The flexibility of the FV approach and the use of $h-$ **refinement** are advantageous
- The **edge-based structure** adopted can provide computational efficiency, since most of the geometric quantities needed can be calculated in a pre-processing stage.

Conclusions

- A 2D unstructured FV numerical model has been developed for solving Nwogu's extended BT equations, formulated as to have identical **flux terms as to the NSWE**.
- The **conservative formulation** and the **higher-order** FV scheme enhance the applicability of the model without altering its dispersion characteristics.
- The **well-balanced** topography and wet/dry front discretizations provided accurate, conservative and stable wave propagation, shoaling and run-up.
- Impose boundary conditions through **weak formulation** and no ghost cells have to be used.
- The flexibility of the FV approach and the use of $h-$ **refinement** are advantageous
- The **edge-based structure** adopted can provide computational efficiency, since most of the geometric quantities needed can be calculated in a pre-processing stage.
- Two different types of **wave breaking** mechanisms are implement with comparable performance.

Conclusions

- A 2D unstructured FV numerical model has been developed for solving Nwogu's extended BT equations, formulated as to have identical **flux terms as to the NSWE**.
- The **conservative formulation** and the **higher-order** FV scheme enhance the applicability of the model without altering its dispersion characteristics.
- The **well-balanced** topography and wet/dry front discretizations provided accurate, conservative and stable wave propagation, shoaling and run-up.
- Impose boundary conditions through **weak formulation** and no ghost cells have to be used.
- The flexibility of the FV approach and the use of $h-$ **refinement** are advantageous
- The **edge-based structure** adopted can provide computational efficiency, since most of the geometric quantities needed can be calculated in a pre-processing stage.
- Two different types of **wave breaking** mechanisms are implement with comparable performance.
- Relatively straight forward to **extend existing NSWE codes** that use (unstructured) FV schemes as to include dispersion characteristics for deeper water simulations.

Thank you for your attention!!

2D solitary wave propagation in a channel

Area: $(x, y) = [-100, 2400m] \times [-5, 5m]$, $A/h = 0.2$, $N = 53, 304$, $CFL = 0.8$.

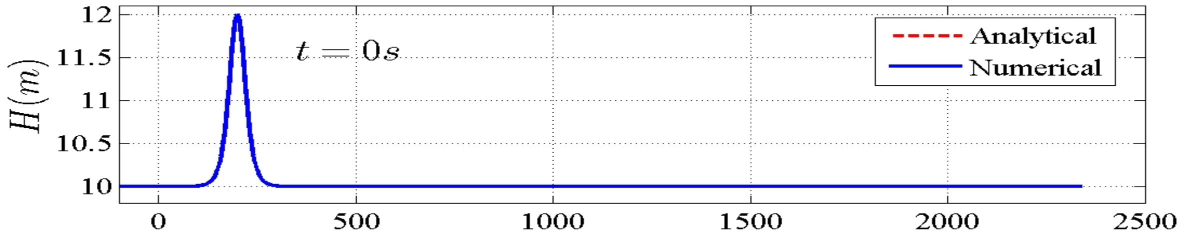

2D solitary wave propagation in a channel

Area: $(x, y) = [-100, 2400m] \times [-5, 5m]$, $A/h = 0.2$, $N = 53,304$, $CFL = 0.8$.

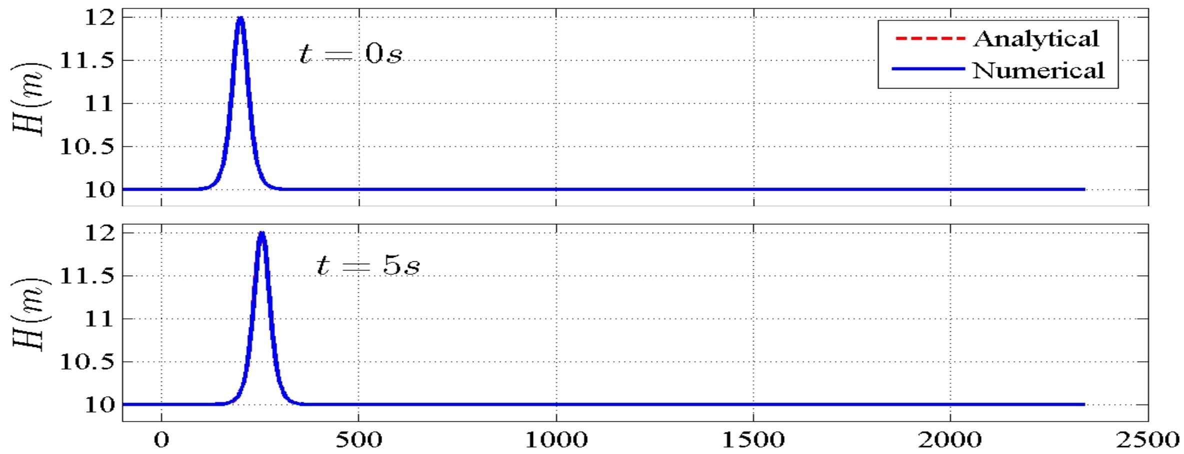

2D solitary wave propagation in a channel

Area: $(x, y) = [-100, 2400m] \times [-5, 5m],\ \ A/h = 0.2,\ \ N = 53,304\ , CFL = 0.8.$

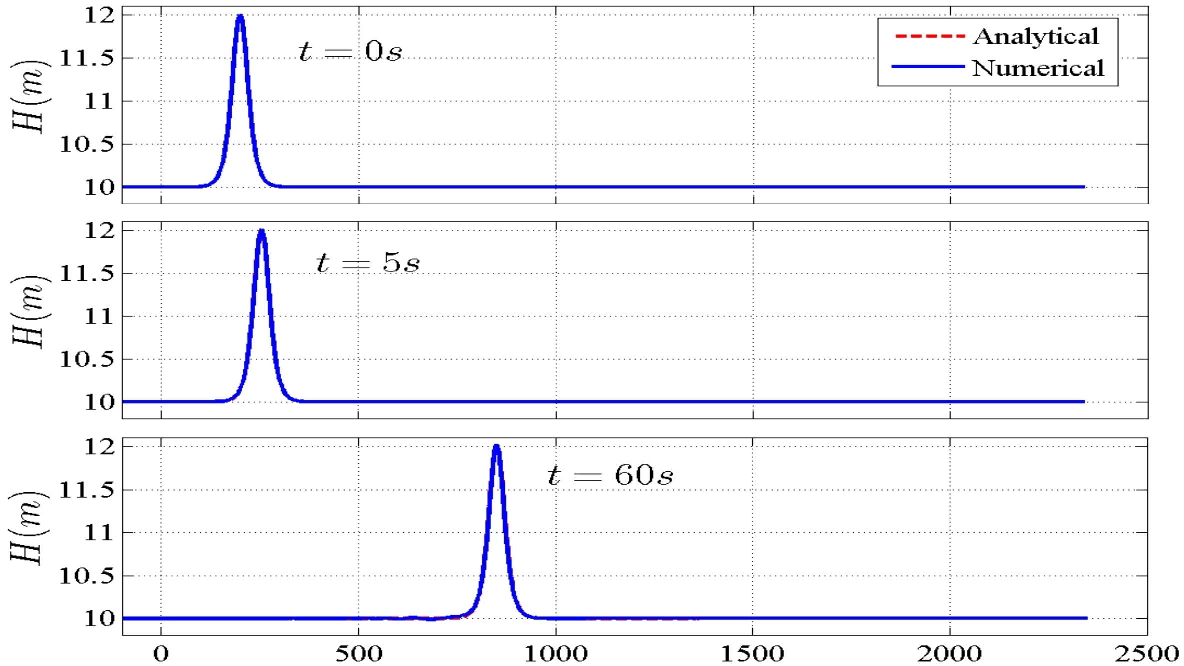

2D solitary wave propagation in a channel

Area: $(x, y) = [-100, 2400m] \times [-5, 5m]$, $A/h = 0.2$, $N = 53,304$, $CFL = 0.8$.

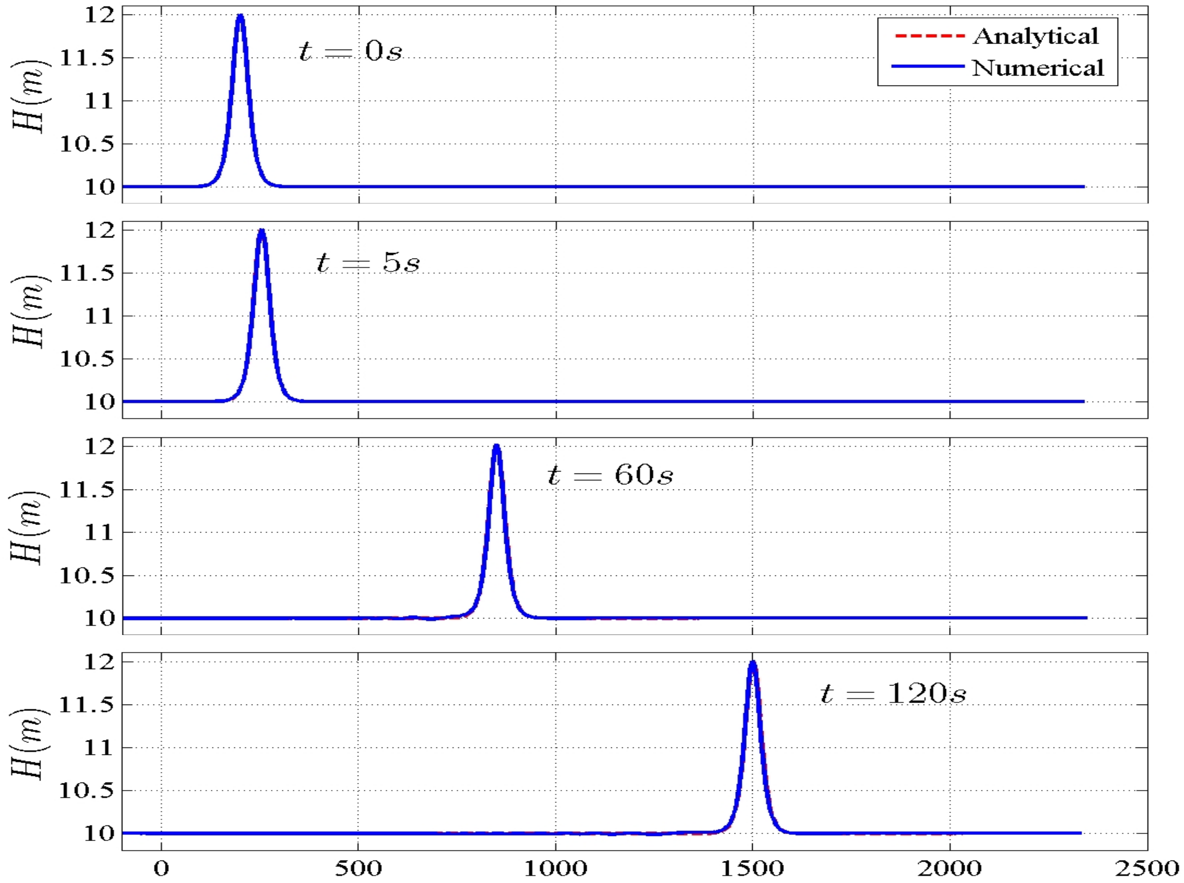

2D solitary wave propagation in a channel

Area: $(x, y) = [-100, 2400m] \times [-5, 5m]$, $A/h = 0.2$, $N = 53,304$, $CFL = 0.8.$

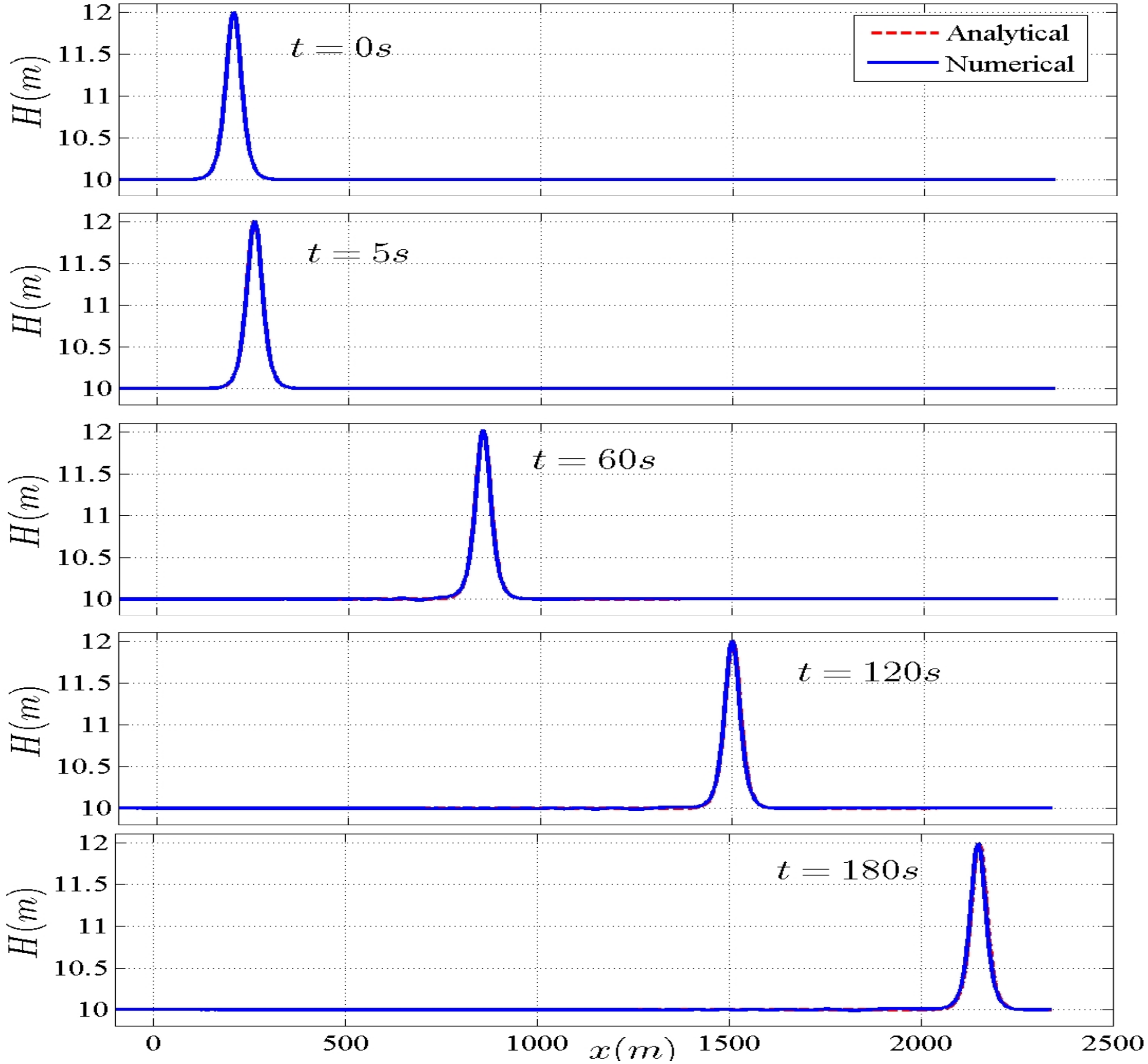

Wave Interaction with a Vertical Circular Cylinder (Antunes do Cormo et al. 1993)

Area: $(x, y) = [-4, 10m] \times [-0, 0.55m],\ \ A/h = 0.25,\ \ N = 10,609$, $CFL = 0.8$

Use of an $h-$ enrichment technique (Nikolos and Delis, 2009)

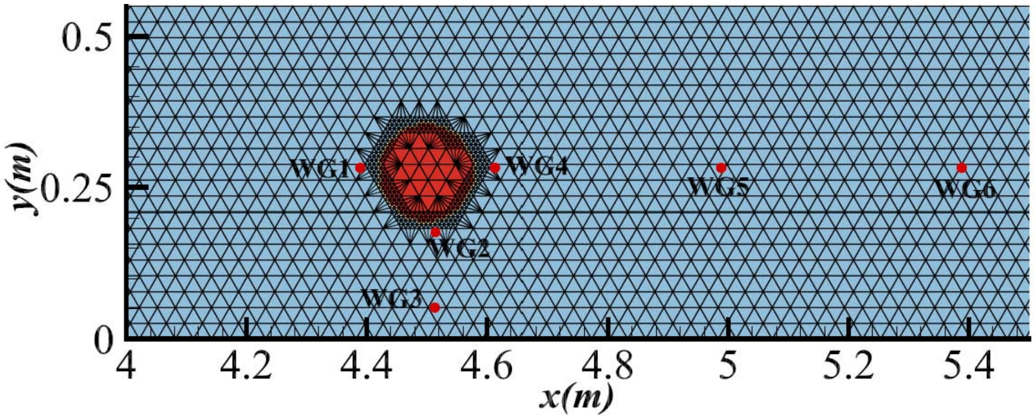

Wave Interaction with a Vertical Circular Cylinder (Antunes do Cormo et al. 1993)

Area: $(x,y) = [-4, 10m] \times [-0, 0.55m]$, $A/h = 0.25$, $N = 10,609$, $CFL = 0.8$

Use of an $h-$ enrichment technique (Nikolos and Delis, 2009)

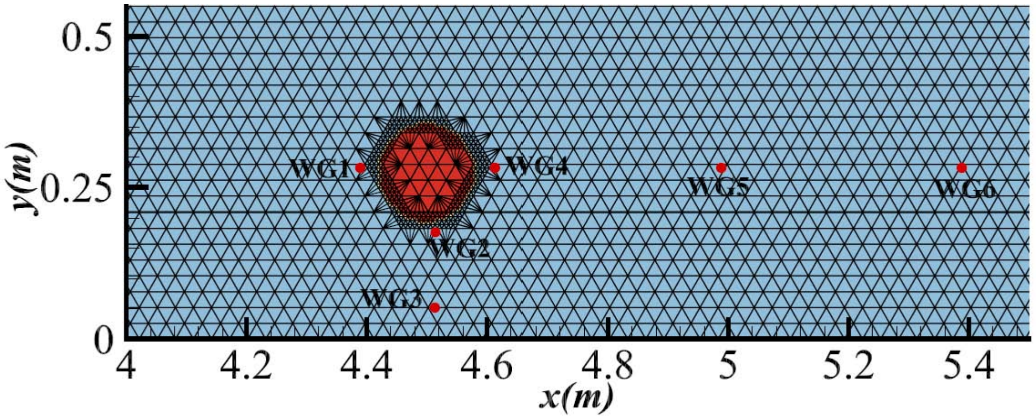

Wave Interaction with a Vertical Circular Cylinder (Antunes do Cormo et al. 1993)

Area: $(x, y) = [-4, 10m] \times [-0, 0.55m]$, $A/h = 0.25$, $N = 10,609$, $CFL = 0.8$

Use of an $h-$ enrichment technique (Nikolos and Delis, 2009)

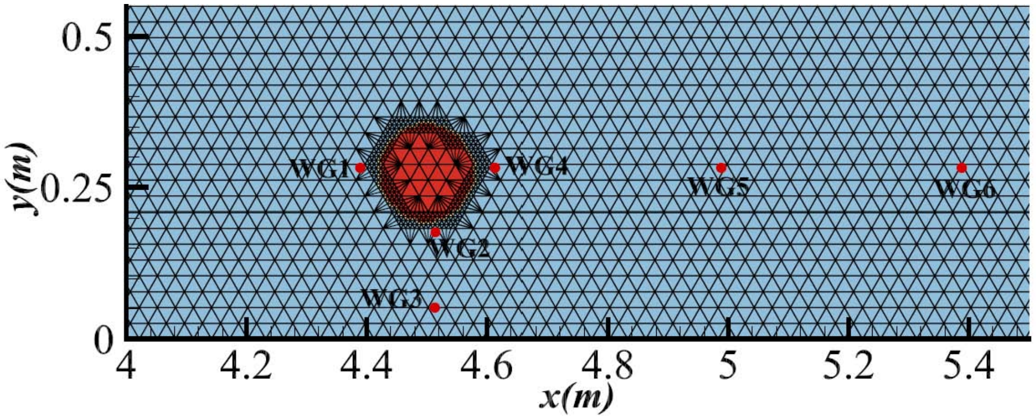

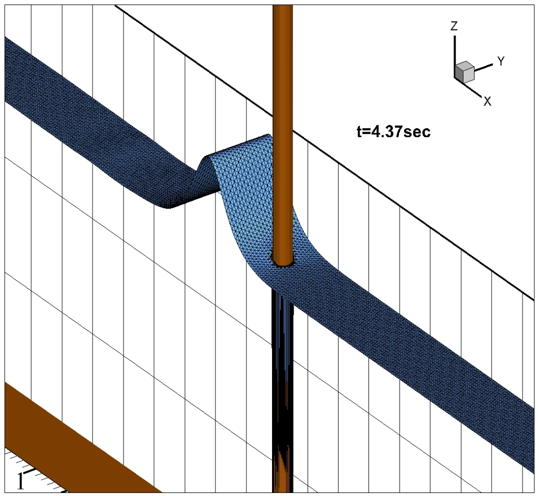

Wave Interaction with a Vertical Circular Cylinder (Antunes do Cormo et al. 1993)

Area: $(x, y) = [-4, 10m] \times [-0, 0.55m]$, $A/h = 0.25$, $N = 10,609$, $CFL = 0.8$

Use of an $h-$ enrichment technique (Nikolos and Delis, 2009)

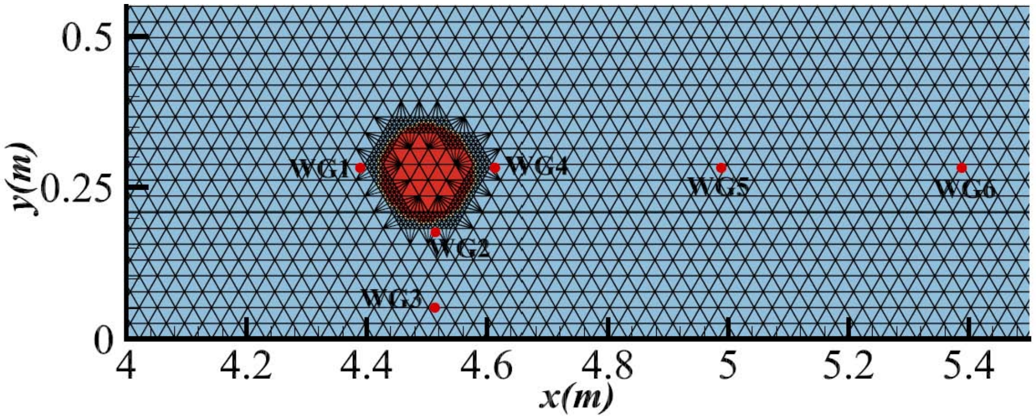

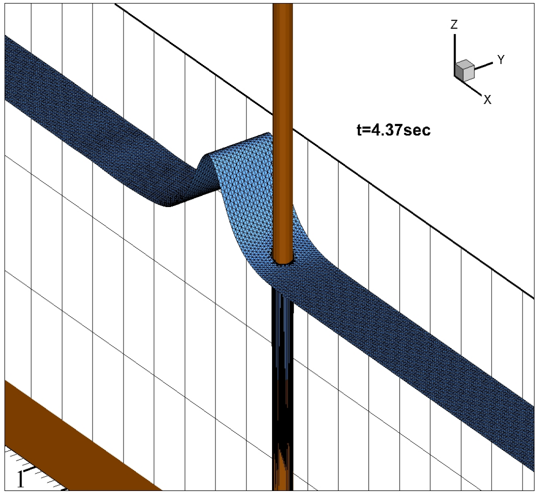

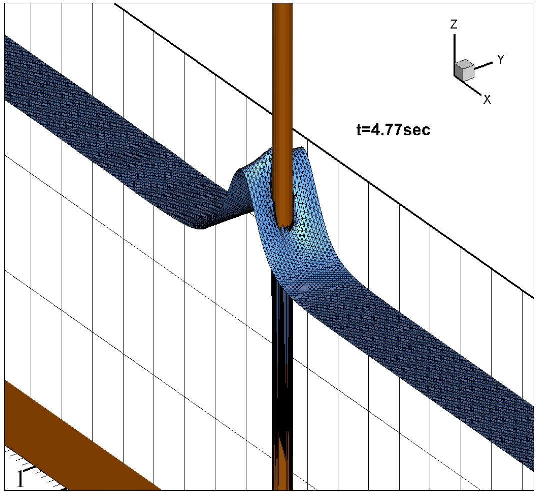

Wave Interaction with a Vertical Circular Cylinder (Antunes do Cormo et al. 1993)

Area: $(x, y) = [-4, 10m] \times [-0, 0.55m]$, $A/h = 0.25$, $N = 10,609$, $CFL = 0.8$

Use of an $h-$ enrichment technique (Nikolos and Delis, 2009)

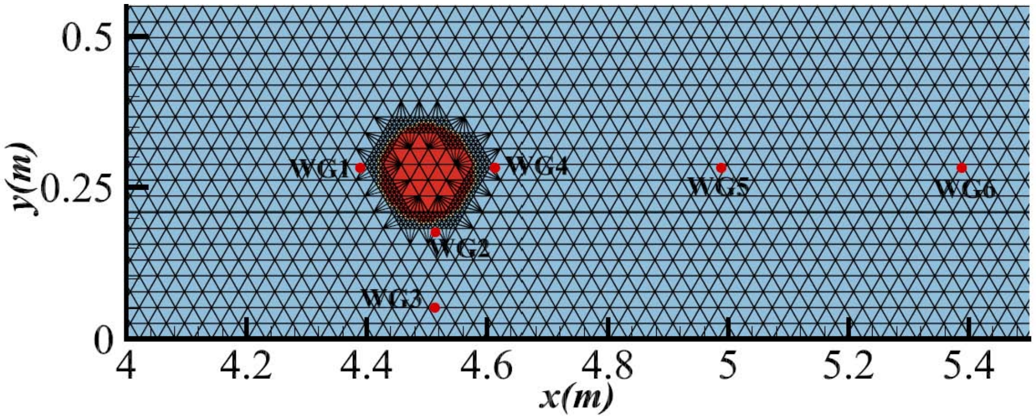

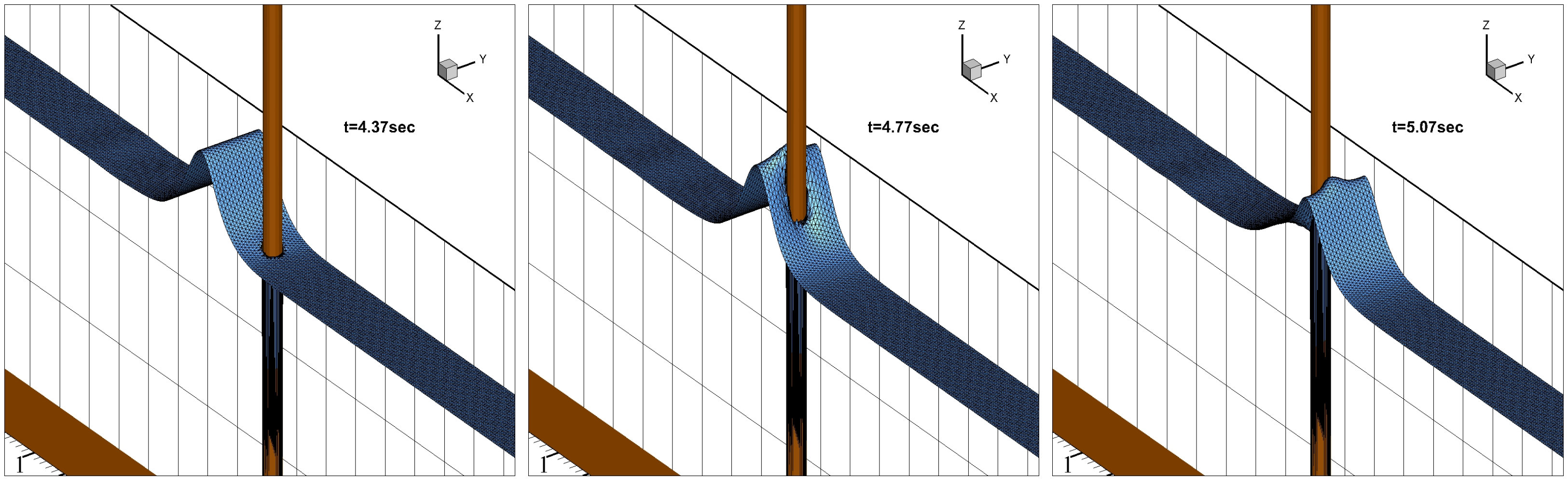

Wave Interaction with a Vertical Circular Cylinder (Antunes do Cormo et al. 1993)

Area: $(x, y) = [-4, 10m] \times [-0, 0.55m]$, $A/h = 0.25$, $N = 10,609$, $CFL = 0.8$

Use of an $h-$ enrichment technique (Nikolos and Delis, 2009)

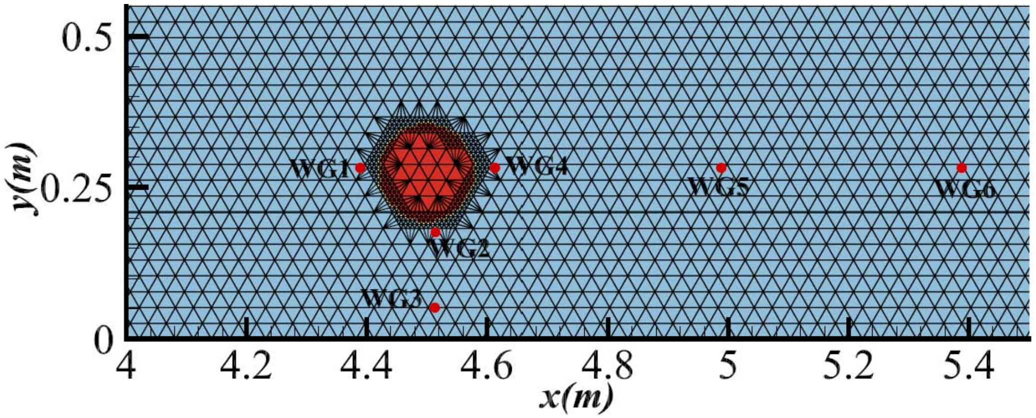

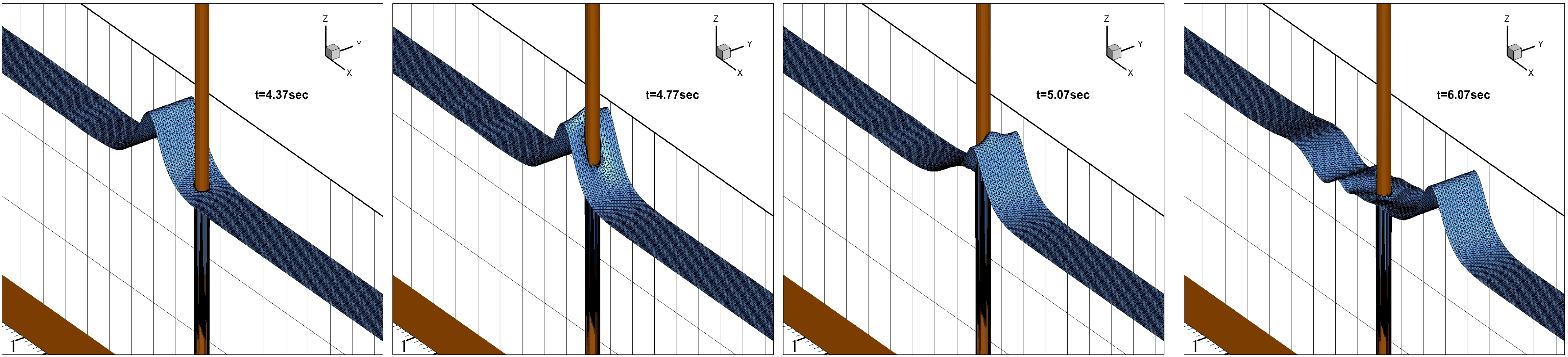

Solitary wave-cylinder interaction: numerical and experimental results for η at WG1-WG6